# Hydrolysis of Polyaluminum Chloride

# and

# its Effect on Coagulation Performance: Role of Inorganic Ions

by
Yize Chen

A dissertation submitted in partial fulfillment of the requirements for the degree of

Doctor of Philosophy

Hokkaido University
2023

## Acknowledgment

To complete this dissertation, I have been supported by many peoples. First of all, I would like to express my sincere gratitude to them.

I would like to express my deepest respect and gratitude to my supervisor, Professor Yoshihiko Matsui (The Environmental Risk Engineering Laboratory), for his guidance and support throughout my research, for his patient instructions when I made mistakes, and for his kindness in receiving me as his student. What he taught me is not only his sophisticated thinking on research but also his wisdom on work and efficiency. Without his guidance, I could not imagine the complication of my research. I believe that the experience I gained through my research life will be a great power and driving force when I am confronted with hardships and difficulties in my future work and life.

I would like to express my sincere respect and gratitude to Associate Professor Taku Matsushita and Associate Professor Nobutaka Shirasaki in this laboratory, for their enthusiastic advice on my research, for their patient instruction on my academic presentation, and for their efforts to make me a good rhythm of research and life.

I would like to express my sincere gratitude to Dr. Yoshifumi Nakazawa, Dr. Shun Saito, Mr. Kouki Shinno, Mr. Hideki Takaesu, and all the rest of laboratory members from 2017 to 2023. They gave me support on my research and experiment and also helped me with the difficulties I met in my daily life in Japan. They activated the air of this laboratory. Talking with them was a good relaxation during my research life.

I would like to express my gratitude to my friends: Dr. Yuanjun Zhao, Dr. Gang Shi, Dr. Long Pan, Ms. Qiuhan Hu, Mr. Jinming Jia, and Mr. Zihao Guan. They helped me a lot in my research and life. We had a lot of fun talking, traveling, and having hobbies. They are excellent with

many strengths which I do not have so I was always inspired by them. Without them, I would not have been able to continue my research here.

I would like to express my deepest gratitude to my parents, Ms. Liqun Liu and Mr. Hui Chen, who always respected and supported my choice. They gave me financial and emotional support during my life in Japan. I was encouraged every time I thought of them.

Finally, I am grateful to Mitsubishi Corporation, who provided me with financial support so that I could focus more on my research.

# Content

# Chapter 1. Introduction

## 1.1 Background

### 1.1.1 Application of PACl coagulants in drinking water treatment process

Coagulation–flocculation is a fundamental process in water treatment and is applied worldwide as a pretreatment not only for traditional sedimentation–rapid sand filtration but also for membrane filtration (Edzwald, 2011). At the beginning of coagulation–flocculation, coagulant is dosed to destabilize particles during coagulation, which plays an important role in the formation of floc particles and particle removal in subsequent processes such as sedimentation and filtration (Bratby, 2016). Among various types of inorganic coagulants, polyaluminum chloride (PACl), which was first used as a coagulant in Japan, has been applied and is popular in water treatment worldwide. The aluminum species in PACl is pre-hydrolyzed and is produced in a way that gives it a high capacity for charge neutralization. The fact that the interaction between PACl and substances to be removed can proceed effectively (Bratby, 2016) leads to superior coagulation performance.

### 1.1.2 Different performance of PACl with various characteristics and preparation methods

Recently, high-basicity (basicity 70%), sulfated PACl has been developed and has rapidly become popular in Japan because its use results in lower aluminum residuality in treated water, higher removal efficiencies of natural organic matter (NOM), and long-term stability without the formation of precipitates during storage (Kimura et al., 2013). Furthermore, compared with normal-basicity (50%), sulfated PACl, high-basicity PACl can attenuate transmembrane pressure rise more when it is applied in coagulation pretreatment before microfiltration (Kimura

et al., 2015). The market share of high-basicity PACl indicates that it is becoming popular, but for some raw water, high-basicity PACl may fail to outperform normal-basicity PACl (personal communication, Taki Chemical Co., Ltd., 2019).

High-basicity and normal-basicity PACls are commercially produced by the $Al(OH)_3$-dissolution method. However, PACls produced by $AlCl_3$-titration methods have been intensively studied in laboratory coagulation experiments, and satisfactory coagulation performance has been reported based on the residual turbidity after sedimentation (Chu et al., 2008; Gao & Yue, 2005). However, Nakazawa et al. (2018a) have reported that high-basicity PACls produced by $Al(OH)_3$-dissolution and by $AlCl_3$-titration perform very differently, although they are identical in terms of aluminum species based on the ferron assay (Wang et al., 2002). The former was very effective, but the latter was ineffective in forming large floc particles. Use of the latter resulted in a high concentration of residual SPAC particles in treated water. Overall, the evaluations of base-titration PACls have not been consistent. Even when water has been treated with several types of $Al(OH)_3$-dissolution PACl coagulants, the performance of the PACls has generally been specific to the raw water. The mechanisms responsible for this specificity have not been fully investigated and are not yet clearly understood.

Moreover, most of the foregoing studies of PACl coagulation have used PACls prepared by the $AlCl_3$-titration method, but the characteristics and coagulation performances of PACls produced by the $Al(OH)_3$-dissolution method, which is quite popular in PACl-production industries, have seldom been studied. Experimental results of a series of CSF processes, rather than jar tests, are still not enough for PACl coagulants.

Plenty of research have investigated the effect of some important factors about PACl on coagulation and flocculation. Thorough studies of PACl coagulation performance have been

conducted on the effects of the amount of PACl added (Hendricks, 2016; Letterman & Yiacoumi, 2010) and the mixing intensity after addition (Lin et al., 2013; Kan et al., 2002; and Nakazawa et al., 2018). There has also been a great deal of research on the properties of various types of PACls, including their basicity and chemical composition. In the case of non-sulfated PACls, the focus has been on aluminum polynuclear species (Kong et al., 2021; Lin et al., 2008; Liu et al., 2021; Matsui et al., 1998; Qu & Liu, 2004; Tang et al., 2015; Wu et al., 2007; Yan et al., 2007). These studies have led to the common understanding that PACls with high basicity containing $Al_{13}$ and/or $Al_{30}$ species are excellent coagulants because of the high charge neutralization capacities of these species. However, it is unclear whether this conclusion is true for all types of raw waters, and the compatibility of PACls and raw water quality is not yet well understood, with the exception of the compounds targeted in coagulation treatment.

On the other hand, another possible reason which can explain the different performances of various types of PACls is the characteristics of the raw water. In other countries and regions, types of PACl similar to those used in Japan are not always used. The implication is that the PACl best suited for a local area depends on the characteristics of the raw water in that area. However, little attention has been focused on the relationship between PACl and raw water quality, especially the concentrations of substances not targeted for removal.

### 1.1.3 Effects of inorganic ions on PACl performance

Because PACl and the conventional coagulant alum are hydrolyzing aluminum salts, it is commonly understood that alkalinity is required for their hydrolysis and that hydrolysis produces the aluminum polynuclear species needed for coagulation. High alkalinity of raw water, therefore, increases the efficiency of removal via coagulation with alum (Letterman et al., 1979; Yan et al., 2008). In contrast, Saxena et al. (2019) have reported that high alkalinity in water has little effect on particle removal via coagulation with high-basicity PACl, though

they do not discuss the mechanism responsible for this phenomenon. It has been reported that Kegging-type e-$Al_{13}$ polycation, which is said to be the active species in PACl, needs to be hydrolyzed prior to interacting with colloidal particles to be removed by coagulation–flocculation (An et al., 2021).

Among other anions commonly found in natural waters, the effect of sulfate ions on alum coagulation was studied long ago (Miller, 1925). It is known that the pH range of aluminum precipitation and the sweep coagulation of aluminum sulfate extends to more acidic side than those of aluminum chloride, which attributed to the complexing of sulfate with aluminum (Hanna et al., 1970; Matijević and Stryker, 1966). Letterman (2010) reports that sulfate ion of a certain concentration in water is required for coagulation at pH 6, while no sulfate ion is needed at pH 7.5. It is explained that sulfate ion destabilizes positively charged aluminum hydroxide possibly by surface ionization and site-specific, complex formation reactions (Edzwald, 2011). The effect of sulfate ion on aluminum precipitation is also reported elsewhere (Duan et al., 2014). Other researchers report that sulfate ion in raw water increases the rate of floc formation (Snodgrass et al., 1984; Sricharoenchaikit and Letterman, 1987; Xiao et al., 2010). These studies have focused mainly on conventional aluminum coagulants such as alum, but there have been a limited number of studies related to the effect of inorganic anions on PACl coagulation, although it is known that sulfate ion content in PACl besides basicity influence the property and coagulation performance of PACl (Gao and Yue, 2005; Nakazawa et al., 2018; Wang et al., 2002). Chu et al (2008) investigate the effect of sulfate ion on floc formation by PACl and report that floc formation is enhanced at low sulfate concentrations, but is reduced at high sulfate concentrations. However, the conclusions were not clearly confirmed because of very limited experiments. Chen et al. (2020) have examined the role of sulfate ions in removing superfine powdered activated carbon particles from water by coagulation, sedimentation, and sand filtration. They have pointed out that the coagulation performance of high-basicity PACl

is highly dependent on the sulfate concentration in the raw water. However, the relevant mechanism and the effects of PACl types have not been fully studied.

The effect of ions other than sulfate in natural waters on PACl coagulation performance has not been fully investigated. Just as nitrate ions have little effect on coagulation by aluminum nitrate except at high concentrations (Hanna et al., 1970), monovalent ions possibly have no effect on coagulation by PACl at normal concentrations in natural surface waters. It is well known that phosphate forms precipitates with aluminum (Hanna et al., 1970), and therefore the efficiency of removal via aluminum coagulation declines as the phosphate concentration increases (Cheng et al., 2004). However, the concentration of phosphate is rarely high enough in sources of drinking water to influence removal by an aluminum coagulant. The effects of cations have rarely been investigated, but Long et al. (2021) have pointed out that the binding affinity of $Ca^{2+}$ and $Al^{3+}$ facilitates formation of large flocs by PACl.

In summary, although inorganic ions are the main dissolved species in natural waters, their effects on the performances of PACls with different basicity and polymerization degree, have not been systematically investigated. Because the concentrations of inorganic ions in surface waters are highly dependent on the type of soil and rock from which the minerals dissolved and entered a body of water (Nikanorov and Brazhnikova, 2009), they vary greatly worldwide and it is necessary to figure out compatibility between PACl and raw water.

## 1.2 Objectives and structure of this study

According to the background, although coagulant and coagulation process are traditional methods for drinking water treatment, there are still many challenges and issues to be solved. This study focused on the different performance when using PACl coagulants, which resulted

from their different properties, preparation methods, and inorganic ion components in the raw water, during coagulation experiment. This study sets the following objectives:

1) To characterize the $AlCl_3$-titration PACl and $Al(OH)_3$-dissolution PACl with different properties. To find a new PACl property that can reflect their different performance.

2) To investigate the correlation between the new property and coagulation performance, when applying PACl to coagulation process in water with different inorganic ions composition.

3) To quantitively investigate the effects of common inorganic ions in natural water on the new property.

4) To investigate the simultaneous effects of inorganic ions on the new property, in order that the PACl coagulation performance could be estimated by analyzing ion components in water.

This dissertation includes 5 chapters. To achieve the above objectives, different research was conducted and can be briefly summarized as follows:

In Chapter 1, the recent states related to the application of PACl coagulant in drinking water treatment process are mentioned. The remained challenges and issues related to the effects of raw water on PACl coagulation are also listed. The objectives and structure of this study are also introduced.

In Chapter 2, the origin of this study: the different performance of $AlCl_3$-titration PACl and $Al(OH)_3$-dissolution PACl in removing superfine powdered activated carbon (SPAC) particles, is introduced. The comparison among $AlCl_3$-titration PACl and $Al(OH)_3$-dissolution PACl,

normal-basicity and high-basicity PACl is conducted by conventional methods. Finally, we found a new factor: PACl hydrolysis-precipitation rate, which can reflect this difference. I also test the effect of sulfate ion on the PACl hydrolysis-precipitation rate.

In Chapter 3, the investigation of hydrolysis-precipitation rate is furtherly improved and comprehensively discussed. The discussion included the effect of alkalinity, PACl dose, and sulfate ion concentration. The discussion in this chapter strengthened the important role of hydrolysis-precipitation rate as a factor related to the coagulation performance.

In Chapter 4, the effects of ion components and NOM on PACl hydrolysis-precipitation rate are fully investigated by experiment. According to the correlation between PACl hydrolysis-precipitation rate and coagulation performance, the overlooked effects of ion components in raw water on PACl coagulation are revealed. The mechanism of why sulfate ion can strongly facilitate hydrolysis-precipitation rate is discussed. Finally, we quantified the effects of ion components and NOM on PACl hydrolysis-precipitation, therefore the hydrolysis-precipitation rate can be a novel indicator for PACl coagulant performance.

In Chapter 5, the findings and conclusions are summarized.

## 1.3 Reference

An, G., Yue, Y., Wang, P., Liu, L., Demissie, H., Jiao, R., & Wang, D. (2021). Deprotonation and aggregation of Al13 under alkaline titration: A simulating study related to coagulation process. *Water Research*, *203*(June), 117562. https://doi.org/10.1016/j.watres.2021.117562

Bratby, J. (2016). *Coagulation and flocculation in water and wastewater treatment*. IWA publishing.

Chen, Y., Nakazawa, Y., Matsui, Y., Shirasaki, N., & Matsushita, T. (2020). Sulfate ion in raw water affects performance of high-basicity PACl coagulants produced by Al(OH)3 dissolution and base-titration: Removal of SPAC particles by coagulation-flocculation, sedimentation, and sand filtration. *Water Research*, *183*, 116093. https://doi.org/10.1016/j.watres.2020.116093

Cheng, W. P., Chi, F. H., & Yu, R. F. (2004). Effect of phosphate on removal of humic substances by aluminum sulfate coagulant. *Journal of Colloid and Interface Science*, *272*(1), 153–157. https://doi.org/10.1016/j.jcis.2003.08.074

Chu, Y., Gao, B., Yue, Q., & Wang, Y. (2008). Investigation of dynamic processing on aluminum floc aggregation: Cyclic shearing recovery and effect of sulfate ion. *Science in China, Series B: Chemistry*, *51*(4), 386–392. https://doi.org/10.1007/s11426-007-0129-2

Duan, J., Wang, J., Guo, T., & Gregory, J. (2014). Zeta potentials and sizes of aluminum salt precipitates - Effect of anions and organics and implications for coagulation mechanisms. *Journal of Water Process Engineering*, *4*(C), 224–232. https://doi.org/10.1016/j.jwpe.2014.10.008

Edzwald, J., & Association, A. W. W. (2011). *Water quality & treatment: a handbook on drinking water*. McGraw-Hill Education.

Gao, B., & Yue, Q. (2005). Effect of SO42-/Al3+ratio and O-/Al3+value on the characterization of coagulant poly-aluminum-chloride-sulfate (PACS) and its coagulation performance in water treatment. *Chemosphere*, *61*(4), 579–584. https://doi.org/10.1016/j.chemosphere.2005.03.013

Hanna, & Rubin, A. J. (1970). Effect of Sulfate and Other Ions in Coagulation With Aluminum(Iii. *Journal / American Water Works Association*, *62*(5), 315–321. https://doi.org/10.1002/j.1551-8833.1970.tb03912.x

Hendricks, D. W. (2016). *Fundamentals of Water Treatment Unit Processes: Physical, Chemical, and Biological*. CRC Press. https://books.google.co.jp/books?id=9dv1wQEACAAJ

Kan, C., Huang, C., & Pan, J. R. (2002). Time requirement for rapid-mixing in coagulation. *Colloids and Surfaces A: Physicochemical and Engineering Aspects*, *203*(1–3), 1–9. https://doi.org/10.1016/S0927-7757(01)01095-0

Kimura, M., Matsui, Y., Kondo, K., Ishikawa, T. B., Matsushita, T., & Shirasaki, N. (2013). Minimizing residual aluminum concentration in treated water by tailoring properties of polyaluminum coagulants. *Water Research*, *47*(6), 2075–2084. https://doi.org/10.1016/j.watres.2013.01.037

Kimura, M., Matsui, Y., Saito, S., Takahashi, T., Nakagawa, M., Shirasaki, N., & Matsushita, T. (2015). Hydraulically irreversible membrane fouling during coagulation-microfiltration and its control by using high-basicity polyaluminum chloride. *Journal of Membrane Science*, *477*, 115–122. https://doi.org/10.1016/j.memsci.2014.12.033

Kong, Y., Ma, Y., Ding, L., Ma, J., Zhang, H., Chen, Z., & Shen, J. (2021). Coagulation behaviors of aluminum salts towards humic acid: Detailed analysis of aluminum speciation and transformation. *Separation and Purification Technology*, *259*(November 2020), 118137. https://doi.org/10.1016/j.seppur.2020.118137

Letterman, R. D., Tabatabaie, M., & Jr, R. S. A. (1979). The Effect of the Bicarbonate Ion Concentration on Flocculation With Aluminum Sulfate. *Journal (American Water Works Association)*, *71*(8), 467–472. https://doi.org/10.1002/j.1551-8833.1979.tb04395.x

Letterman, R. D., & Yiacoumi, S. (2010). Coagulation and flocculation. In J. K. Edzwald (Ed.), *Water Quality and Treatment A Handbook on Drinking Water* (Sixth Edit, pp. 8.1-8.81). McGrawHill.

Lin, J. L., Chin, C. J. M., Huang, C., Pan, J. R., & Wang, D. (2008). Coagulation behavior of Al13aggregates. *Water Research*, *42*(16), 4281–4290. https://doi.org/10.1016/j.watres.2008.07.028

Lin, J. L., Pan, J. R., & Huang, C. (2013). Enhanced particle destabilization and aggregation by flash-mixing coagulation for drinking water treatment. *Separation and Purification Technology*, *115*(August 2013), 145–151. https://doi.org/10.1016/j.seppur.2013.05.013

Liu, L., Lu, S., Demissie, H., Yue, Y., Jiao, R., An, G., & Wang, D. (2021). Formation of Al30 aggregates and its correlation to the coagulation effect. *Chemosphere*, *278*, 130493. https://doi.org/10.1016/j.chemosphere.2021.130493

Long, Y., Yu, G., Dong, L., Xu, Y., Lin, H., Deng, Y., You, X., Yang, L., & Liao, B. Q. (2021). Synergistic fouling behaviors and mechanisms of calcium ions and polyaluminum chloride associated with alginate solution in coagulation-ultrafiltration (UF) process. *Water Research*, *189*, 116665. https://doi.org/10.1016/j.watres.2020.116665

Matijević, E., & Stryker, L. J. (1966). Coagulation and reversal of charge of lyophobic colloids by hydrolyzed metal ions. III. Aluminum Sulfate. *Journal of Colloid And Interface Science*, *22*(1), 68–77. https://doi.org/10.1016/0021-9797(66)90068-3

Matsui, Y., Yuasa, A., Furuya, Y., & Kamei, T. (1998). Dynamic analysis of coagulation with alum and PACl. *Journal-American Water Works Association*, *90*(10), 96–106.

Miller, L. B. . (1925). A Study of the Effects of Anions upon the Properties of " Alum Floc ". *Public Health Reports*, *40*(8), 351–367.

Nakazawa, Y., Matsui, Y., Hanamura, Y., Shinno, K., Shirasaki, N., & Matsushita, T. (2018). Minimizing residual black particles in sand filtrate when applying super-fine powdered activated carbon: Coagulants and coagulation conditions. *Water Research*, *147*, 311–320. https://doi.org/10.1016/j.watres.2018.10.008

Nikanorov, A. M., & Brazhnikova, L. V. (2009). Water Chemical Composition of Rivers, Lakes and Wetlands. In *Encyclopedia of Life Support Systems (EOLSS)* (Vol. 2). https://www.eolss.net/Sample-Chapters/C07/E2-03-04-02.pdf

Qu, J., & Liu, H. (2004). Optimum conditions for Al13 polymer formation in PACl preparation by electrolysis process. *Chemosphere*, *55*(1), 51–56. https://doi.org/10.1016/j.chemosphere.2003.10.058

Saxena, K., Brighu, U., & Choudhary, A. (2019). Coagulation of humic acid and kaolin at alkaline pH: Complex mechanisms and effect of fluctuating organics and turbidity. *Journal of Water Process Engineering*, *31*(February), 100875. https://doi.org/10.1016/j.jwpe.2019.100875

Snodgrass, W. J., Clark, M. M., & O'Melia, C. R. (1984). Particle formation and growth in dilute aluminum(III) solutions. Characterization of particle size distributions at pH 5.5. *Water Research*, *18*(4), 479–488. https://doi.org/10.1016/0043-1354(84)90157-X

Sricharoenchaikit, P., & Letterman, R. D. (1987). Effect of Al(III) and sulfate ion on flocculation kinetics. *Journal of Environmental Engineering -ASCE*, *113*(5), 1120–1138. https://doi.org/10.1061/(ASCE)0733-9372(1987)113:5(1120)

Tang, H., Xiao, F., & Wang, D. (2015). Speciation, stability, and coagulation mechanisms of hydroxyl aluminum clusters formed by PACl and alum: A critical review. *Advances in Colloid and Interface Science*, *226*, 78–85. https://doi.org/10.1016/j.cis.2015.09.002

Wang, D., Tang, H., & Gregory, J. (2002). Relative importance of charge neutralization and precipitation on coagulation of kaolin with PACI: Effect of sulfate ion. *Environmental Science and Technology*, *36*(8), 1815–1820. https://doi.org/10.1021/es001936a

Wu, X., Ge, X., Wang, D., & Tang, H. (2007). *Distinct coagulation mechanism and model between alum and high Al 13 -PACl*. *305*, 89–96. https://doi.org/10.1016/j.colsurfa.2007.04.046

Xiao, F., Yi, P., Pan, X. R., Zhang, B. J., & Lee, C. (2010). Comparative study of the effects of experimental variables on growth rates of aluminum and iron hydroxide flocs during coagulation and their structural characteristics. *Desalination*, *250*(3), 902–907. https://doi.org/10.1016/j.desal.2008.12.050

Yan, M., Wang, D., Qu, J., He, W., & Chow, C. W. K. (2007). Relative importance of hydrolyzed Al(III) species (Ala, Alb, and Alc) during coagulation with polyaluminum chloride: A case study with the typical micro-polluted source waters. *Journal of Colloid and Interface Science*, *316*(2), 482–489. https://doi.org/10.1016/j.jcis.2007.08.036

Yan, M., Wang, D., Yu, J., Ni, J., Edwards, M., & Qu, J. (2008). Enhanced coagulation with polyaluminum chlorides: Role of pH/Alkalinity and speciation. *Chemosphere*, *71*(9), 1665–1673. https://doi.org/10.1016/j.chemosphere.2008.01.019

# Chapter 2. Comparing PACl coagulants with different properties and preparation methods: role of PACl hydrolysis

## 2.1 Introduction

With the recent development of milling technology, it is possible to produce superfine powdered activated carbon (SPAC) by micro-milling conventionally sized PAC (powdered activated carbon) to a mean diameter of ~1 μm (Matsui et al., 2004; Matsui et al., 2013). The larger adsorption capacity and faster adsorption kinetics of SPAC compared with PAC lead to superior adsorptive removal of organic pollutants from water by SPAC (Ando et al., 2010; Bonvin et al., 2016; Matsui et al., 2012, 2015; Partlan et al., 2016). These advantages of SPAC have led to the expectation that it will be used in water and wastewater treatment (Bonvin et al., 2016). However, there is a concern that the risk of leakage from the treatment process may be higher for SPAC than for conventionally sized PAC. The application of high-basicity (basicity 70%) PACl (polyaluminum chloride) coagulant instead of normal-basicity (basicity 50%) PACl coagulant has been proposed as an effective way to minimize the loss of SPAC particles during the CSF (coagulation-flocculation, sedimentation, and sand filtration) process, but not all types of high-basicity PACls are effective coagulants (Nakazawa et al., 2018b). High-basicity PACls produced by $Al(OH)_3$-dissolution and by $AlCl_3$-titration perform very differently, although they are identical in terms of aluminum species based on the ferron assay (Wang et al., 2002). The reason is not yet clear.

To solve this problem, many characteristics methods were applied to find the difference between PACls produced by $Al(OH)_3$-dissolution method and $AlCl_3$-titration method. The different performances of PACls in removing SPAC particles were explained in this chapter. Because the conventional PACl characterize methods can not reflect the different performance

of $Al(OH)_3$-dissolution PACl and $AlCl_3$-titration PACl, the more important objective is to find or establish a factor or method which can reflect this difference.

The contents introduced in this chapter have been published by Elsevier, and the information is described as follows:

Title: Sulfate ion in raw water affects performance of high-basicity PACl coagulants produced by $Al(OH)_3$ dissolution and $AlCl_3$-titration: removal of SPAC particles by coagulation-flocculation, sedimentation, and sand filtration

Author: Yize Chen, Yoshifumi Nakazawa, Yoshihiko Matsui, Nobutaka Shirasaki, Taku Matsushita

Name of journal: Water Research

Year: 2020

Volume: 183

Pages: 116093

DOI: https://doi.org/10.1016/j.watres.2020.116093

## 2.2 Materials and methods

### 2.2.1 PACl coagulants preparation

Three kinds of PACls were used in this study. Among them, HB-PACl ("HB" represents "high-basicity", basicity 70%) and NB-PACl ("NB" represents "normal-basicity", basicity 50%) are commercially available PACls and were provided by Taki Chemical Co., Ltd. (Hyogo. Japan), which produced them by dissolving $Al(OH)_3$ in HCl and $H_2SO_4$ [as described in Sato and Matsuda (2009)]. Briefly, a mixture of $AlCl_3$, $Al_2(SO_4)_3$, and $Al(OH)_3$ was heated to obtain a solution with basicity of 50% ($Al(OH)_3$-dissolution method). The basicity was then raised to 70% at <85 °C by adding a solution of sodium carbonate (Fig. 2-1). The basicity was calculated by the following formula:

$$Basicity\ (\%) = \frac{[OH^-]}{3[Al_t]} \times 100$$

where $[Al_t]$ is the total aluminum concentration, and $[OH^-]$ is the concentration of hydroxyl groups from the ingredients $Al(OH)_3$ and sodium carbonate.

The third kind of PACl used, HB-PACl-t ("t" represents "titration"), was produced in the authors' laboratory by titrating a NaOH solution into an $AlCl_3$ solution. The procedure, which is called the $AlCl_3$-titration method, consists of the following steps. A NaOH solution (1 mol/L; Kanto Chemical Co., Inc., Tokyo, Japan) is diluted with ultrapure water (Milli-Q water) produced by an ultrapure lab water system (Milli-Q Advantage; Merck KGaA, Darmstadt, Germany) to a concentration of 0.26 mol/L. Then, $AlCl_3 \cdot 6H_2O$ and $Al_2(SO_4)_3 \cdot 16H_2O$ (FUJIFILM Wako Pure Chemical Corporation) are dissolved to obtain 80 mL of a 0.5-M Al solution. A pump and tubes are prepared for titrating the NaOH solution with the Al solution. After the NaOH solution and Al solution are heated to 50–60 °C and 85–90 °C, respectively,

the titration is started. The flow rate of the NaOH solution is set at 4 mL/min to avoid the appearance of a precipitate during the titration. After the titration is finished, the resultant solution is preserved in a refrigerator at 4 °C for one night and then heated at 90–95 °C for 3 hours (Fig. 2-2). After the temperature has returned to room temperature, the solution is preserved at 4 °C until the time of the experiment. Table 2-1 lists the basic properties of the PACl coagulants. During the experiment, PACls from the stock were first diluted to 0.1 mol-Al/L using Milli-Q water. The dosage of PACl coagulant was 2.5 mg-Al/L in this chapter unless otherwise noted.

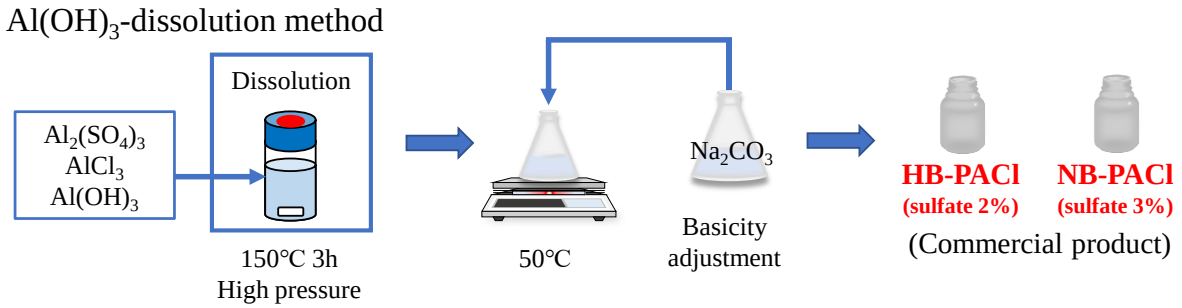


Fig. 2-1. Preparation method for $Al(OH)_3$-dissolution PACls.

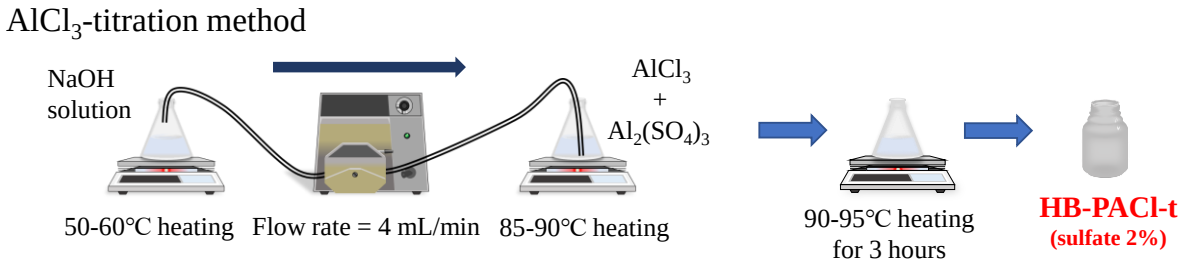


Fig. 2-2. Preparation method for $AlCl_3$-titration PACls. This method was introduced in Nakazawa et al. (2018b).

Table 2-1.
Properties of PACl coagulants used in this study.

| | HB-PACl-t | HB-PACl | NB-PACl |
|---|---|---|---|
| Al content (mol/L) | 0.1 | 2.5 | 2.5 |
| $SO_4^{2-}$/Al (mole ratio) | 0.11 | 0.11 | 0.14 |
| $Na^+$/Al (mole ratio) | 2.18 | 0.27 | 0.00 |
| $Cl^-$/Al (mole ratio) | 3.86 | 1.04 | 1.25 |
| Basicity (%) | 70 | 70 | 50 |

### 2.2.2 Superfine powdered activated carbon (SPAC)

A commercially available wood-based PAC (Taiko W) was obtained from Futamura Chemical Co., Ltd. (Nagoya, Japan) and was milled with a bead mill (LMZ015; Ashizawa Finetech, Ltd., Chiba, Japan) to produce a SPAC. The details of the procedure are described elsewhere (Pan et al., 2017).

### 2.2.3 PACl coagulants characterization by conventional methods

The ferron assay was conducted with the 3 PACls. Immediately after being diluted with Milli-Q water to a concentration of 0.1 mol-Al/L, the PACls were added to the ferron reagent (8-hydroxy-7-indo-5-quinoline sulfonic acid; FUJIFILM Wako Pure Chemical Corporation) to initiate the reaction. The absorbance at 366 nm was then measured using an ultraviolet light meter (UV-1800; Shimadzu, Kyoto, Japan). Dilution of the PACls was acceptable because dilution has little effect on the distribution of ferron (Kimura et al., 2013; Wang et al., 2002). The aluminum species in the PACl were divided based on their reaction time with the ferron reagent into Ala (monomeric species, within 30 s), Alb (polymeric species, from 30 s to 120 min), and Alc (colloidal species, did not react within 120 min) (Wang et al., 2004; Yan et al., 2007).

The colloid charges of the PACls were measured via colloid titration. A PACl was diluted with Milli-Q water into 0.1 mol-Al/L and was titrated with a potassium polyvinyl sulfate titration solution (N/400, for colloidal titration; FUJIFILM Wako Pure Chemical Corporation) using an automatic titrator (COM-555; Hiranuma Sangyo Co., Inc., Ibaraki, Japan) (Matsui et al., 2017).

For the ESI-MS analyses, PACls were diluted to a concentration of 0.1 mol-Al/L and introduced into an Orbitrap LC-MS system (Exactive; Thermo scientific, Bremen, Germany) under the following conditions: scan range *m*/*z* 200–2000; spray voltage 3.0 kV; capillary temperature 300 °C; capillary voltage 32.5 V; heater temperature 250 °C. Peaks and the possible formulas of aluminum species were calculated by Xcalibur 2.2 (Thermo Fisher Scientific).

$^{27}$Al-NMR analysis was conducted with a JNM-ECA Series FT NMR (ECA 600; JEOL Ltd., Tokyo, Japan). $NaAl(OH)_4$ (FUJIFILM Wako Pure Chemical Corporation) solution (0.01 mol-Al/L) was used as the internal standard. $AlCl_3$ (FUJIFILM Wako Pure Chemical Corporation) solution (0.1 mol-Al/L) was used as the reference material. Parameters for the measurement were as follows: field strength, 14.09 T; frequency, 78247 Hz; resonance frequency, 156.39 MHz; number of scans, 8000; temperature 70 °C. The data and peaks were processed with the data-processing software provided with Nakamura (2009).

The molecular weight (MW) distributions of aluminum species were measured by using membrane filters with nominal MW cutoffs of 1 and 10 kDa (regenerated cellulose membrane, Ultracel PL; Merck KGaA, Darmstadt, Germany). The membrane filters were set in 50-mL stirred cells (Amicon 8050 series; Merck KGaA, Darmstadt, Germany). Coagulants with concentrations higher than 0.1 mol-Al/L were diluted to 0.1 mol-Al/L using Milli-Q water in the stirred cell. The filtration was then started by applying 0.5-MPa pressure at 30 s after dilution. The filtration continued until 2 mL of filtrate had been collected from the 50-mL

sample. The aluminum concentrations in the filtrates were measured with an inductively coupled plasma mass spectrometer (ICPMS, 7700x; Agilent Technologies, Inc., Santa Clara, CA, USA).

### 2.2.4 Water

Three kinds of water (C, E, and J series) were prepared and used (Table 2-2). Water of the C series was prepared from natural water (designated as C-0) that was sampled from the Chibaberi River (Rumoi City, Hokkaido, Japan). Water C-0 was diluted with pure water (Elix water, Elix Advantage; Merck KGaA, Darmstadt, Germany), and its ion concentrations were adjusted by adding $NaHCO_3$ or $Na_2SO_4$ to prepare Waters C-1 and C-2. Waters of the E series (E-1–7) were ionic waters prepared by adding $MgSO_4$, $CaCl_2$, $HNO_3$, KOH, $Na_2SO_4$, and $NaHCO_3$ (FUJIFILM Wako Pure Chemical Corporation) to Elix water. There were two waters in the J series: water sampled from the Joganji River (Toyama, Japan) and the same water adjusted by addition of $Na_2SO_4$. Alkalinity, which might affect the coagulation, was adjusted at each constant for C-2–3, E-1–7, and J-1–2 waters. These waters were stored at 4 °C. The waters were ready for a PACl hydrolysis-precipitation test after their temperatures had returned to room temperature (~20 °C). The waters were ready for CSF experiments after their temperatures had returned to room temperature and SPAC (the target for removal) had been added at a concentration of 2 mg/L. Concentrations of ions in the water were measured by ion chromatography (ICS-1000 and ICS-1100; Thermo Scientific, Bremen, Germany). The alkalinity was measured by titrating the water with 0.01 M $H_2SO_4$. For the measurement of dissolved organic carbon (DOC), the water sample was filtered through a membrane filter (0.45-μm pore size; Toyo Roshi Kaisha, Ltd., Tokyo, Japan), and the DOC was then measured with a TOC analyzer (TOC900; GE Analytical Instruments, Inc., Boulder, CO, USA).

Table 2-2.

Ion components, alkalinity, and DOC of waters used in this study.

| Series | Water | $Na^+$ | $K^+$ | $Mg^{2+}$ | $Ca^{2+}$ | $Cl^-$ | $NO_3^-$ | $SO_4^{2-}$ | Alkalinity | DOC | Source |
|---|---|---|---|---|---|---|---|---|---|---|---|
| | | mg/L | mg/L | mg/L | mg/L | mg/L | mg/L | mg/L | mg-$CaCO_3$/L | mg/L | |
| C Series | C-0 | 13.8 | 1.7 | 4.5 | 5.8 | 11.9 | 0.3 | 18.8 | 27 | 2.4 | Chibaberi River |
| | C-1 | 33.0 | 1.7 | 4.3 | 5.7 | 14.4 | 0.0 | 15.9 | 50 | 0.9 | |
| | C-2 | 28.3 | 1.7 | 4.5 | 5.7 | 21.6 | 0.0 | 6.4 | 50 | NM | |
| E Series | E-1 | 24.2 | 0.6 | 0.0 | 12.5 | 22.5 | 0.9 | 0.0 | 50 | NM | Elix water |
| | E-2 | 24.1 | 0.5 | 0.6 | 12.3 | 22.1 | 0.9 | 3.5 | 50 | NM | |
| | E-3 | 24.0 | 0.6 | 1.3 | 12.5 | 22.3 | 1.0 | 6.4 | 50 | NM | |
| | E-4 | 25.3 | 0.5 | 3.9 | 12.5 | 25.7 | 1.1 | 15.8 | 50 | NM | |
| | E-5 | 30.5 | 0.6 | 0.0 | 12.5 | 22.1 | 0.9 | 15.7 | 50 | NM | |
| | E-6 | 20.5 | 0.5 | 6.1 | 12.3 | 25.3 | 1.0 | 28.2 | 50 | NM | |
| | E-7 | 21.0 | 0.5 | 10.2 | 12.3 | 25.7 | 1.0 | 48.8 | 50 | NM | |
| J Series | J-1 | 1.9 | 0.4 | 0.9 | 6.6 | 1.7 | 0.6 | 4.0 | 16 | 0.5 | Joganji River |
| | J-2 | 8.0 | 0.4 | 0.9 | 6.6 | 1.7 | 0.6 | 15.3 | 16 | 0.5 | |

(NM: Not measured, DOC: dissolved organic carbon)

### 2.2.5 Coagulation-flocculation, sedimentation, and sand filtration experiments

CSF experiments were used to evaluate the coagulation performances of the PACls. Four liters of raw water were placed in a rectangular plastic beaker. A predetermined volume of HCl or NaOH (0.1N) was added to the water to adjust the coagulation pH to 7.0. After 30 min of mixing, PACl was added. Rapid mixing conducted at a G value of 600 $s^{-1}$ for 40 s was followed by three stages of slow mixing at G values (in chronological order) of 50 $s^{-1}$ for 170 s, 20 $s^{-1}$ for 170 s, and 10 $s^{-1}$ for 320 s, respectively (Table 2-3). The total GT value for the rapid and slow mixing was 39,100. After mixing, the water was allowed to stand for 1 hour for sedimentation. The supernatant was then transferred at a constant rate to the sand-filtration column for sand filtration. Sand filtration was conducted at a rate of 90-m/d with a 50-cm–deep column containing sand (effective diameter, 0.6 mm; uniformity, 1.3). Filtrate was collected from 13 to 40 min after the start of filtration. After the filtration was finished, the sand filter was backwashed with tap water and then forward washed with Milli-Q water (Fig. 2-3).

Table 2-3.
Mixing condition for coagulation-flocculation, sedimentation, and sand filtration experiment

| Rapid mixing | | Slow mixing 1 | | Slow mixing 2 | | Slow mixing 3 | | Total |
|---|---|---|---|---|---|---|---|---|
| G ($s^{-1}$) | T (s) | G ($s^{-1}$) | T (s) | G ($s^{-1}$) | T (s) | G ($s^{-1}$) | T (s) | GT |
| 600 | 40 | 50 | 170 | 20 | 170 | 10 | 320 | 39100 |

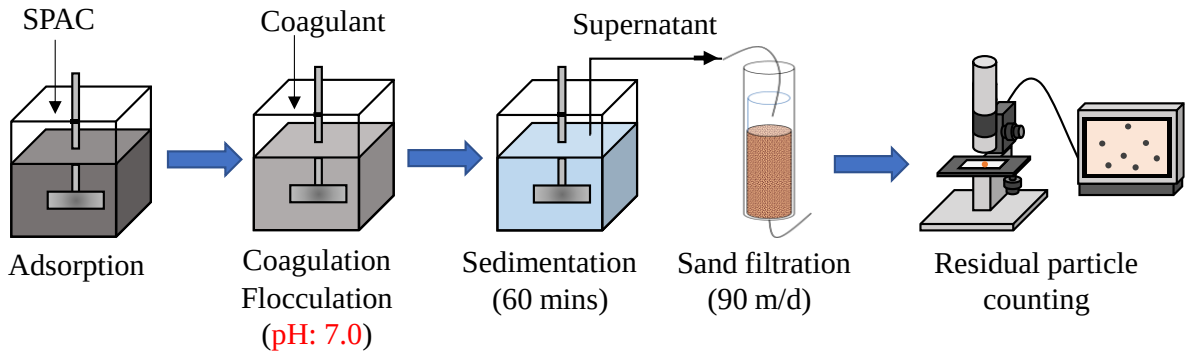


Fig. 2-3. The flow of coagulation-flocculation, sedimentation, and sand-filtration experiment.

### 2.2.6 Zeta potential measurement and floc size analysis by photography

The Zeta potentials of the water before coagulation, the water after rapid mixing, and the supernatant were measured with a Zeta potential meter (Zetasizer Nano ZS; Malvern Panalytical Ltd., Almelo, Netherlands) using a dip cell. The turbidity of the water before coagulation, the supernatant, and the sand filtrate were measured with a turbidity meter (2100Q portable turbidimeter; Hach Company, Loveland, CO, USA). Formation of floc particles was evaluated based on pictures of the beaker taken with a DSLR (digital single lens reflex) camera (EOS 60D; Canon Ltd., Tokyo, Japan) at the end of rapid mixing and during slow mixing. For a correct exposure and sharp image, the parameters for photography were set as follows: ISO 3200, aperture F9.0, shutter speed 1/250 s, with flash.

### 2.2.7 Membrane filtration and microscopic image analysis

The carbon particles that remained in the sand filtrate were enumerated via membrane filtration and image analysis. The details of this method have been described by Nakazawa et al. (2018b) but can be briefly described as follows. Sample water was filtered through a membrane filter (pore size 0.1 μm, PTFE, Φ25 mm; Merck KGaA), and then the filter was allowed to dry under natural conditions. Photographs of the filter were taken with a microscope (VHX-2000; Keyence corporation, Osaka, Japan) at 1000× magnification, and the SPAC particles on the photographs were counted with the software built into the microscope. (Fig. 2-4 and Fig. 2-5).

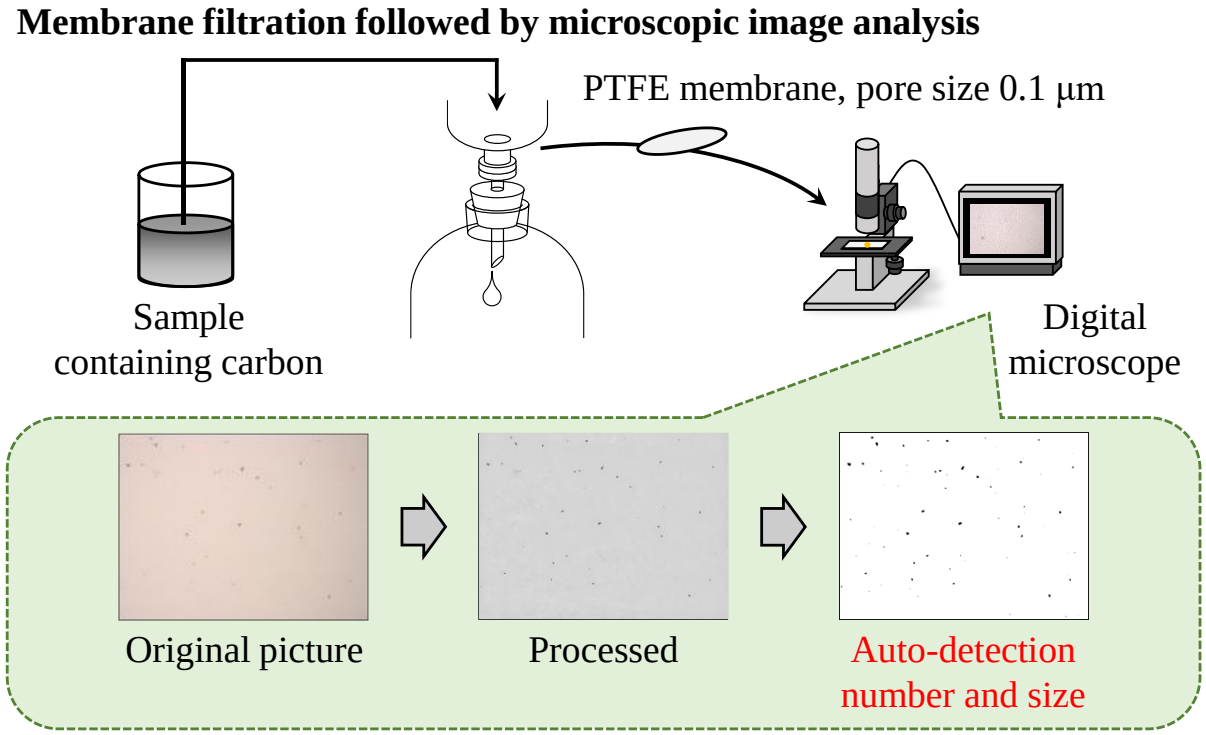


Fig. 2-4. The flow of membrane filtration and microscope image analysis. The detail of this flow is described in Nakazawa et al. (2018a).

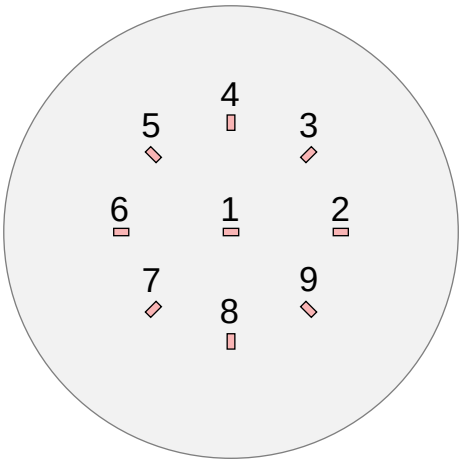


Fig. 2-5. The position of observation zones on a membrane filter. The observation was conducted with 9 zones.

### 2.2.8 Hydrolysis-precipitation rate test

The following procedure was used to determine the rate of hydrolysis-precipitation of the aluminum species in PACl. E-series water was placed in a 1-L rectangular plastic beaker. HCl or NaOH (0.1N) was added to bring the final pH to 7.0, and then PACl was added so that the

concentration of aluminum was 2.5 mg/L. The solution was mixed at a G value (velocity gradient) of 600 $s^{-1}$ for 40 s and then at a G value of 50 $s^{-1}$ for 80 s. Ten-milliliter samples of water were taken at times of 15 s, 30 s, 60 s, and 120 s after the PACl injection. A portion of the sample was immediately filtered through a polytetrafluoroethylene (PTFE) membrane (Φ47 mm; Merck KGaA, Darmstadt, Germany) with a pore size of 0.1, 1, or 10 mm. The total process of hydrolysis-precipitation rate test was shown in Fig. 2-6, and the mixing condition was shown in Table 2-4. A PTFE membrane was used in this experiment because PTFE membranes have been reported to have the lowest tendency to adsorb aluminum (Matsui et al., 2013). The Al concentration in the filtrate was measured by ICPMS.

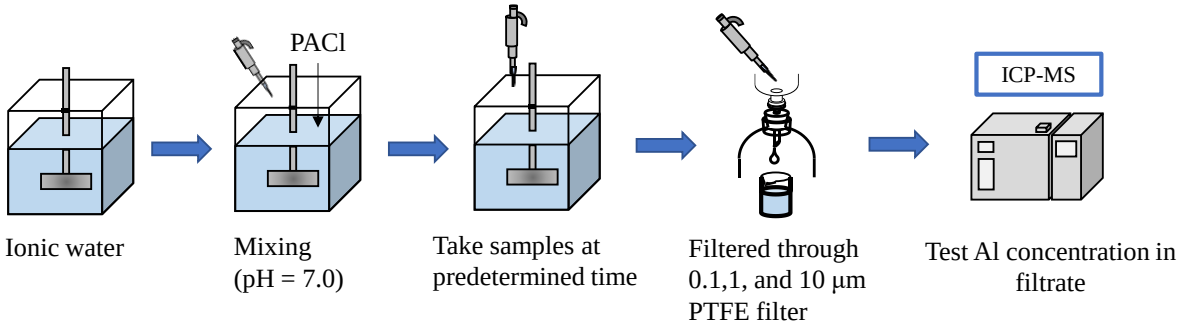


Fig. 2-6. The flow of hydrolysis-precipitation rate test.

Table 2-4.

The mixing condition of hydrolysis-precipitation rate test.

| Rapid mixing | | Slow mixing | |
|---|---|---|---|
| G ($s^{-1}$) | T (s) | G ($s^{-1}$) | T (s) |
| 600 | 40 | 50 | 80 |

## 2.3 Results and discussion

### 2.3.1 Characteristics of PACl coagulants

As shown in Fig. 2-7 (Panel A), the ferron distributions of HB-PACl-t and HB-PACl were almost the same: Alc species accounted for more than 65% of total aluminum, Alb for ~15%, and Ala for ~20%. Among the three PACls, the percentage of Ala was highest (40%) in NB-PACl. The similarity of the charge neutralization abilities of HB-PACl-t and HB-PACl (Fig. 2-7 (Panel B)) reflected the similarities of their ferron distributions. The fact that the charge neutralization ability was smaller for NB-PACl than for HB-PACl-t and HB-PACl reflected the lower percentage in NB-PACl of Alc + Alb (aluminum colloid and polymer), which are generally regarded as the aluminum species with high charge neutralization capacity (Yan et al., 2008).

Marked differences between the three PACls were observed in the MW distributions determined by membrane filtration (Panel C of Fig. 2-7). HB-PACl-t contained a relatively large amount of polymerized aluminum species with MWs ranging from 1 to 10 kDa compared with HB-PACl. NB-PACl contained a relatively large amount of aluminum species with low MWs (<1 kDa), which should include Al monomers. Differences were also observed in the ESI-MS spectrum of the three PACls (Fig. 2-8), although the formulas of the aluminum species could not be identified.

The $^{27}$Al-NMR analysis spectra are shown in Fig. 2-7 (Panel D). The peak at $\delta$ = 0 ppm, which is the indication of an Al monomer, was observed for all three PACls, but the fact that it was relatively high in the NB-PACl spectrum compared with the other spectra was consistent with the ferron assay results. A peak at $\delta$ = 62.5 ppm is assigned to tetrahedrally coordinated Al in the Keggin $Al_{13}$ structure ($Al(O)_4$) and is related to the presence of an e-$Al_{13}$ polycation (Allouche et al., 2002; Sposito, 1995). This peak was found in all three PACl coagulants and was relatively intense in HB-PACl. The Keggin-type e-$Al_{13}$ polycation is considered to be equivalent to Alb (Chen et al., 2007; Parker & Bertsch, 1992; Sposito, 1995), but this

equivalence was not supported by the data of the present study: the percentages of Alb were similar in HB-PACl and HB-PACl-t and relatively small in NB-PACl. The broad resonance observed at δ = 10–12 ppm in HB-PACl-t and HB-PACl (but not in NB-PACl) was assigned to octahedral aluminum sites [$Al(O)_6$] in oligomers (Casey, 2006; Tang et al., 2015). The larger area and higher intensity of the resonance at δ = 10–12 ppm in HB-PACl-t versus HB-PACl meant that the amount of $Al(O)_6$ oligomer was higher in HB-PACl-t than in HB-PACl. The broad resonance at δ = ~70 ppm, which is an indication of a Keggin-type δ-$Al_{30}$ polycation, was not observed. HB-PACl-t and HB-PACl therefore differed with respect to their aluminum species, although the ferron analysis could not distinguish this difference. Finally, the three PACls were different.

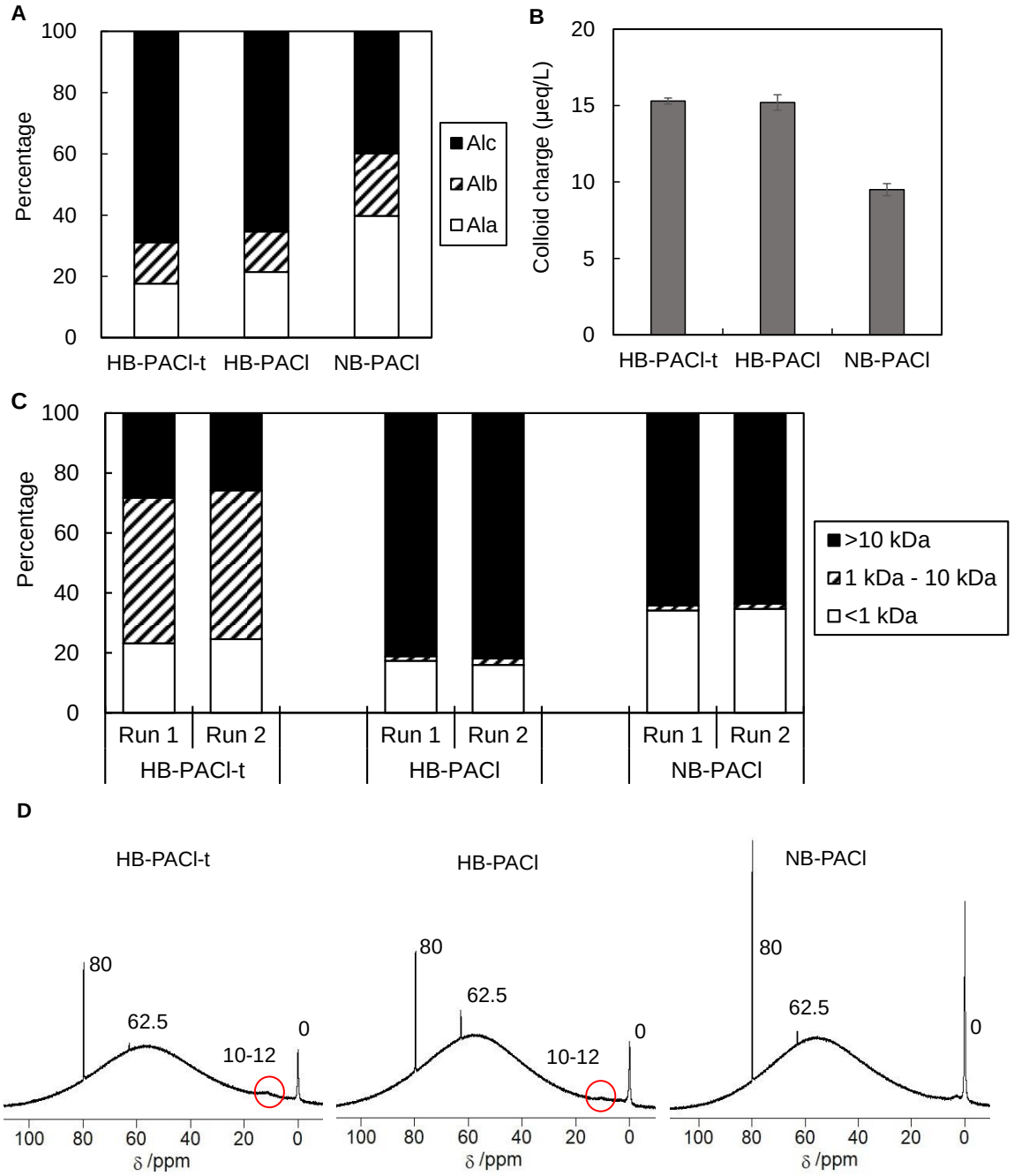


Fig. 2-7. Characteristics of HB-PACl-t, HB-PACl, and NB-PACl. Panel A: ferron distributions. Panel B: colloid charges. Panel C: molecular weight distribution of aluminum species (This experiment was conducted twice at the same condition. Panel D: of $^{27}$Al-NMR spectra (The peaks at δ = 80 ppm are due to the internal standard, $NaAl(OH)_4$. The red circles indicate broad peaks at δ = 10-12 ppm).

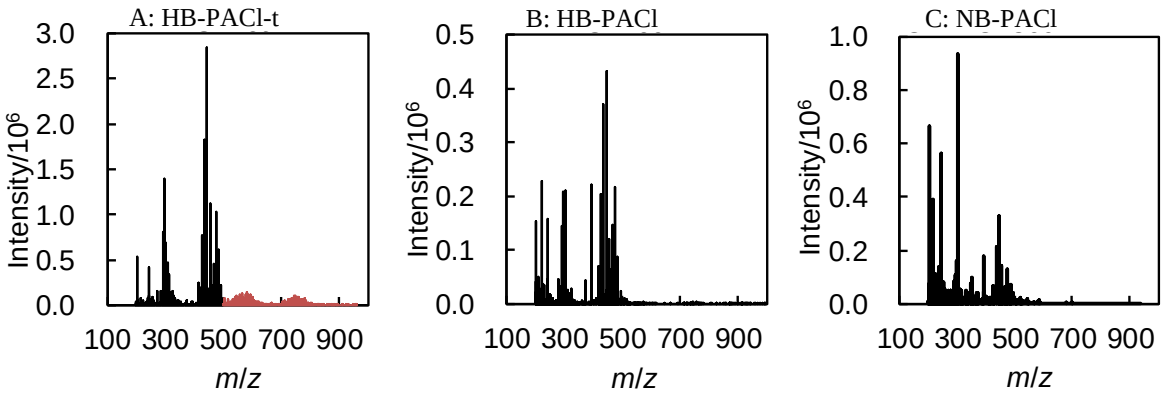


Fig. 2-8. ESI-MS spectra of HB-PACl-t, HB-PACl, and NB-PACl.

### 2.3.2 Comparison of PACls in CSF experiments

The turbidity and residual SPAC particles during the CSF experiments are shown in Fig. 2-9 (Panels A and B) and Fig. 2-10 for Waters C-1 and E-4, respectively. Turbidities in the supernatant after sedimentation were very low when either HB-PACl or NB-PACl was used to treat the water, and the turbidities in the sand filtrate after the rapid filtration process reached an even lower level (Fig. 2-10). In contrast, use of HB-PACl-t resulted in a relatively high residual turbidity in the supernatant for Water C-1 (Panel A of Fig. 2-9) and so little turbidity removal after sedimentation for Water E-4 (Figs. 2-10) that we could not conduct a sand-filtration experiment. Photographs taken during the coagulation flocculation process are shown in Fig. 2-9 (Panel C) and Fig. 2-11. At the end of slow mixing, the floc size was very small when HB-PACl-t was used. In contrast, relatively large floc particles were observed for both NB-PACl and HB-PACl. Although the rate of floc formation seemed higher for NB-PACl because of the greater number of micro-floc particles that were clearly observed at the end of rapid mixing, the residual SPAC particles in the sand filtrate when NB-PACl was used was at the same level or higher versus HB-PACl (Fig. 2-9 Panel B, Fig. 2-10). Although NB-PACl was superior in terms of floc formation, this superiority did not lead to lower numbers of residual SPAC particles in the sand filtrate because of the low charge-neutralization ability of the NB-PACl, which was apparent from the results of the ferron assay and colloid charge (Panels A and

B of Fig. 2-1). Nakazawa et al. (2018a and 2018b) have revealed that particles with un-neutralized charge leak through CSF processes, and high-basicity PACls have a high charge-neutralizing capacity.

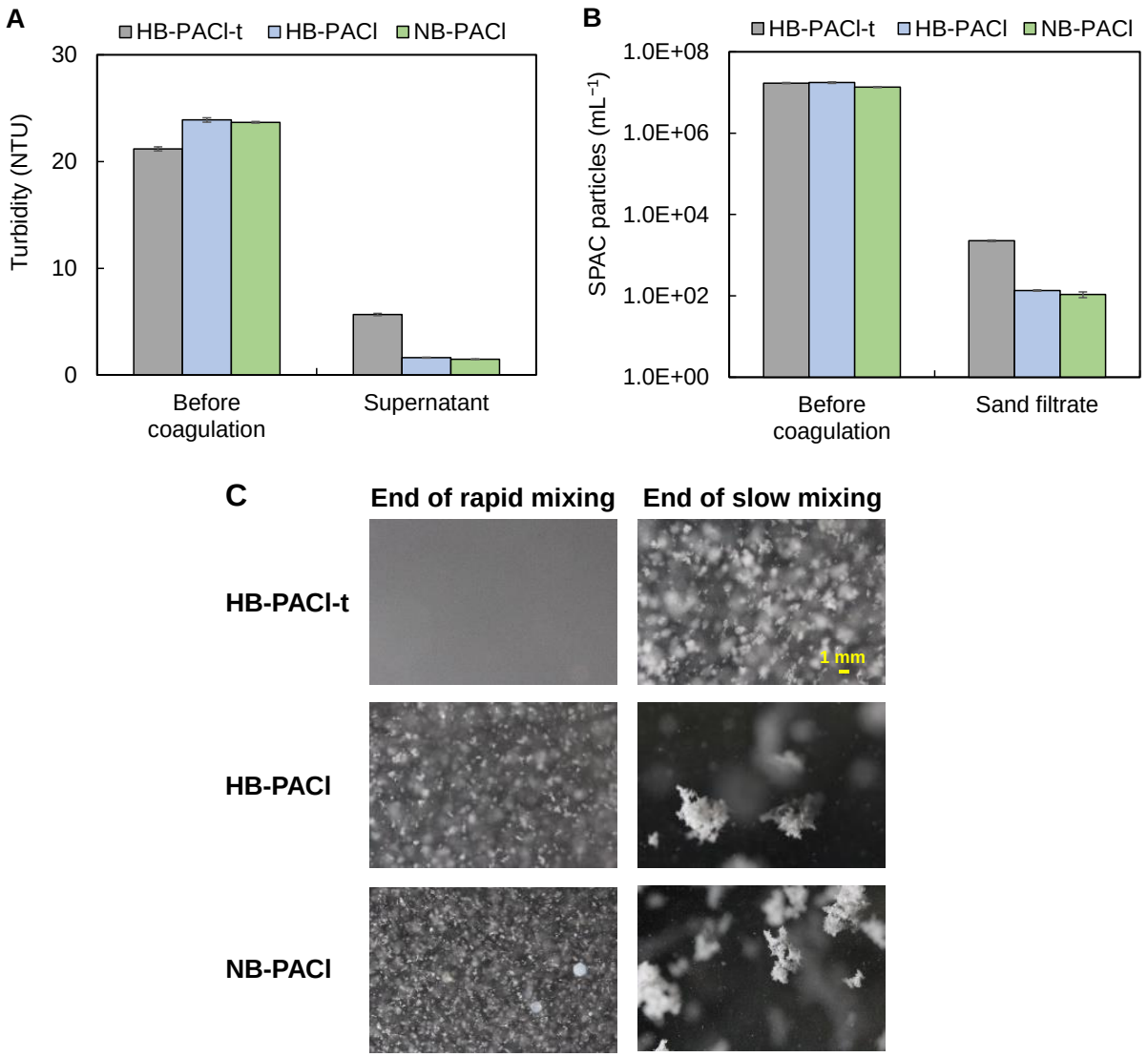


Fig. 2-9. Turbidity in supernatant (Panel A), residual SPAC particles in sand filtrate (Panel B), and photographs taken at the ends of rapid mixing and slow mixing (Panel C). Water C-1 was used. Initial SPAC concentration was 2 mg/L. HB-PACl-t, HB-PACl, and NB-PACl were used at a dosage of 2.5 mg-Al/L. Coagulation pH was 7.0. Turbidities of sand filtrates were also measured, but they were very low: <0.1 NTU.

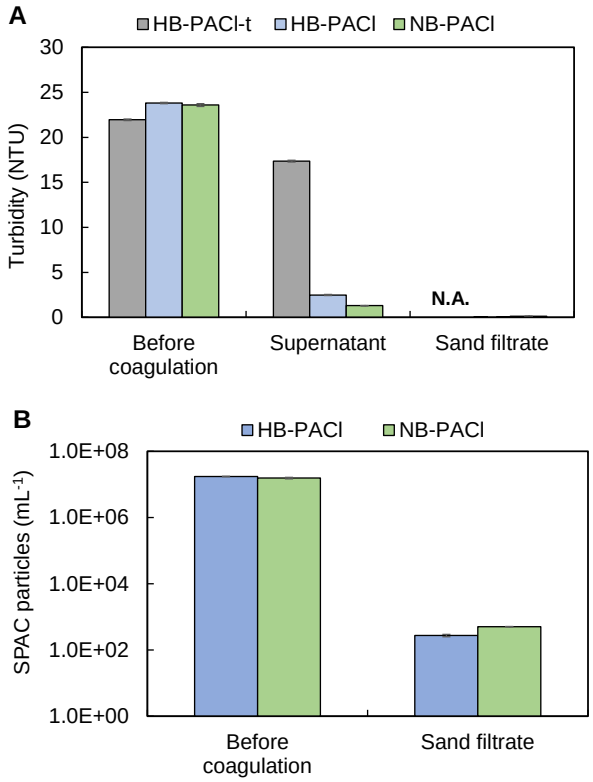


Fig. 2-10. Turbidity in supernatant and sand filtrate (Panel A) and residual SPAC particles in sand filtrate (Panel B). Water E-4 was used. Initial SPAC concentration was 2 mg/L. HB-PACl-t, HB-PACl, and NB-PACl were used with the dosage of 2.5 mg-Al/L. Coagulation pH was 7.0. The sand filtration was not conducted for HB-PACl-t, so the turbidity in sand filtrate of HB-PACl-t was not available (N.A.).

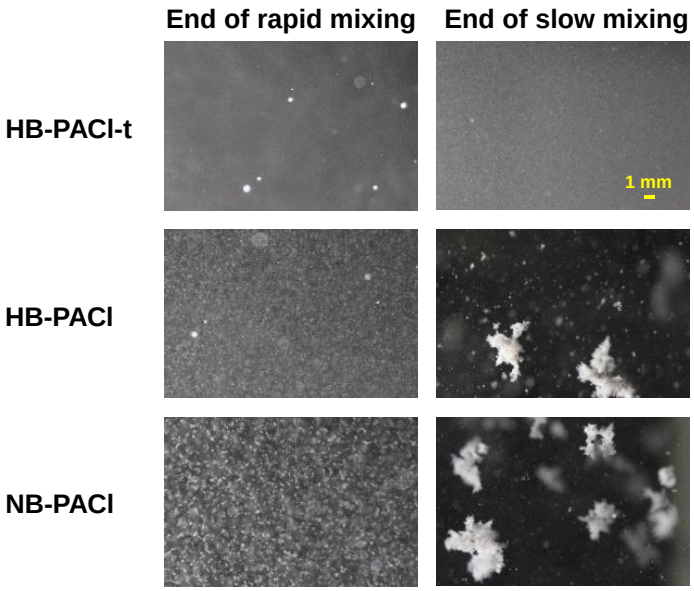


Fig. 2-11. Photographs taken at the end of rapid mixing and slow mixing. Water E-4 was used. Initial SPAC concentration was 2 mg/L. HB-PACl-t, HB-PACl, and NB-PACl were used at a dosage of 2.5 mg-Al/L. Coagulation pH was 7.0.

The performance of HB-PACl and HB-PACl-t differed to a great extent, although they had nearly the same ferron distribution and colloid charge. The zeta potentials during coagulation using HB-PACl and HB-PACl-t are shown in Fig. 2-12. The higher charge neutralization ability of HB-PACl-t versus HB-PACl has also been reported by Nakazawa et al. (2018a). The fact that the zeta potential of particles became close to zero after coagulation by HB-PACl-t meant that charge neutralization progressed well. However, floc formation was much slower with HB-PACl-t than with HB-PACl. The reason might be the difference in the aluminum species in the PACls, a difference that was seen in the MW distributions and ESI-MS and that was faintly apparent in the $^{27}$Al-NMR spectra. The difference, however, was not reflected in the ferron species distribution (Ala, Alb, and Alc) and colloid charge (see Section 2.3.1). Feng et al. (2007) have differentiated Alb (polymeric aluminum species) into two fractions: the faster-reacting polymers and the slower-reacting polymers. However, the main aluminum species in HB-PACl and HB-PACl-t was Alc (colloid aluminum species), not Alb. The large difference in coagulation performance between HB-PACl and HB-PACl-t may therefore not be attributable to the difference in the polymeric aluminum species (Alb). The colloid aluminum species (Alc) may include a variety of species with very different reaction rates. Such species differences were observed in the MW distributions and ESI-MS.

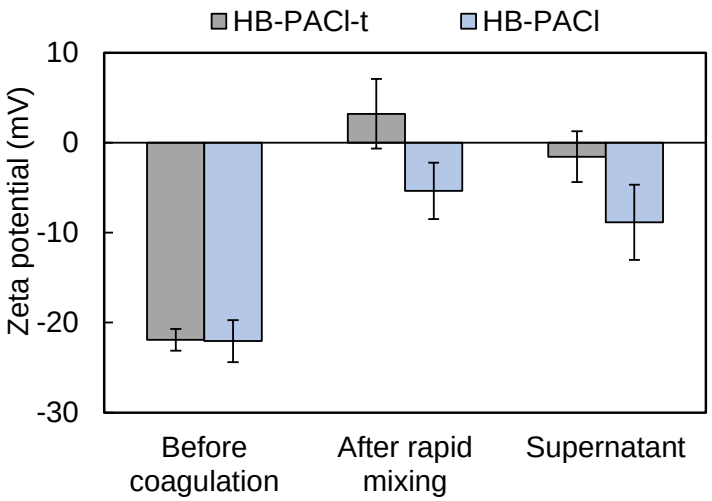


Fig. 2-12. Change of zeta potential during CSF experiment. Water C-1 was used. Initial SPAC concentration was 2 mg/L. HB-PACl-t and HB-PACl were used at a dosage of 2.5 mg-Al/L. Coagulation pH was 7.0.

### 2.3.3 Hydrolysis-precipitation analysis of PACls

Aluminum coagulants, including PACls, are hydrolyzing aluminum salt coagulants. The aluminum species in PACl react with alkalinity after it is dosed to water, and the unstable aluminum hydroxide that is finally formed plays an important role in sweep coagulation (Letterman & Yiacoumi, 2010). In this study, we evaluated the speed of aluminum hydrolysis-precipitation by measuring the concentrations of aluminum after filtration through membranes of different pore sizes (0.1, 1, and 10 μm, Fig. 2-13). The rapid hydrolysis-precipitation of HB-PACl and NB-PACl resulted in the most large (>10 μm) Al particles within 15 s after the PACl was injected into the water. The HB-PACl-t hydrolyzed at a much slower rate: more than half of the Al particles were still <10 μm in size 60 s after injection. The very different rates of hydrolysis-precipitation of HB-PACl-t and HB-PACl may have reflected differences in the aluminum species that were observed in the MW distributions and ESI-MS. The difference of coagulation performance could not be explained solely on the basis of charge neutralization ability. Hydrolysis, which can be evaluated with a hydrolysis-precipitation test, also plays an important role in coagulation performance.

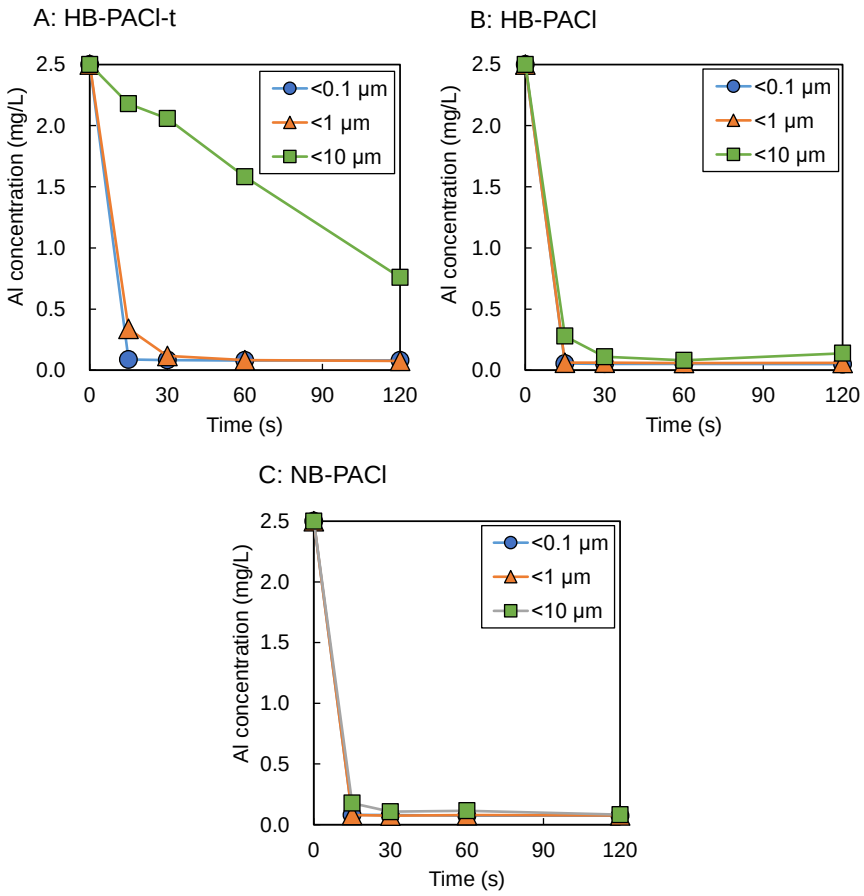


Fig. 2-13. Rate of hydrolysis-precipitation of HB-PACl-t (Panel A), HB-PACl (Panel B), and NB-PACl (Panel C). Water E-4 was used. HB-PACl-t, HB-PACl, and NB-PACl were used at a dosage of 2.5 mg-Al/L. Coagulation pH was 7.0.

### 2.3.4 Effect of sulfate ion on CSF performance

The sulfate ion in PACl is known to change the characteristics of the PACl (Nakazawa et al., 2018b). However, HB-PACl-t and HB-PACl had the same sulfate ion content, and therefore the sulfate ions in the PACls could not have caused a large difference in their coagulation performance. We then focused on the sulfate ions in the raw water. The effect of the sulfate ions was first investigated by using adjusted natural waters (C-1 and C-2) with different sulfate concentrations. There was no obvious difference in turbidity and removal of SPAC particles between sulfate concentrations of 15.9 mg/L and 6.4 mg/L (Fig. 2-14). However, the slower rate of formation of floc at 6.4 mg/L than at 15.9 mg/L (Fig. 2-15) suggested that there was a sulfate effect.

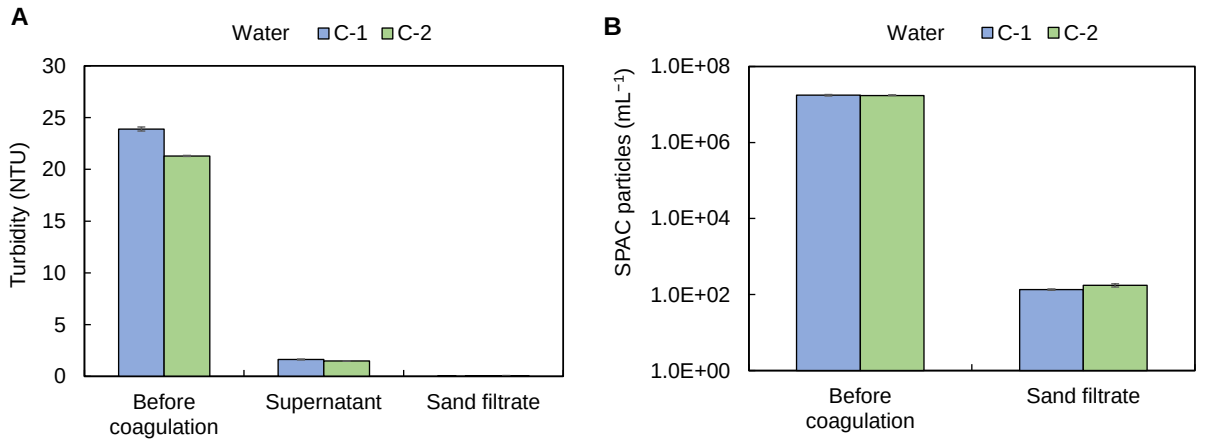


Fig. 2-14. Changes of turbidity (Panel A) and SPAC-particle number concentration (Panel B) during CSF. Waters C-1 (sulfate ion concentration 15.9 mg/L) and C-2 (sulfate ion concentration 6.4 mg/L) were used. Initial SPAC concentration was 2 mg/L. HB-PACl was used at a dosage of 2.5 mg-Al/L. Coagulation pH was 7.0.

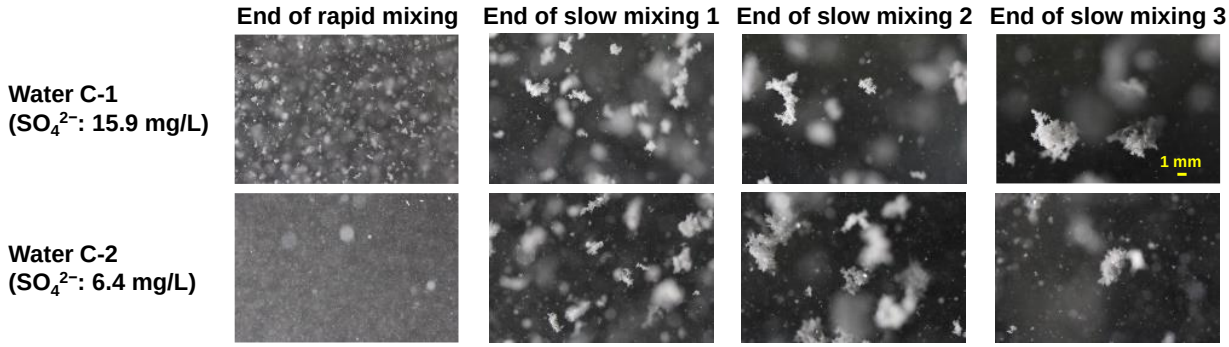


Fig. 2-15. Photographs taken at the end of rapid mixing and each slow mixing stage. Waters C-1 (upper pictures) and C-2 (lower pictures), including sulfate ion concentrations of 15.9 and 6.4 mg/L, respectively, were used. Initial SPAC concentration was 2 mg/L. HB-PACl was used at a dosage of 2.5 mg-Al/L. Coagulation pH was 7.0.

We further investigated the effect of sulfate ions by preparing artificial raw waters with various sulfate ion concentration (E-1–7 in Table 2-2). Fig. 2-16 shows the rates of turbidity removal by HB-PACl-t, HB-PACl, and NB-PACl. As the concentration of the sulfate ion in the raw water decreased, the removal of turbidity by HB-PACl-t and HB-PACl in sedimentation supernatant decreased dramatically. In the absence of sulfate ion, there was almost no turbidity removal. Compared with HB-PACl and HB-PACl-t, on the other hand, treatment with NB-PACl resulted in high turbidity removal, regardless of the sulfate ion concentration in the water. Even

when the sulfate ion concentration was zero, NB-PACl produced supernatant with a low residual turbidity that was comparable to the turbidity attained with 15.8-mg/L sulfate ion. Photographs of floc formation were consistent with this result (Fig. 2-17). When NB-PACl was used to treat the water, visible floc particles were observed at the rapid-mixing stage when the water contained sulfate ion concentration at 3.5–15.8 mg/L, and during the first stage of slow mixing, visible floc particles were also observed, even when the water contained no sulfate ions (Fig. 2-20). For HB-PACl, however, the rate of floc formation slowed as the sulfate ion concentration decreased. When the sulfate ion concentration was 3.5 mg/L, visible floc particles were not formed during the rapid-mixing stage; instead, they were formed only after slow mixing. At a sulfate ion concentration of zero, floc particles were not formed at all. At low sulfate concentrations, the floc formation ability was therefore stronger for NB-PACl than for HB-PACl. HB-PACl-t required a very high sulfate ion concentration (48.8 mg/L) for floc formation, but even at such a high sulfate ion concentration, large floc particles did not form.

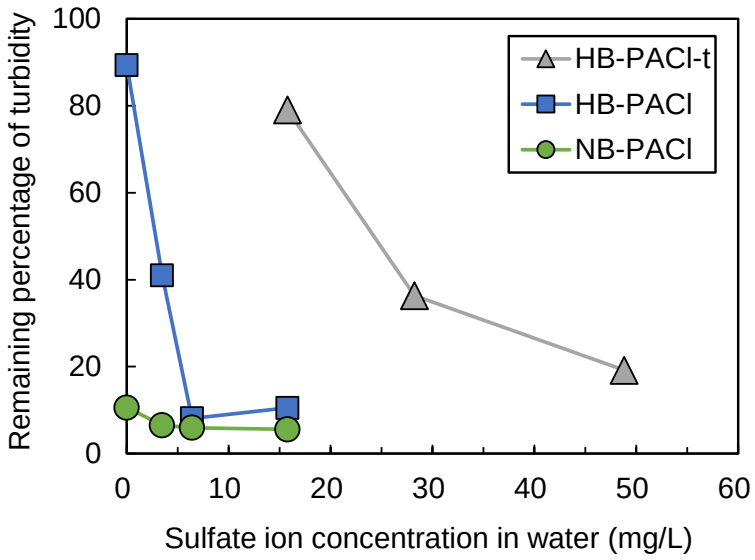


Fig. 2-16. Plots of the percentage of turbidity remaining after coagulation and sedimentation against sulfate ion concentration in raw water. Waters E-1–4 and E-6–7 were used. Initial SPAC concentration was 2 mg/L. HB-PACl-t, HB-PACl, and NB-PACl were used at a dosage of 2.5 mg-Al/L. Coagulation pH was 7.0.

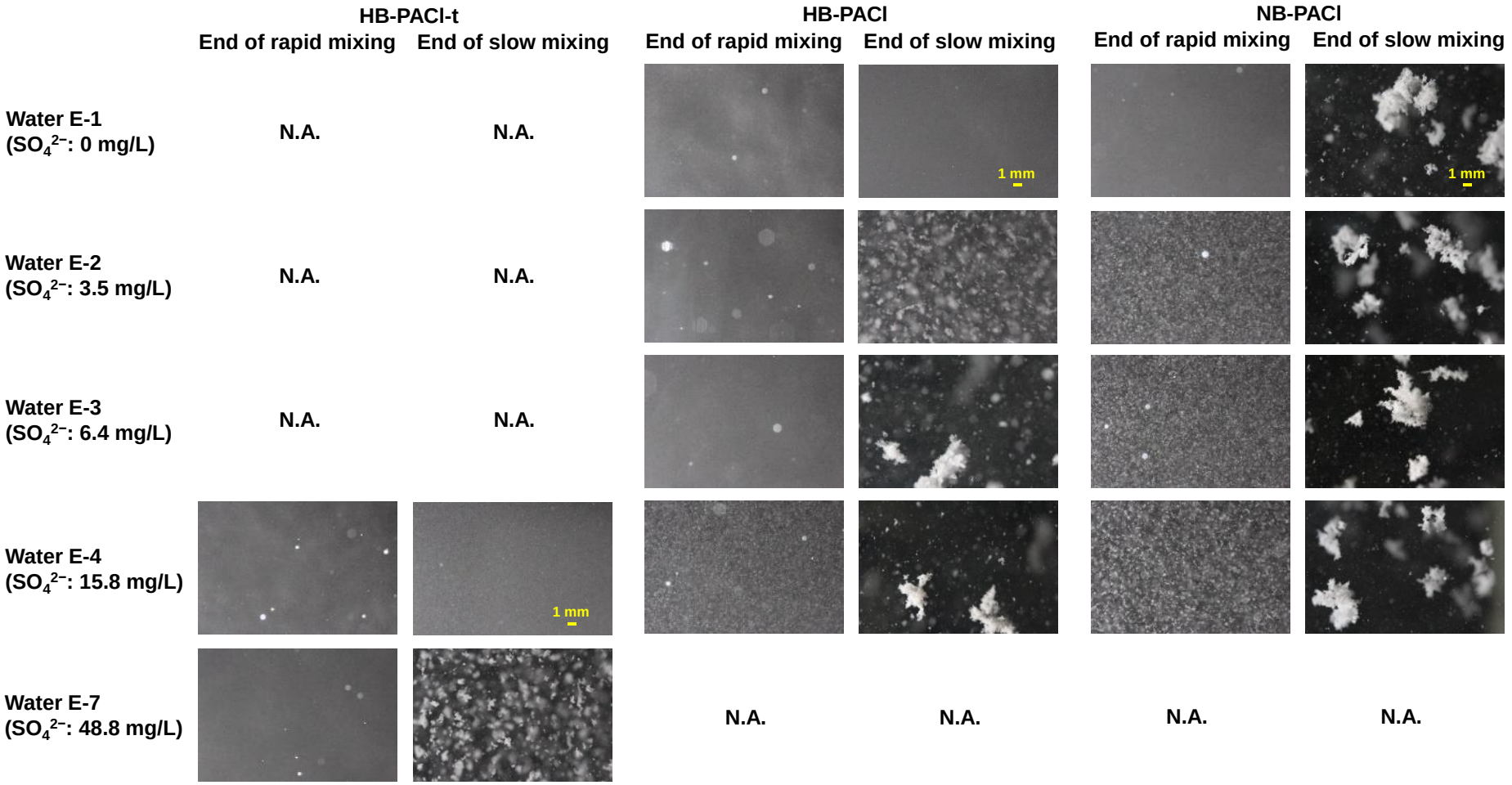


Fig. 2-17. Photographs taken at the end of slow mixing. Waters E-1, E-2, E-3, E-4, and E-7 were used. Initial SPAC concentration was 2 mg/L. HB-PACl-t, HB-PACl, and NB-PACl were used at a dosage of 2.5 mg-Al/L. Coagulation pH was 7.0. All the pictures during slow mixing are shown in Fig. 2-18, Fig. 2-19, and Fig. 2-20.

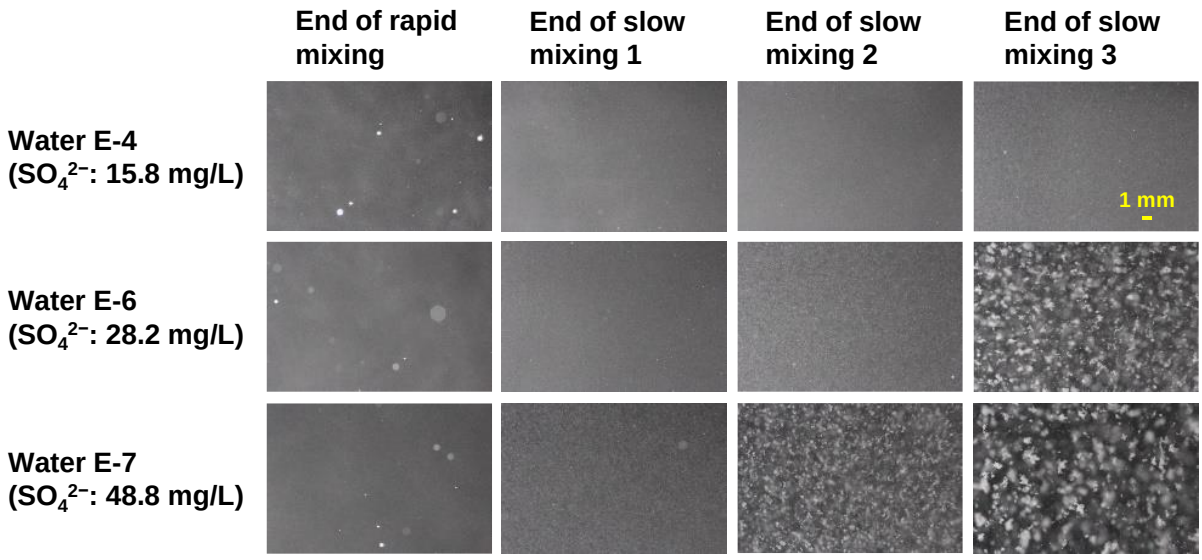


Fig. 2-18. Photographs taken at the ends of rapid mixing, slow mixing 1, slow mixing 2, and slow mixing 3. Waters E-4, E-6 and E-7 with sulfate ion concentrations of 15.8, 28.2, and 48.8 mg/L, respectively, were used. Initial SPAC concentration was 2 mg/L. HB-PACl-t was used at a dosage of 2.5 mg-Al/L. Coagulation pH was 7.0.

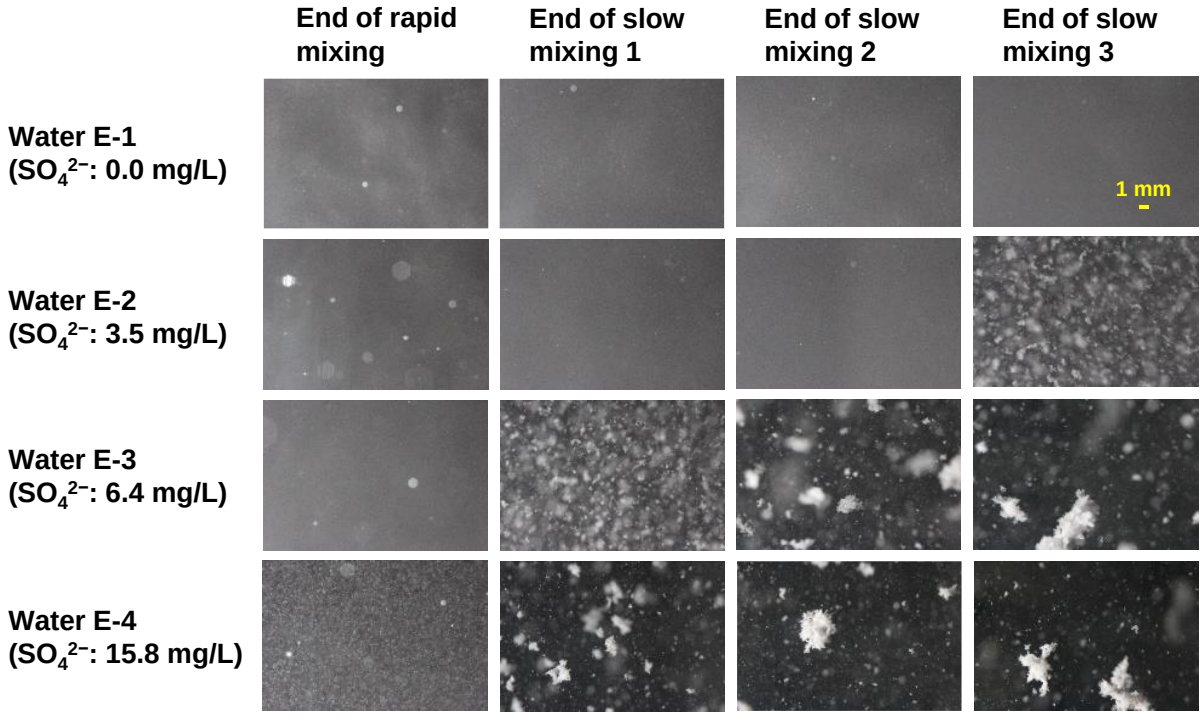


Fig. 2-19. Photographs taken at the end of rapid mixing, slow mixing 1, slow mixing 2, and slow mixing 3. Waters E-1, E-2, E-3, and E-4 with sulfate ion concentrations of 0.0, 3.5, 6.4 and 15.8 mg/L, respectively, were used. Initial SPAC concentration was 2 mg/L. HB-PACl was used at a dosage of 2.5 mg-Al/L. Coagulation pH was 7.0.

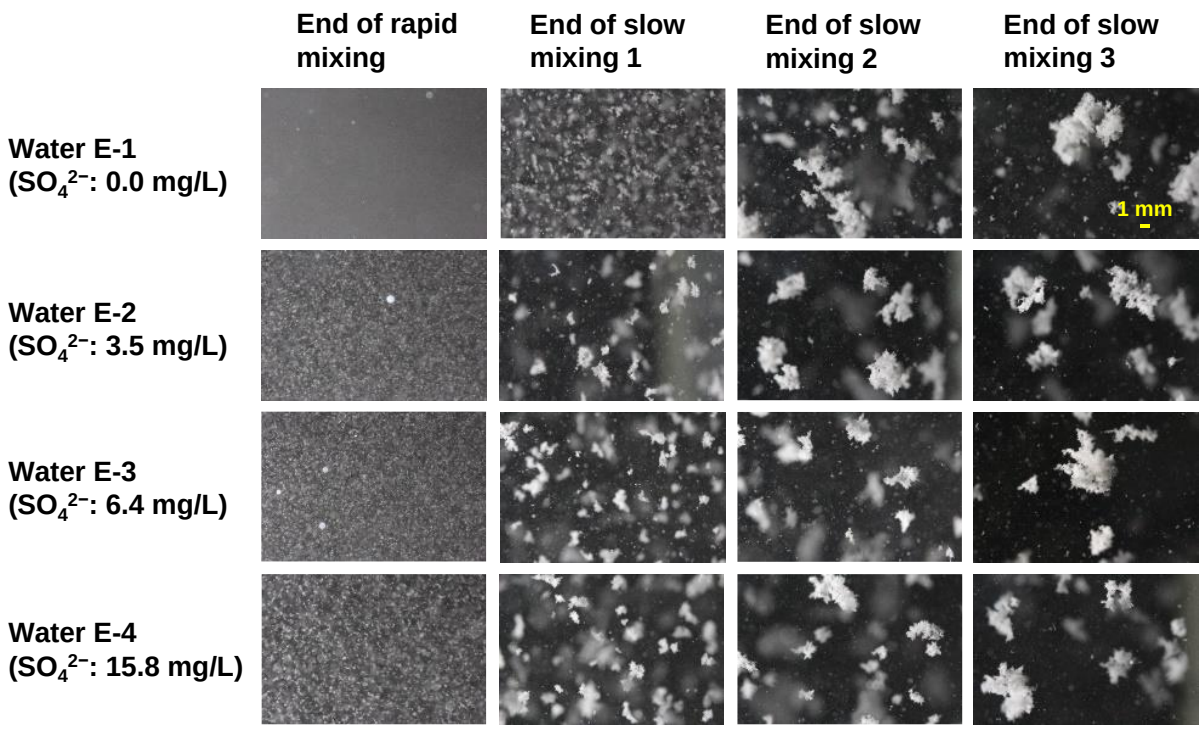


Fig. 2-20. Photographs taken at the end of rapid mixing, slow mixing 1, slow mixing 2, and slow mixing 3. Waters E-1, E-2, E-3, and E-4 with sulfate ion concentrations of 0.0, 3.5, 6.4 and 15.8 mg/L, respectively, were used. Initial SPAC concentration was 2 mg/L. NB-PACl was used at a dosage of 2.5 mg-Al/L. Coagulation pH was 7.0.

The sulfate ion in PACl is known to enhance the precipitation of aluminum ions in water (De Hek et al., 1978). All commercially available PACls in Japan contain sulfate ions, but JIS (Japanese Industrial Standards) standard JIS K 1475-1996 stipulates that the sulfate ion content of PACl should be lower than 3.5% (Japanese Industrial Standards Committee, 1996). The sulfate contents of HB-PACl and NB-PACl were 2% and 3%, respectively. The unsatisfactory performance of HB-PACl at low sulfate ion concentrations might have resulted from its relatively low sulfate content. In order to test this hypothesis, Fig. 2-16 was redrawn using the total sulfate ion concentration (sulfate ion concertation in raw water plus sulfate ion added with the PACl) as the independent variable (Fig. 2-21). The total sulfate ion concentration did not explain the difference in the coagulation performances of HB-PACl and NB-PACl. Moreover, when HB-PACl-t and HB-PACl were compared, the requirement for sulfate ions was larger for HB-PACl-t than for HB-PACl, although the two PACls had the same sulfate content. Nakazawa

et al. (2018a) have prepared a set of high-basicity PACl coagulants prepared by the $Al(OH)_3$-dissolution method and have reported that SPAC particle removal ability via PACl coagulation depends little on $SO_4^{2-}$/Al ratios in the range 0.11–0.15. These results indicate that the requirement of HB-PACl for sulfate ions in raw water is not related to its low sulfate content.

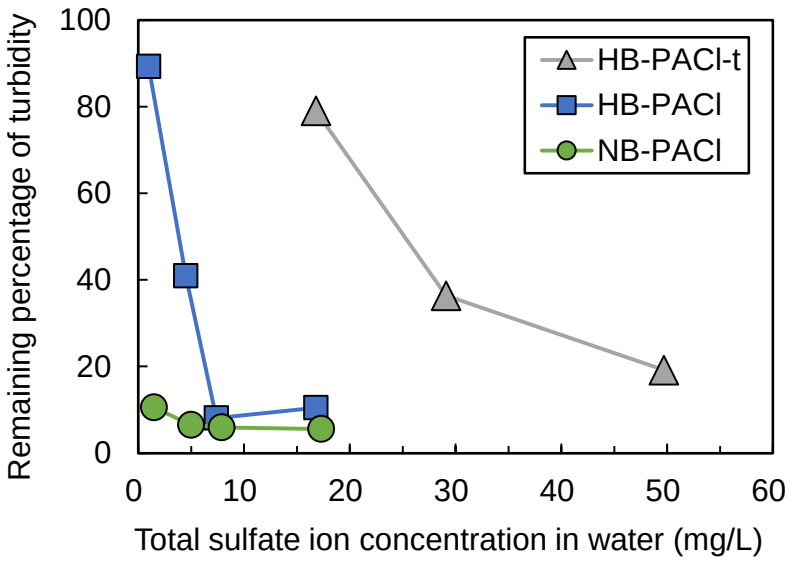


Fig. 2-21. Plots of the percentage of turbidity remaining after coagulation and sedimentation against total sulfate ion concentration in raw water. Waters E-1–4, and E-6–7 with different sulfate ions were used. Initial SPAC concentration was 2 mg/L. HB-PACl-t, HB-PACl, and NB-PACl were used at a dosage of 2.5 mg-Al/L. Coagulation pH was 7.0.

A dependence of HB-PACl coagulation on sulfate ion concentrations in water was also observed in the concentrations of residual SPAC particles after CSF (Fig. 2-22). When sulfate ion concentrations were at a low level of 3.5 mg/L, the residual SPAC particle concentration was quite high, 1790 particles/mL, a concentration that was higher than the concentration of 345 particles/mL achieved with NB-PACl at the same sulfate ion concentration. At a sulfate ion concentration of zero, residual SPAC particles were too numerous to count. Nakazawa et al. (2018a) have observed the superiority of HB-PACl over NB-PACl in reducing residual SPAC particles in water containing sulfate ion at a concentration of 16 mg/L, and this trend was also observed in our study when the sulfate ion concentration exceeded 6.4 mg/L. Our results show,

however, that at relatively low sulfate ion concentrations, normal-basicity PACl is superior to high-basicity PACl.

The effect of sulfate ions was further confirmed by the experiments using natural water and sulfate ion -adjusted natural water. For HB-PACl, floc did not form during the mixing process (Panel A of Fig. 2-23), and the result was high residual turbidity in the supernatant (Panel B of Fig. 2-23). With the increase of the sulfate ion concentration in the water, the coagulation performance improved: formation of large floc particles was observed, and turbidity in the supernatant became satisfactorily low. In contrast, the performance of NB-PACl was fairly good, regardless of whether or not there was an increase of the sulfate ion concentration (Fig. 2-23). Our results showed that HB-PACl, which is superior in reducing residual SPAC particles after CSF, requires a certain concentration of sulfate ion in the raw water to work efficiently.

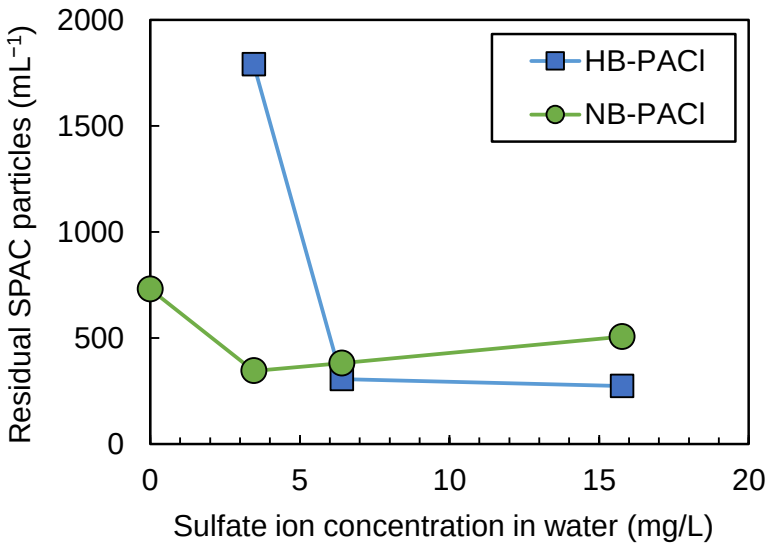


Fig. 2-22. Plots of residual SPAC particle concentration in sand filtrate against sulfate concentration in raw water. Waters E-1, E-2, E-3, and E-4 with sulfate ion concentrations of 0.0, 6.4, 15.8, and 28.2 mg/L, respectively, were used. Initial SPAC concentration was 2 mg/L. PACl dosage was 2.5 mg-Al/L. Coagulation pH was 7.0.

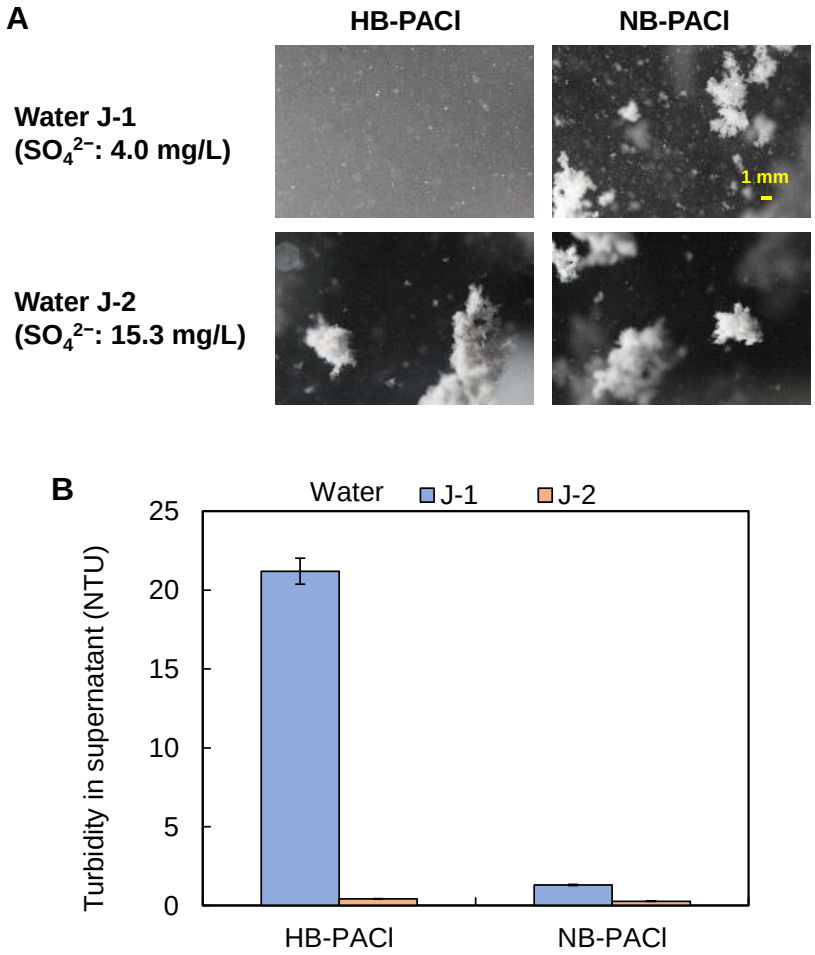


Fig. 2-23. Photographs taken at the end of slow mixing 3 (Panel A) and residual turbidities of supernatants (Panel B). Waters J-1 and J-2 with different sulfate ion concentrations of 4.0 and 15.3 mg/L, respectively, were used. Initial SPAC concentration was 2 mg/L. HB-PACl and NB-PACl were used at a dosage of 4.0 mg-Al/L. Coagulation pH was 7.0.

### 2.3.5 Effect of sulfate ion on PACl hydrolysis

The rates of hydrolysis-precipitation of HB-PACl-t, HB-PACl, and NB-PACl at different sulfate concentrations were investigated, and the results are shown in Fig. 2-24. There was little effect of sulfate ions on the rate of hydrolysis-precipitation for NB-PACl: the aluminum species in NB-PACl grew larger than 10 μm within 15 s, no matter what the sulfate concentration in the water was. In contrast, the aluminum species in HB-PACl hydrolyzed relatively slowly and grew a little slower at a sulfate ion concentration of 6.4 mg/L (Water E-3). They barely hydrolyzed without sulfate ions and did not grow larger than 10 μm (Water E-1). They grew

rapidly at a sulfate ion concentration of 15.8 mg/L (Waters E-4 and E-5). Although the concentrations of $Na^{+}$ and $Mg^{2+}$ differ in Waters E-4 and E-5, the rates of the hydrolysis-precipitation were about the same. The aluminum species in HB-PACl-t grew very slowly, even at a sulfate concentration of 15.8 mg/L. The growth trend of HB-PACl-t at a sulfate concentration of 48.8 mg/L was similar to that of HB-PACl at a sulfate concentration of 6.4 mg/L. Therefore, the results indicate that sulfate ions are essential for the hydrolysis of HB-PACl and HB-PACl-t, and they show that HB-PACl-t requires a much higher concentration of sulfate for its rapid hydrolysis-precipitation than HB-PACl.

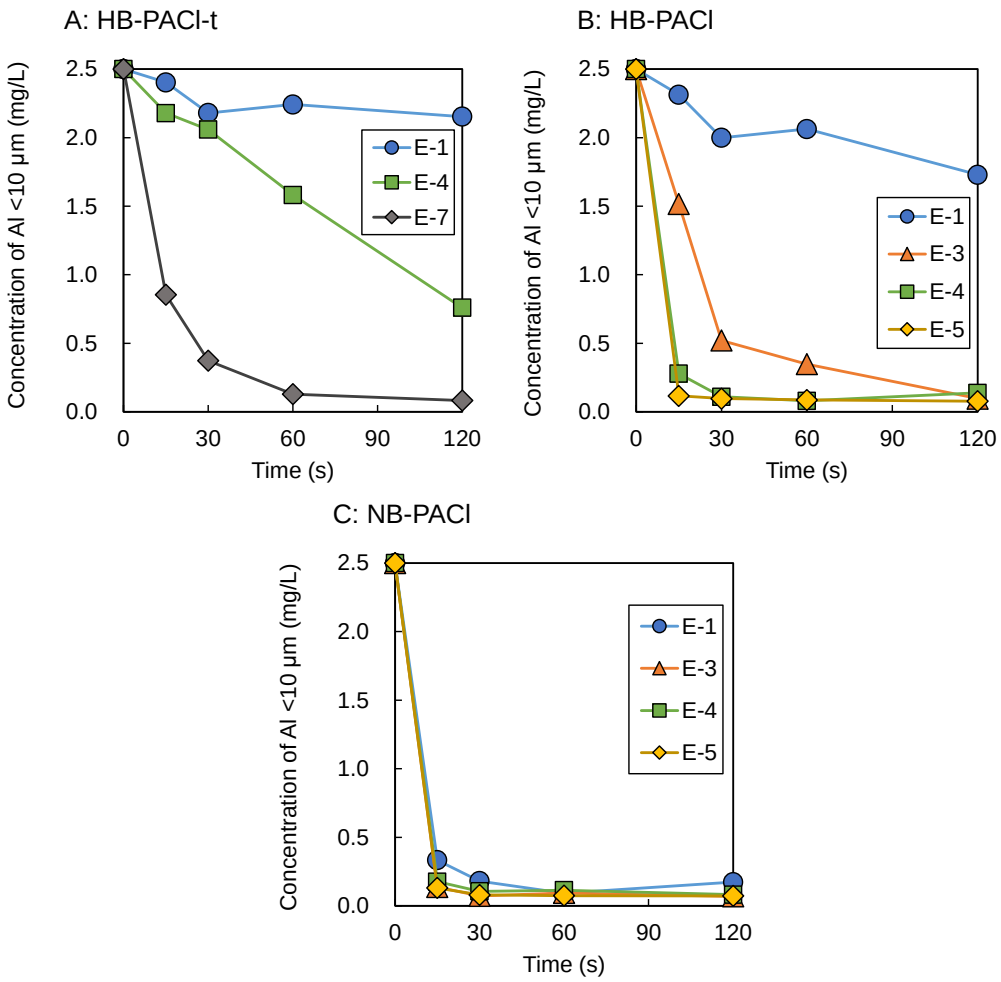


Fig. 2-24. Change of concentration of aluminum that passed through a membrane with a 10-µm pore size. Waters E-1, E-3, E-4, E-5, and E-7 with sulfate ion concentrations of 0.0, 6.4, 15.8, 15.7, and 48.8 mg/L, respectively, were used. HB-PACl-t (Panel A), HB-PACl (Panel B), and NB-PACl (Panel C) were dosed at 2.5 mg-Al/L. pH during mixing was 7.

The pattern of hydrolysis-precipitation rates was similar to the trend of coagulation performance, including floc formation and the concentration of residual particles after CSF. On the other hand, charge neutralization capacity, which was evaluated via the ferron assay and colloid charge, did not explain the different coagulation performances of HB-PACl and HB-PACl-t, as described in the sections 2.3.1 and 2.3.2. Hydrolysis-precipitation rate rather than charge neutralization capacity, therefore determined coagulation performance. Wang et al. (2002) have reported an enhancement of coagulation performance with increasing $SO_4^{2-}$/Al ratio in PACl and have explained the sulfate ion effect by a charge neutralization mechanism.

Our results are new in terms of three points. First, we focused on sulfate ion in raw water, not in PACl. Second, there was a sulfate ion effect on high-basicity PACl (HB-PACl and HB-PACl-t) but not on normal-basicity PACl (NB-PACl). Third, the effect of sulfate ion in raw water was not explained by the charge neutralization mechanism. Sulfate ion in raw water accelerate hydrolysis-precipitation of aluminum species in high-basicity PACls, but its mechanism is not cleared yet. A possible mechanism is related to ionic strength and double-layer compression. Sulfate ion in raw water may change charge-neutralization capacity of aluminum species formed after PACl is dosed into raw water. These require further study.

Moderately polymerized aluminum species with MWs ranging from 1 to 10 kDa were observed in HB-PACl-t. These moderately polymerized species may have been related to the distinctive hydrolysis-precipitation of HB-PACl-t. HB-PACl contained a high percentage of highly polymerized species with MWs >10 kDa. Among the three PACls, NB-PACl had the highest percentage of species with molecular weights <1 kDa, including monomer Al. We hypothesized that the resistance to hydrolysis-precipitation was strong for moderately polymerized species followed by highly polymerized species. HB-PACl-t was produced through a high-temperature (90–95 °C) process, whereas HB-PACl was prepared through a low-temperature process (<85 °C). HB-PACl-t contains more sodium and chloride ions per aluminum than HB-PACl (Table 2-1). The production temperature and/or salt content, in addition to basicity, may therefore determine hydrolysis-precipitation resistance and coagulation ability.

## 2.4 Chapter summary

This chapter comprehensively investigated the difference between HB-PACl ($Al(OH)_3$-dissolution PACl) and HB-PACl-t ($AlCl_3$-titration PACl) as well as the difference between HB-PACl (high-basicity PACl) and NB-PACl (normal-basicity PACl) in terms of their coagulation ability to form floc particles and to reduce the concentration of SPAC particles in CSF-treated water.

The coagulation performance of HB-PACl was superior to that of HB-PACl-t, although the ferron distribution, colloid charge, and sulfate ion content were the same. Charge neutralization capacities were likewise sufficient for HB-PACl-t and HB-PACl, but the very low hydrolysis-precipitation of aluminum species in HB-PACl-t versus HB-PACl resulted in poor floc formation by the former.

HB-PACl was superior to NB-PACl in reducing residual carbon particles after CSF, although the rate of floc particle formation was somewhat slower for HB-PACl than for NB-PACl. The similarities of the residual turbidities after coagulation sedimentation could have been due to the high charge neutralization capacity of HB-PACl. However, sulfate ion was required in raw water for HB-PACl to be effective.

When the raw water contained very low concentrations of sulfate ions, the aluminum species in HB-PACl hydrolyzed very slowly and did not form floc particles. In contrast, NB-PACl did not need sulfate ions. Finally, HB-PACl was inferior to NB-PACl when sulfate ion concentrations in raw water were very low.

The three PACls were clearly different in terms of their MW distributions and their $m/z$ values determined by ESI-MS, but they did not necessarily differ based on the ferron assay.

Polymerized aluminum species, in particular those with MWs of 1–10 kDa, might be highly resistant to hydrolysis-precipitation and may require sulfate ions for hydrolysis-precipitation and for effective coagulation.

Hydrolysis-precipitation of aluminum species as well as charge neutralization capacity are key determinants of coagulation effectiveness.

## 2.5 Reference

Allouche, L., Gérardin, C., Loiseau, T., Férey, G., & Taulelle, F. (2002). Al30: A Giant Aluminum Polycation. Angewandte Chemie International Edition, 39(3), 511–514. https://doi.org/10.1002/(sici)1521-3773(20000204)39:3<511::aid-anie511>3.0.co;2-n

Ando, N., Matsui, Y., Kurotobi, R., Nakano, Y., Matsushita, T., & Ohno, K. (2010). Comparison of natural organic matter adsorption capacities of super-powdered activated carbon and powdered activated Carbon. Water Research, 44(14), 4127–4136. https://doi.org/10.1016/j.watres.2010.05.029

Bonvin, F., Jost, L., Randin, L., Bonvin, E., & Kohn, T. (2016). Super-fine powdered activated carbon (SPAC) for efficient removal of micropollutants from wastewater treatment plant effluent. Water Research, 90, 90–99. https://doi.org/10.1016/j.watres.2015.12.001

Casey, W. H. (2006). Large aqueous aluminum hydroxide molecules. Chemical Reviews, 106(1), 1–16. https://doi.org/10.1021/cr040095d

Chen, Z., Luan, Z., Fan, J., Zhang, Z., Peng, X., & Fan, B. (2007). Effect of thermal treatment on the formation and transformation of Keggin Al13 and Al30 species in hydrolytic polymeric aluminum solutions. Colloids and Surfaces A: Physicochemical and Engineering Aspects, 292(2–3), 110–118. https://doi.org/10.1016/j.colsurfa.2006.06.005

De Hek, H., Stol, R. J., & De Bruyn, P. L. (1978). Hydrolysis-precipitation studies of aluminum(III) solutions. 3. The role of the sulfate ion. Journal of Colloid And Interface Science, 64(1), 72–89. https://doi.org/10.1016/0021-9797(78)90336-3

Feng, C., Tang, H., & Wang, D. (2007). Differentiation of hydroxyl-aluminum species at lower OH/Al ratios by combination of 27Al NMR and Ferron assay improved with kinetic resolution. Colloids and Surfaces A: Physicochemical and Engineering Aspects, 305(1–3), 76–82. https://doi.org/10.1016/j.colsurfa.2007.04.043

Japanese Industrial Standards Committee. (1996). Poly aluminum chloride for water works. https://www.jisc.go.jp/app/jis/general/GnrJISNumberNameSearchList?toGnrJISStandardDetailList

Kimura, M., Matsui, Y., Kondo, K., Ishikawa, T. B., Matsushita, T., & Shirasaki, N. (2013). Minimizing residual aluminum concentration in treated water by tailoring properties of polyaluminum coagulants. Water Research, 47(6), 2075–2084. https://doi.org/10.1016/j.watres.2013.01.037

Letterman, R. D., & Yiacoumi, S. (2010). Coagulation and flocculation. In J. K. Edzwald (Ed.), Water Quality and Treatment A Handbook on Drinking Water (Sixth Edit, pp. 8.1-8.81). McGrawHill.

Matsui, Y., Ishikawa, T. B., Kimura, M., Machida, K., Shirasaki, N., & Matsushita, T. (2013). Aluminum concentrations of sand filter and polymeric membrane filtrates: A comparative study. Separation and Purification Technology, 119, 58–65. https://doi.org/10.1016/j.seppur.2013.09.006

Matsui, Y., Murase, R., Sanogawa, T., Aoki, N., Mima, S., Inoue, T., & Matsushita, T. (2004). Micro-ground powdered activated carbon for effective removal of natural organic matter during water treatment. Water Science and Technology: Water Supply, 4(4), 155–163. https://doi.org/10.2166/ws.2004.0073

Matsui, Y., Nakao, S., Sakamoto, A., Taniguchi, T., Pan, L., Matsushita, T., & Shirasaki, N. (2015). Adsorption capacities of activated carbons for geosmin and 2-methylisoborneol vary with activated carbon particle size: Effects of adsorbent and adsorbate characteristics. Water Research, 85, 95–102. https://doi.org/10.1016/j.watres.2015.08.017

Matsui, Y., Nakao, S., Taniguchi, T., & Matsushita, T. (2013). Geosmin and 2-methylisoborneol removal using superfine powdered activated carbon: Shell adsorption and branched-pore kinetic model analysis and optimal particle size. Water Research, 47(8), 2873–2880. https://doi.org/10.1016/j.watres.2013.02.046

Matsui, Y., Shirasaki, N., Yamaguchi, T., Kondo, K., Machida, K., Fukuura, T., & Matsushita, T. (2017). Characteristics and components of poly-aluminum chloride coagulants that enhance arsenate removal by coagulation: Detailed analysis of aluminum species. Water Research, 118, 177–186. https://doi.org/10.1016/j.watres.2017.04.037

Matsui, Y., Yoshida, T., Nakao, S., Knappe, D. R. U., & Matsushita, T. (2012). Characteristics of competitive adsorption between 2-methylisoborneol and natural organic matter on superfine and conventionally sized powdered activated carbons. Water Research, 46(15), 4741–4749. https://doi.org/10.1016/j.watres.2012.06.002

Nakamura, H. (2009). FT-NMR data processing by computer (Secong edi). Sankyo Shuppan. https://opac.lib.hokudai.ac.jp/opac/opac_link/bibid/2001632616

Nakazawa, Y., Matsui, Y., Hanamura, Y., Shinno, K., Shirasaki, N., & Matsushita, T. (2018a). Identifying, counting, and characterizing superfine activated-carbon particles remaining after coagulation, sedimentation, and sand filtration. Water Research, 138, 160–168. https://doi.org/10.1016/j.watres.2018.03.046

Nakazawa, Y., Matsui, Y., Hanamura, Y., Shinno, K., Shirasaki, N., & Matsushita, T. (2018b). Minimizing residual black particles in sand filtrate when applying super-fine powdered activated carbon: Coagulants and coagulation conditions. Water Research, 147, 311–320. https://doi.org/10.1016/j.watres.2018.10.008

Pan, L., Nishimura, Y., Takaesu, H., Matsui, Y., Matsushita, T., & Shirasaki, N. (2017). Effects of decreasing activated carbon particle diameter from 30 Mm to 140 nm on equilibrium adsorption capacity. Water Research, 124, 425–434. https://doi.org/10.1016/j.watres.2017.07.075

Parker, D. R., & Bertsch, P. M. (1992). Identification and Quantification of the "Al13" Tridecameric Aluminum Polycation Using Ferron. Environmental Science and Technology, 26(5), 908–914. https://doi.org/10.1021/es00029a006

Partlan, E., Davis, K., Ren, Y., Apul, O. G., Mefford, O. T., Karanfil, T., & Ladner, D. A. (2016). Effect of bead milling on chemical and physical characteristics of activated carbons pulverized to superfine sizes. Water Research, 89, 161–170. https://doi.org/10.1016/j.watres.2015.11.041

Sato, F., & Matsuda, S. (2009). Novel Basic Aluminum Chloride, Its Manufacturing Method and Its Application. Japanese Patent, Application, 2008–047932.

Sposito, G. (1995). The Environmental Chemistry of Aluminum, Second Edition. Taylor & Francis. https://books.google.co.jp/books?id=lNxltQeVP9UC

Tang, H., Xiao, F., & Wang, D. (2015). Speciation, stability, and coagulation mechanisms of hydroxyl aluminum clusters formed by PACl and alum: A critical review. Advances in Colloid and Interface Science, 226, 78–85. https://doi.org/10.1016/j.cis.2015.09.002

Wang, D., Sun, W., Xu, Y., Tang, H., & Gregory, J. (2004). Speciation stability of inorganic polymer flocculant-PACl. Colloids and Surfaces A: Physicochemical and Engineering Aspects, 243(1–3), 1–10. https://doi.org/10.1016/j.colsurfa.2004.04.073

Wang, D., Tang, H., & Gregory, J. (2002). Relative importance of charge neutralization and precipitation on coagulation of kaolin with PACI: Effect of sulfate ion. Environmental Science and Technology, 36(8), 1815–1820. https://doi.org/10.1021/es001936a

Yan, M., Wang, D., Ni, J., Qu, J., Chow, C. W. K., & Liu, H. (2008). Mechanism of natural organic matter removal by polyaluminum chloride: Effect of coagulant particle size and hydrolysis kinetics. Water Research, 42(13), 3361–3370. https://doi.org/10.1016/j.watres.2008.04.017

Yan, M., Wang, D., Qu, J., He, W., & Chow, C. W. K. (2007). Relative importance of hydrolyzed Al(III) species (Ala, Alb, and Alc) during coagulation with polyaluminum chloride: A case

study with the typical micro-polluted source waters. Journal of Colloid and Interface Science, 316(2), 482–489. https://doi.org/10.1016/j.jcis.2007.08.036

# Chapter 3. PACl hydrolysis as a indicator of PACl performance and effects of inorganic ions

## 3.1 Introduction

Because PACl and the conventional coagulant alum are hydrolyzing aluminum salts, it is commonly understood that hydrolysis produces the aluminum polynuclear species need for coagulation. The important role of hydrolysis on PACl performance has been revealed in Chapter 2 by investigating the removal of SPAC particles in coagulation-flocculation process. PACl hydrolysis-precipitation is highly correlated with PACl performance in coagulation, irrespectively the type and characteristics of PACl. Sulfate ion was found to strongly affect PACl hydrolysis-precipitation, especially for the high-basicity PACl. However, the above conclusion based on the artificial ionic water and only one type of natural raw water. On the other hand, aluminum ion in the PACl must undergo hydrolysis to become species that can affect coagulation and the hydrolysis allows protons to react with alkalinity (Ye et al., 2007). An et al. (2021) also mentioned the importance of hydrolysis on aluminum species formation. To furtherly establish and strengthen the hydrolysis-precipitation rate as a factor of coagulation performance, in this chapter, the universality of hydrolysis-precipitation at various pH, PACl dose, alkalinity condition in natural raw water was studied. Two PACls: HB-PACl and NB-PACl were applied in coagulation experiments in different natural waters, and their hydrolysis-precipitation in these waters were also evaluated. The removal of turbidity, which is the common removal target in coagulation-flocculation process, and the floc formation rate at each condition, are the indices for the coagulation performance. The main objective of the study in this chapter is to confirm the universality of hydrolysis-precipitation rate under different coagulation condition and establish the correlation between PACl hydrolysis-precipitation and its coagulation performance.

## 3.2 Materials and methods

### 3.2.1 PACl coagulants

We used sulfated PACl coagulants with high basicity (HB-PACl, basicity 70%) and normal basicity (NB-PACl, basicity 50%) (Taki Chemical Co., Ltd., Hyogo, Japan) in this study. They were produced by the dissolution method described in Sato and Matsuda (2009). Briefly, NB-PACl was produced by heating a mixture of $AlCl_3$, $Al_2(SO_4)_3$, and $Al(OH)_3$. HB-PACl was producing from NB-PACl by adding a sodium carbonate solution to raise the basicity to 70% at a temperature <85 °C. Table 3-1 lists the basic properties of the PACl coagulants. These two PACls are the same as which used in Chapter 2. The characteristics of the PACl were analyzed by ferron assay, colloid titration, and $^{27}$Al-NMR analysis (Fig. 2-7, Section 2.3.1, Chapter 2). The details of these analytical methods are described in Section 2.2.3 (Chapter 2.) (Chen et al., 2020). Stock PACls were diluted to 0.1 mol-Al/L using ultrapure water (Milli-Q water) produced by an ultrapure lab water system (Milli-Q Advantage; Merck KGaA, Darmstadt, Germany) before they were used in the experiments.

Table 3-1.
Properties of the PACls used in this study

| | HB-PACl | NB-PACl |
|---|---|---|
| Al content (mol/L) | 2.5 | 2.5 |
| $SO_4^{2-}$/Al (mole ratio) | 0.11 | 0.14 |
| Basicity (%) | 70 | 50 |

### 3.2.2 Water

Waters tested in this chapter were given 5 designations. Table 3-2 show the water characteristics. Waters designated Y-1, J-1, M-1, T-1, and S-1 (Table 3-2) were natural waters sampled from the Kuromorigawa Reservoir (Akita, Japan), Jyoganji River (Toyama, Japan),

Toyohira River (Hokkaido, Japan), Jyoganji River, and Shiraikawa Treatment Plant (Hokkaido, Japan), respectively. Waters J-1 and T-1 were sampled from the same river on different dates. Waters designated Y-2–6, J-2, M-2, and T-2 were prepared by adding $Na_2SO_4$ and $NaHCO_3$ to the respective natural water.

These waters were stored at 4 °C prior to experiments, which were begun after the temperature of the waters had returned to room temperature (~20 °C). Concentrations of ions in the water were measured by ion chromatography (Integrion and ICS-1100; Thermo Scientific, Bremen, Germany). At the experimental pH of 7.0, almost all the alkalinity is associated with bicarbonate ions. The alkalinity was measured by titration with sulfuric acid (0.01 M $H_2SO_4$, FUJIFILM Wako Pure Chemical Corporation), and then the concentration of bicarbonate ions was determined from the alkalinity. For measurements of dissolved organic carbon (DOC) and ultraviolet (UV) light absorbance, a water sample was filtered through a membrane filter (0.45-μm pore size; Toyo Roshi Kaisha, Ltd., Tokyo, Japan). The DOC was measured with a TOC analyzer (TOC900; GE Analytical Instruments, Inc., Boulder, CO, USA). The UV absorbance was measured at 260 nm (UV260 value) with a spectrophotometer (UV-1800; Shimadzu, Kyoto, Japan). Turbidity was measured with a turbidity meter (WA7700; Nippon Denshoku Industries Co., Ltd; Tokyo, Japan).

Table 3-2.

Ion components, alkalinity, DOC, UV260, and turbidity of the Y, J, M, T, and S water series used in this study

| Series | Water | $Na^+$ | $K^+$ | $Mg^{2+}$ | $Ca^{2+}$ | $Cl^-$ | $NO_3^-$ | $SO_4^{2-}$ | Alkalinity (meq/L) ≈ $HCO_3^-$ (mmol/L) | DOC | UV260 | Turbidity | Source |
|---|---|---|---|---|---|---|---|---|---|---|---|---|---|
| | | mmol/L | mmol/L | mmol/L | mmol/L | mmol/L | mmol/L | mmol/L | | mg-C/L | $cm^{-1}$ | NTU | |
| Y | Y-1 | 0.34 | 0.02 | 0.05 | 0.04 | 0.37 | 0.00 | 0.04 | 0.08 | 1.9 | 0.04 | 5.2 | Kuromorigawa Reservoir |
| | Y-2 | 0.40 | 0.02 | 0.05 | 0.03 | 0.34 | 0.01 | 0.07 | 0.08 | 1.8 | 0.04 | 5.6 | |
| | Y-3 | 0.51 | 0.02 | 0.05 | 0.04 | 0.33 | 0.01 | 0.12 | 0.08 | 1.8 | 0.04 | 5.4 | |
| | Y-4 | 0.62 | 0.02 | 0.05 | 0.04 | 0.34 | 0.01 | 0.04 | 0.34 | 1.9 | 0.04 | 4.9 | |
| | Y-5 | 0.68 | 0.02 | 0.05 | 0.04 | 0.34 | 0.00 | 0.07 | 0.34 | 1.8 | 0.04 | 5.1 | |
| | Y-6 | 1.10 | 0.02 | 0.05 | 0.04 | 0.34 | 0.02 | 0.12 | 0.66 | 1.9 | 0.04 | 5.9 | |
| J | J-1 | 0.08 | 0.01 | 0.04 | 0.16 | 0.05 | 0.01 | 0.04 | 0.32 | 0.5 | NM | NM | Joganji River |
| | J-2 | 0.35 | 0.01 | 0.04 | 0.16 | 0.05 | 0.01 | 0.16 | 0.32 | 0.5 | NM | NM | |
| M | M-1 | 0.24 | 0.02 | 0.05 | 0.14 | 0.19 | 0.01 | 0.09 | 0.20 | 0.4 | 0.03 | 3.2 | Toyohira River |
| | M-2 | 0.45 | 0.04 | 0.09 | 0.23 | 0.37 | 0.02 | 0.15 | 0.34 | 0.4 | 0.03 | 1.1 | |
| T | T-1 | 0.08 | 0.01 | 0.04 | 0.18 | 0.04 | 0.01 | 0.06 | 0.32 | 0.4 | 0.02 | 1.4 | Jyoganji River |
| | T-2 | 0.55 | 0.01 | 0.04 | 0.18 | 0.04 | 0.01 | 0.12 | 0.66 | 0.4 | 0.02 | 1.6 | |
| S | S-1 | 0.31 | 0.04 | 0.06 | 0.18 | 0.29 | 0.02 | 0.13 | 0.23 | 2.9 | 0.10 | 67.7 | Shiraikawa Treatment Plant |

NM: Not measured.

### 3.2.3 Coagulation experiment and hydrolysis-precipitation rate test

Coagulation experiments (including flocculation and sedimentation processes) were performed in a rectangular plastic beaker. Four liters of raw water were placed in the beaker, and a predetermined volume of HCl or NaOH (0.1N) was added to the water to bring the coagulation pH to 7.0 or 7.5. After 30 min of mixing, PACl was added. Rapid mixing conducted at a G value of 600 $s^{-1}$ for 40 s was followed by three stages of slow mixing at G values (in chronological order) of 50 $s^{-1}$ for 170 s, 20 $s^{-1}$ for 170 s, and 10 $s^{-1}$ for 320 s. During the rapid and slow mixing, portions of water were withdrawn from the beaker and filtered through a 10-μm pore size membrane filter (Chen et al., 2020). Aluminum concentrations in the water were measured with an inductively coupled plasma mass spectrometer (ICPMS, 7700x; Agilent Technologies, Inc., Santa Clara, CA, USA). The time required to reduce the Al concentration fourfold from the initial concentration (calculation method explained in following section 3.2.5), and this one-quarter concentration time was used as the index of the rate of PACl hydrolysis-precipitation (the one-quarter concentration was chosen because it was considered important that most of the aluminum be hydrolyzed and precipitated). After mixing, the water was allowed to stand for 1 h for sedimentation. The turbidities of the raw water and the supernatant after sedimentation were measured with a turbidity meter. The zeta potentials of the water sampled after rapid mixing were measured with a zeta potential meter (Zetasizer Nano ZS; Malvern Panalytical Ltd., Almelo, Netherlands) using a dip cell.

### 3.2.4 Floc particle size measurement

Floc particle size was measured by using a particle-size analyzer (Microtrac MT3300EXII; MicrotracBEL Corp., Osaka, Japan). Throughout the time of mixing, water in the beaker was introduced into the analyzer by a peristaltic pump at a flow rate of 0.5 mL/s (a sufficiently slow speed to avoid floc breakage). The outflow from the analyzer was discarded directly without

circulation (Fig. 3-1). As an index of floc formation speed, we used the time until the D50 (median diameter) of floc particles grew to 500 μm. Because the maximum D50 values were approximately 1 mm, the size was set to 0.5 mm. The time until the D50 grew to 500 μm and its 95% confidence interval were determined from the model-fit (Chassagne, 2021) by using Minitab (Minitab, LLC, Pennsylvania, USA).

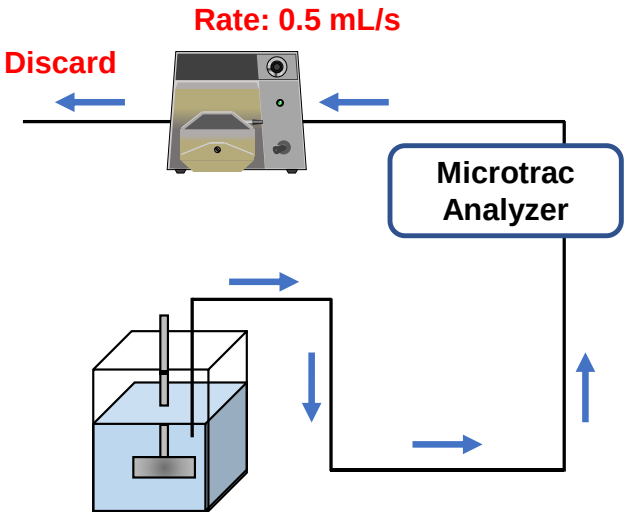


Fig. 3-1. The flow of the coagulation experiment and floc particle size measurement.

### 3.2.5 Calculation method for one-quarter concentration

During hydrolysis-precipitation rate test, samples were taken at pre-determined time and the Al concentration in the filtrate that passed through a 10-μm pore size membrane filter was measured by an inductively coupled plasma mass spectrometer (ICPMS, 7700x; Agilent Technologies, Inc., Santa Clara, CA, USA). Using Minitab (Minitab, LLC, Pennsylvania, USA), the experimental data were fitted to a model (initial exponential decrease followed by a plateau at a very low concentration) to determine the one-half concentration time, one-quarter concentration time (the time to reduce Al concentration to one-half and one-quarter, respectively, of the initial value) and their 95% confidence intervals. If no such change was observed (which was often the case for NOM water), the one-half concentration time and one-quarter concentration time were determined by interpolation of the experimental data.

## 3.3 Results and discussion

### 3.3.1 Effect of sulfate ion, pH, and PACl dose on PACl hydrolysis-precipitation

The discussion in Chapter 2 has revealed that the removability of superfine powdered activated carbon (SPAC) particles by coagulation and sedimentation varies greatly as a function of the basicity of PACl and the sulfate ion concentration of the raw water (J-1 water and J-2 water, Fig. 3-2) (Chen et al., 2020). For HB-PACl, the residual turbidity of the supernatant water was high in J-1 water (low sulfate ion concentration), but the residual turbidity was very low in J-2 water (high sulfate ion concentration). In contrast, when NB-PACl was applied, the residual turbidity was low in both J-1 and J-2 water. To confirm the universality of this phenomenon for the turbidity components (not SPAC), we conducted experiments using Y-, M-, and T-series waters (because the J-series water was consumed), and we varied the amount of PACl added and the coagulation pH. In addition to measuring the turbidity of the supernatant after sedimentation, we measured floc particle size during rapid and slow mixing (Fig. 3-3 and Fig. 3-4).

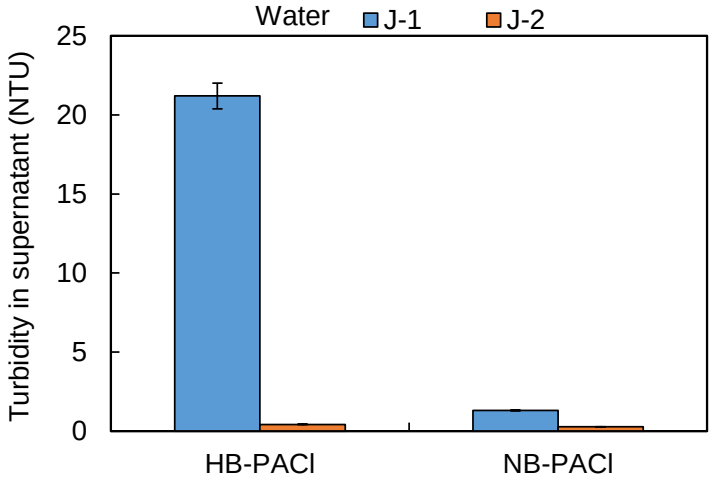


Fig. 3-2. The residual turbidities of supernatants. Waters J-1 and J-2 with sulfate ion concentrations of 4.0 mg/L and 15.3 mg/L, respectively, were used. Superfine powdered activated carbon was used as the removal target substance. HB-PACl and NB-PACl were used at a dose of 4.0 mg-Al/L. The coagulation pH was 7.0 (Chen et al., 2020).

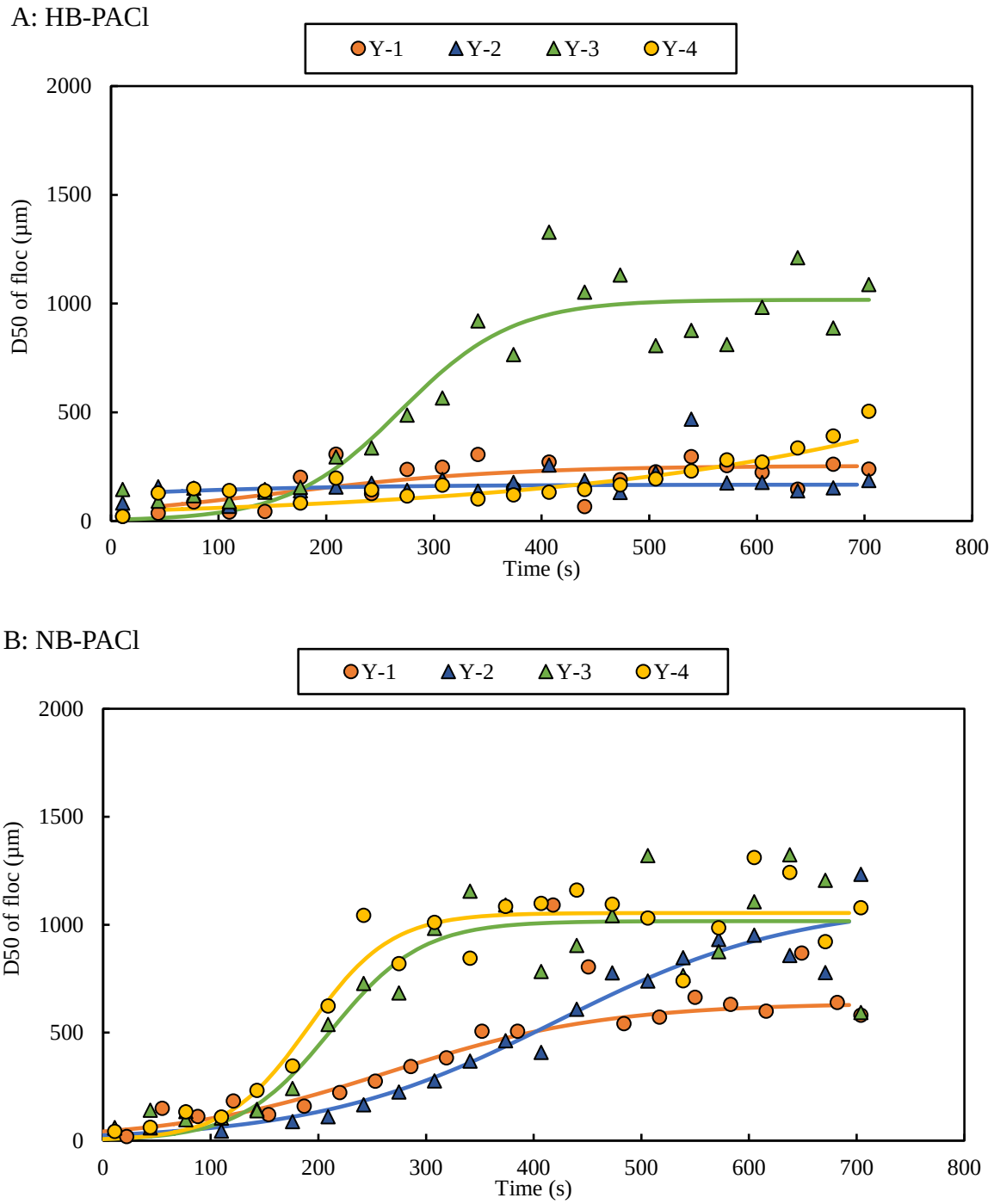


Fig. 3-3. Change of D50 of floc particles in coagulation experiments using HB-PACl (Panel A) and NB-PACl (Panel B). Particle size measurements were conducted every 10 s, and the average value of triplicate measurements is shown (plots). The lines are the fits to the semi-empirical model equation proposed by Chassagne (2021). The time until the D50 of floc particles grew to 500 μm was determined from the model-fit lines. Y series waters (Y-1–4) were used in these experiments. The PACl dose was 2.5 mg-Al/L. The coagulation pH was 7.0.

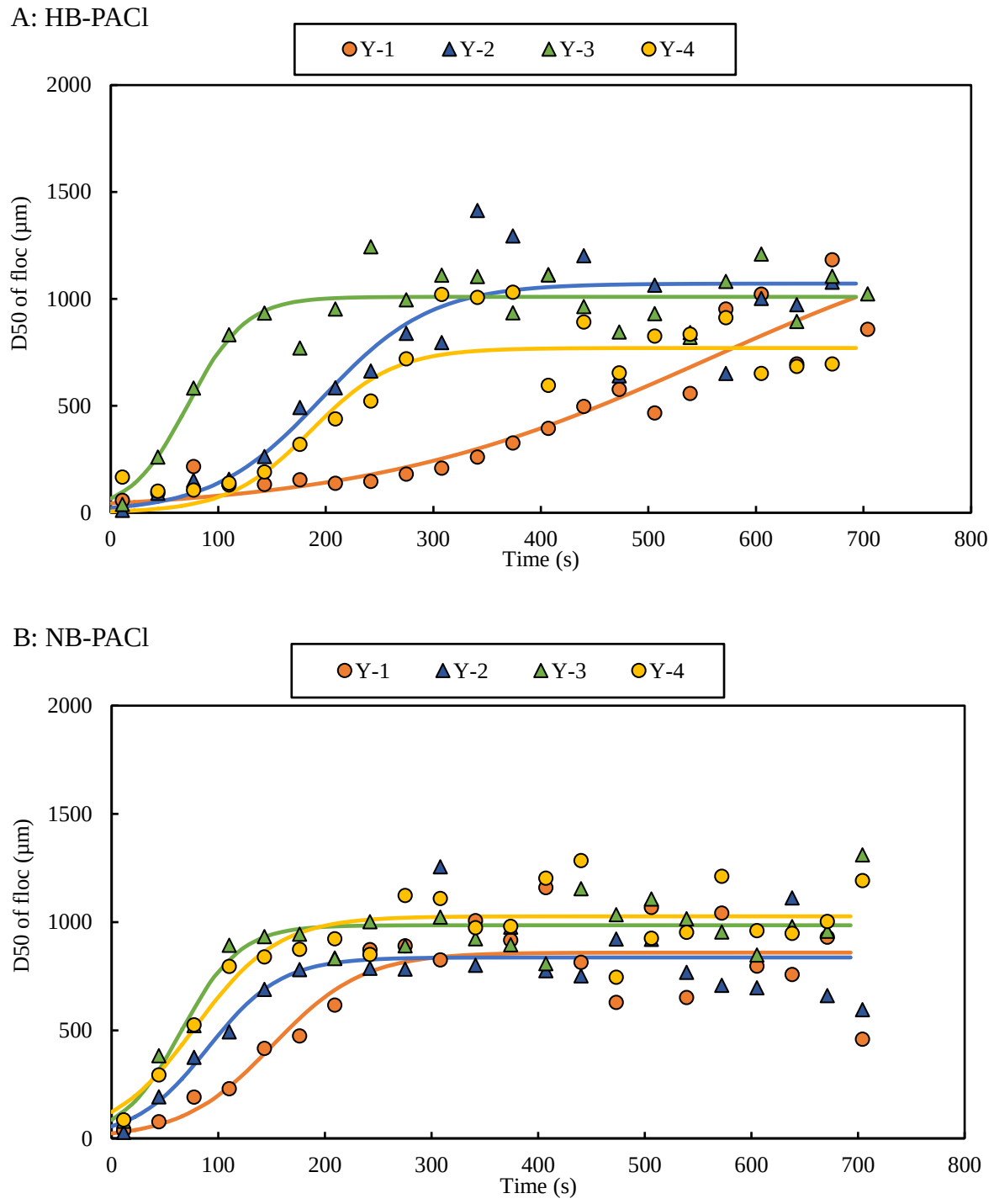


Fig. 3-4. Change of D50 of floc particles in coagulation experiments using HB-PACl (Panel A) and NB-PACl (Panel B). A particle size measurement was conducted every 10 s and the averages of triplicate measurements are shown (symbols). The lines are the fits to the semi-empirical model equation proposed by Chassagne (2021). The time until the D50 of the floc particles grew to 500 μm was determined from the model-fit lines. Y series waters (Y-1–4) were used in these experiments. The PACl dose was 2.5 mg-Al/L. The coagulation pH was 7.5.

Because the sulfate ion concentrations in the Y-1 and T-1 waters used in the experiment were low (< 0.06 mmol-$SO_4^{2-}$/L), coagulation with HB-PACl in these waters took more than 11 min to form floc particles with a D50 > 500 μm or did not form floc particles > 500 μm (Fig. 3-5). As a result, the rate of removal of turbidity after sedimentation was also generally low (Fig. 3-5). However, because floc formation was faster in M-1 water with higher sulfate ion concentrations, turbidity removal rates were higher. When sufficient sulfate ions were added to the Y-1 water, which had the lowest concentration of ions, to increase the concentration of sulfate ions to greater than 0.1 mmol/L, floc formation was faster, and the rate of turbidity removal was higher. In the case of NB-PACl, flocs with a D50 of 500 μm or greater were formed within 7 min in raw water with low as well as high sulfate ion concentrations, and the turbidities of the supernatants were low. On the weak alkaline side of pH 7.5, the coagulation pH at which PACls of high basicity excel (Kimura et al., 2013), floc formation was faster than at pH 7.0, but floc formation still required a longer time if the sulfate ion concentration in the water was low (0.04 mmol/L) than with the NB-PACl (Fig. 3-6 panel A). Furthermore, even when the dose was increased for HB-PACl, floc particles did not form in raw water with low sulfate ion concentrations, and the rate of turbidity removal was low (Fig. 3-7 panel A, B). Therefore, the reason why coagulation-flocculation by HB-PACl does not work well in raw water with low sulfate ion concentrations does not appear to be the insufficiency of its dose. In contrast, when the sulfate ion concentration in the raw water was high, the rate of floc formation also increased with an increase of PACl dose (Fig. 3-7 panel C), as is normally observed.

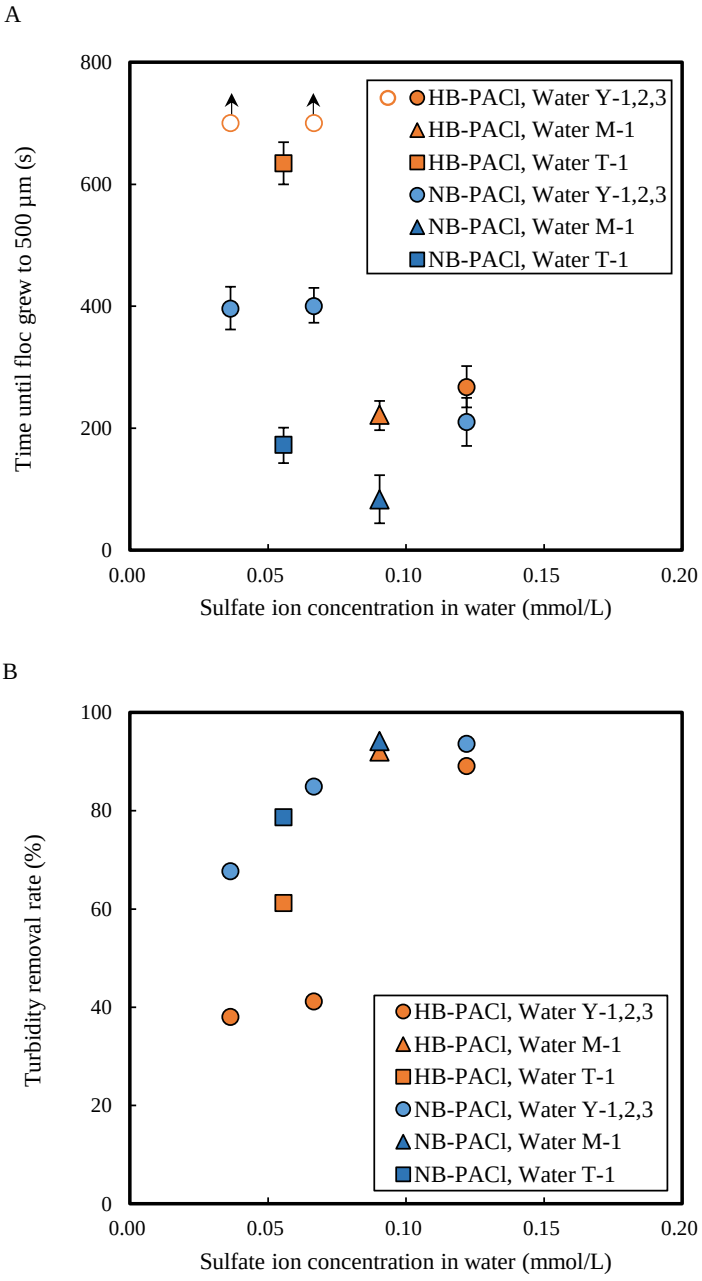


Fig. 3-5. Time until floc grew to 500 µm (Panel A) and the rate of turbidity removal (Panel B) of HB-PACl and NB-PACl in coagulation–flocculation experiments. Y-1–3, M-1, and T-1 waters were used in these experiments. The PACl dosage was 2.5 mg-Al/L. The coagulation pH was 7.0. Open circles with an arrow show data for HB-PACl in Y-1 and 2. In those experiments, no 500-µm floc formed by the end of mixing. Error bars in Panel A indicate 95% confidence intervals.

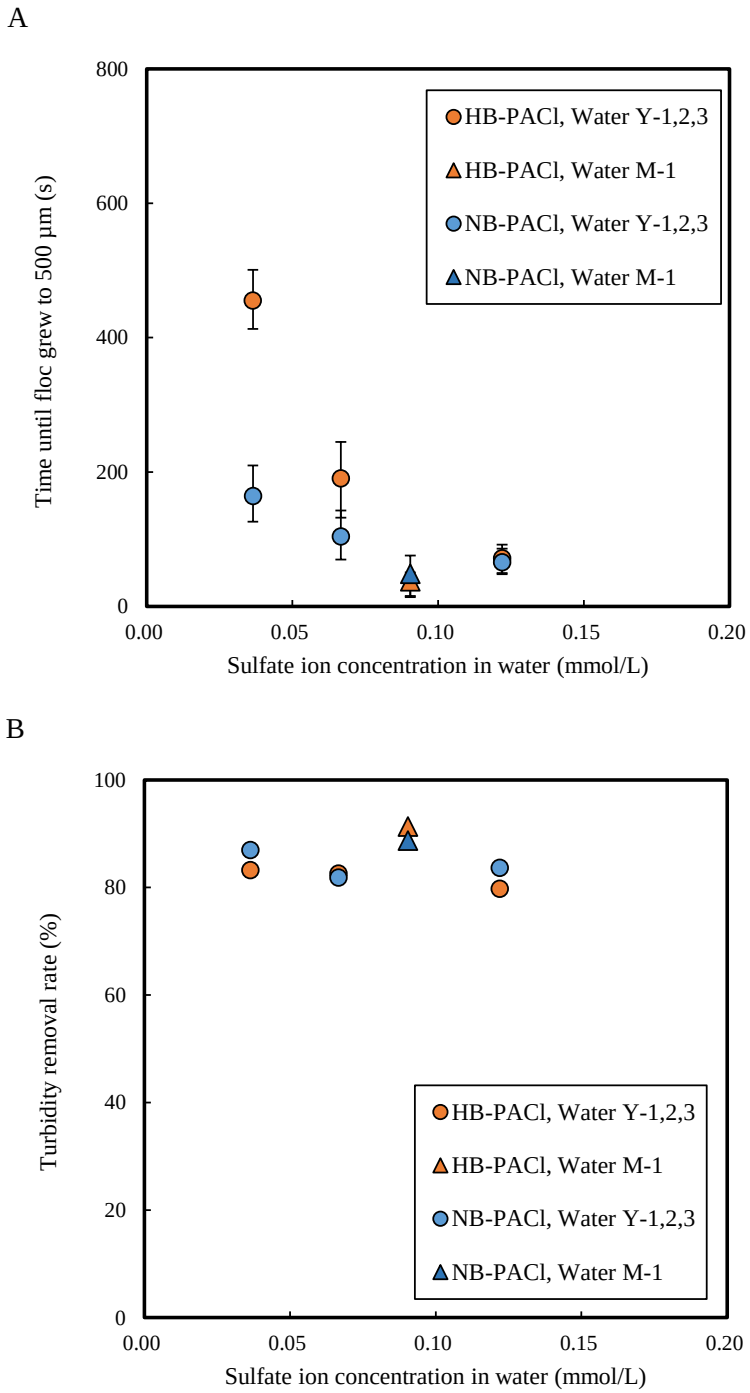


Fig. 3-6. Plots of the time until the floc grew to 500 µm (Panel A) and rate of turbidity removal (Panel B) against sulfate ion concentration. HB-PACl and NB-PACl were used. Y-1–3 and M-1 waters were used. The PACl dose was 2.5 mg-Al/L. The coagulation pH was 7.5. Error bars in Panel A indicate 95% confidence intervals.

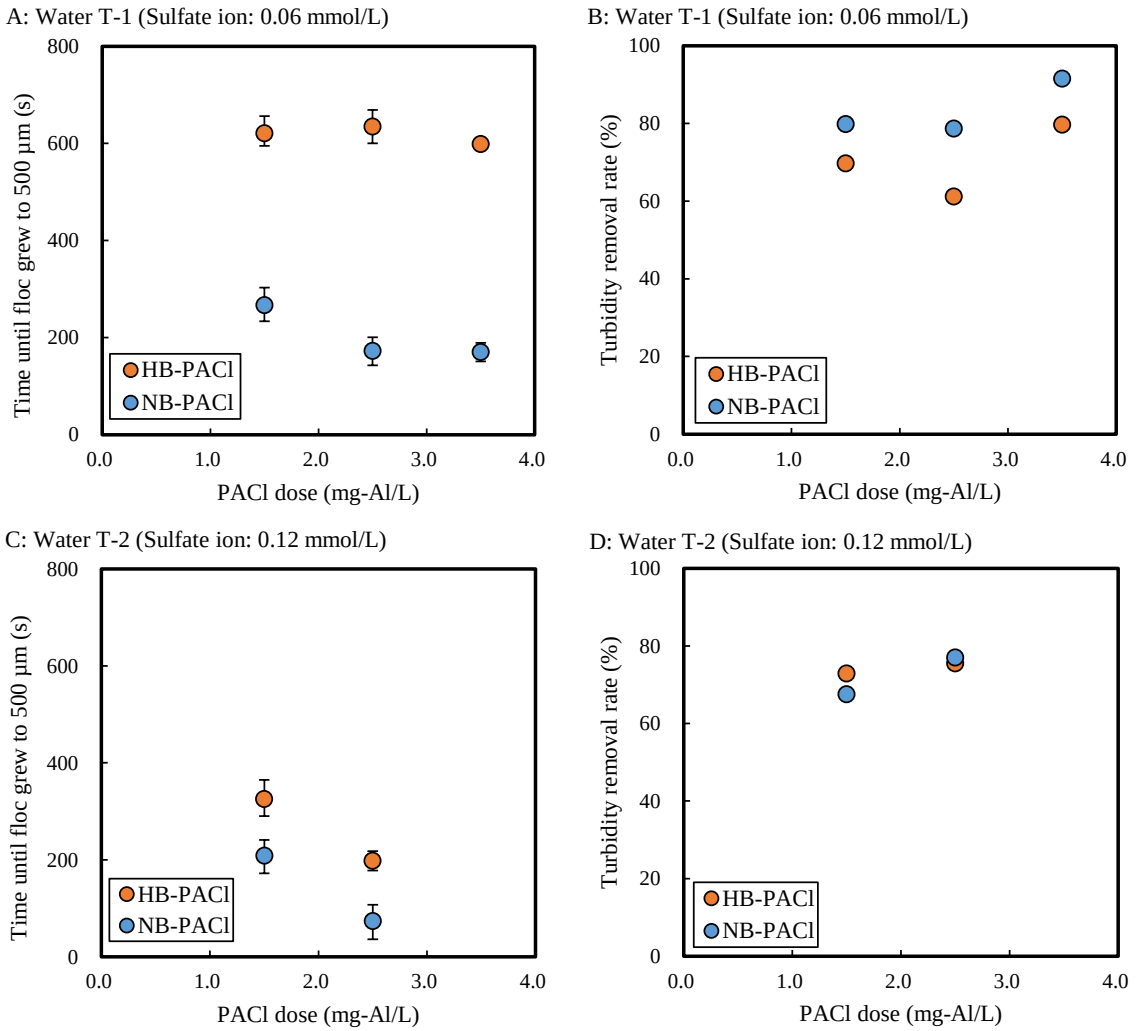


Fig. 3-7. Plots of the time till floc grew to 500 µm and rate of turbidity removal against PACl dose. Panels A and B show the data for HB-PACl and NB-PACl in water T-1. Panels C and D show the data in water T-2. The coagulation pH was controlled at 7.0. The PACls were 1.5, 2.5, and 3.5 mg-Al/L. Error bars in Panel A and C indicate 95% confidence intervals.

PACl dose of 5.6 mg-Al/L was applied in the experiment in S-1 water. To investigate the effect of PACl dose, the results of time till floc grow to 500 µm and the sulfate ion concentration in water are plotted in Fig. 3-8. Both HB-PACl and NB-PACl formed floc within a short time period in S-1 water. Plot in Fig. 3-8 were gained from experiments in different PACl dose and raw water characteristics (especially the very high turbidity water S-1), but the data at sulfate ion concentration at 0.12 mmol/L showed that at this sulfate ion concentration, the increase of PACl dose led to a faster floc formation, which supported the explanation for Fig. 3-7.

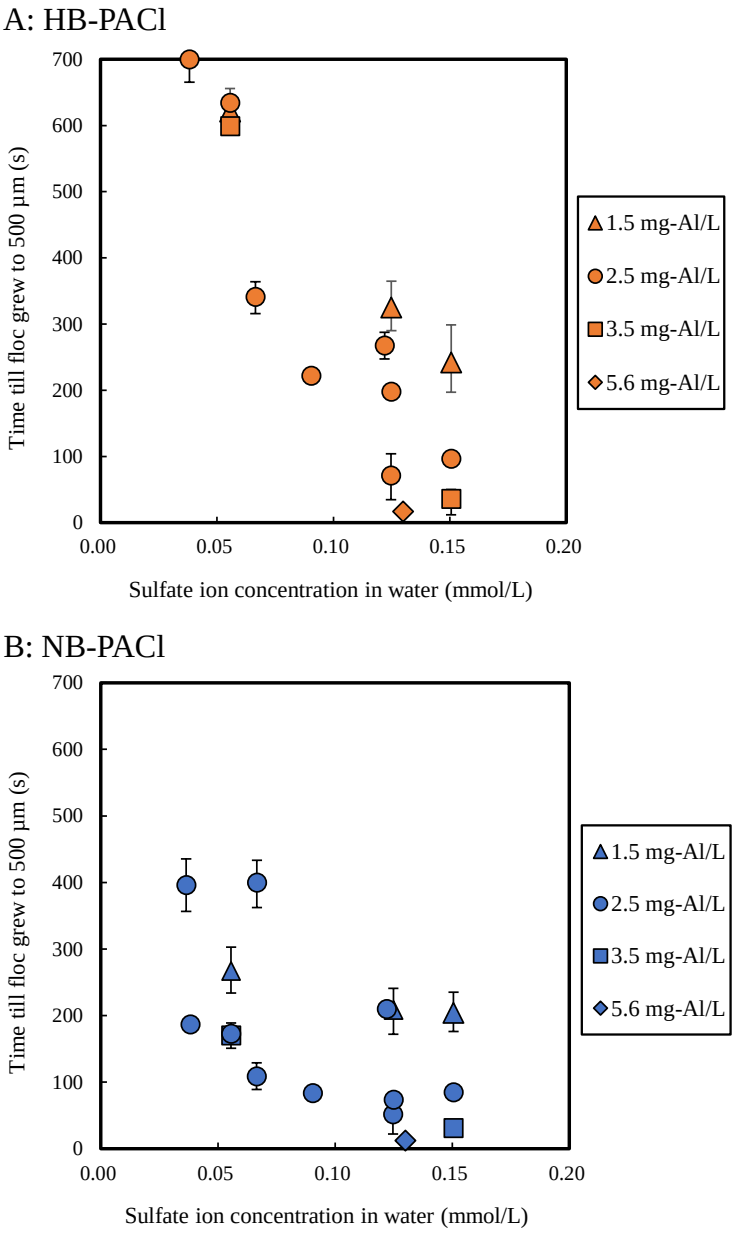


Fig. 3-8. Plots of the time till floc grew to 500 µm against sulfate ion concentration in water. Panels A and B show the data for HB-PACl and NB-PACl respectively. Y-1–6, M-1,2, T-1,2, and S-1 water were used. The coagulation pH was controlled at 7.0. Error bars indicate 95% confidence intervals.

### 3.3.2 Effect of alkalinity on PACl hydrolysis-precipitation

Because aluminum coagulants such as PACl consume alkalinity in the coagulation reaction, bicarbonate ions may also have an effect on PACl coagulation and floc formation. In NB-PACl, floc formation was faster in raw water with bicarbonate ion concentrations greater than 0.2

mmol/L than in raw water with bicarbonate ion concentrations less than 0.2 mmol/L, and floc particles with D50s of 500 μm or more were formed in a shorter time (Fig. 3-9 panel B). The effect of bicarbonate ion concentration was not clearly apparent in HB-PACl (Fig. 3-9 panel A). Overall, the rate of floc formation depended on the raw water, and in raw water with low concentrations of sulfate ions, the rate of floc formation with HB-PACl was inferior to that with NB-PACl.

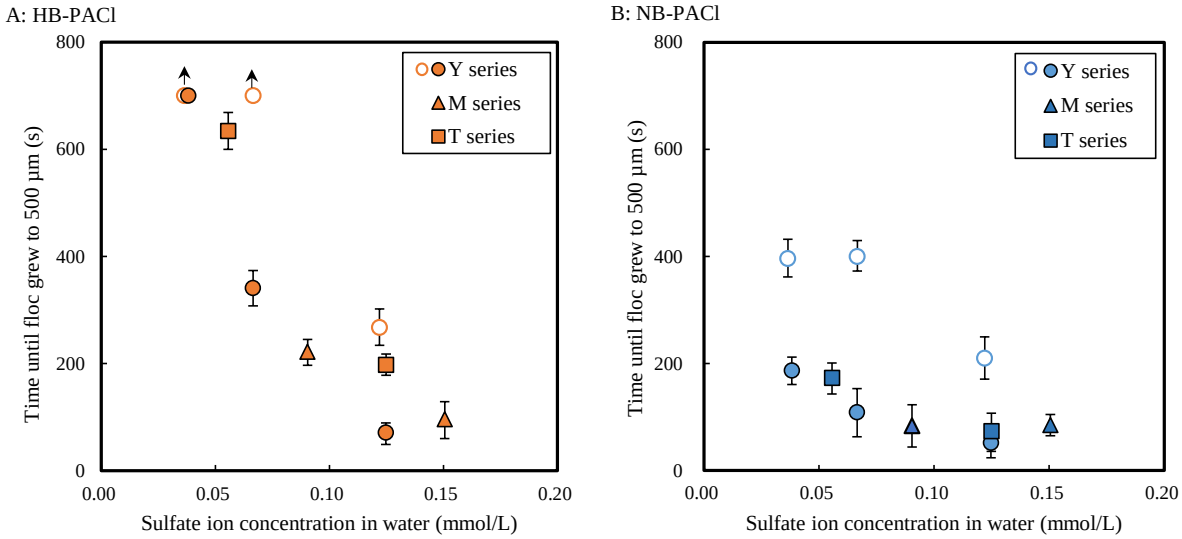


Fig. 3-9. Time until flocs of HB-PACl and NB-PACl grew to 500 μm in waters containing different concentrations of sulfate ions. Y series waters (Y-1–6), M-1,2, and T-1,2 waters were used in these experiments. The PACl dose was 2.5 mg-Al/L. The coagulation pH was 7.0. Open circles indicate that bicarbonate ion concentrations in the waters were lower than 0.2 mmol/L. Error bars indicate 95% confidence intervals.

### 3.3.3 Limitation of conventional indices of coagulant properties

Conventional indices of coagulant properties include the ferron distribution of Al species, the colloid charge, and $^{27}$Al nuclear magnetic resonance (NMR). The analytical results for the two PACls used in this study are shown in Fig. 2-7 (Section 2.3.1 in Chapter 2). The ferron distribution (Panel A) indicated that HB-PACl had a higher content of $Al_b$ + $Al_c$, which are generally regarded as the aluminum species with the highest charge-neutralization capacity

(Yan et al., 2008). The colloid charge was actually higher for HB-PACl than for NB-PACl (Panel B). The peak at 62.5 ppm in the $^{27}$Al-NMR spectrum (Panel C) indicated that the concentration of Kegging-type e-$Al_{13}$ polycations, which have relatively high charge neutralization ability (Z. Chen et al., 2007; Parker & Bertsch, 1992; Sposito, 1995), was higher in HB-PACl than in NB-PACl. This superior charge neutralization ability of HB-PACl suggests that it should be a better coagulant than NB-PACl.

The zeta potential has commonly been used as an indicator of whether the neutralization of the particle charge necessary for coagulation is sufficient. In our experiments, we measured the zeta potential of the floc particles after rapid mixing for coagulation. The zeta potentials of floc particles seemed closer to zero when they were formed by HB-PACl than by NB-PACl (Panel A of Fig. 3-10), and the former particles were better destabilized because of the higher charge-neutralization capacity of the HB-PACl, but HB-PACl coagulation removed less turbidity than NB-PACl coagulation. Even when HB-PACl reduced the zeta potential of the flocs closer to zero than NB-PACl, floc formation took a longer time (Panel A). The zeta potential could therefore not explain why the coagulation performance of HB-PACl and NB-PACl depended on the raw water, and it was unclear why the charge neutralization mechanism was unrelated to the inferior coagulation performance of HB-PACl compared with NB-PACl when raw water with a low concentration of sulfate ions was treated. In contrast, moderate correlations were apparent between the zeta potential and turbidity removal for each HB-PACl and NB-PACl (Panel B of Fig. 3-10). However, the rates of turbidity removal by HB-PACl and NB-PACl were very different, even when the zeta potentials were the same. Although charge neutralization as measured by the zeta potential is still a necessary requirement for coagulation by HB-PACl and NB-PACl, comparison of the turbidity removal abilities of HB-PACl and NB-PACl is not possible based on zeta potential alone.

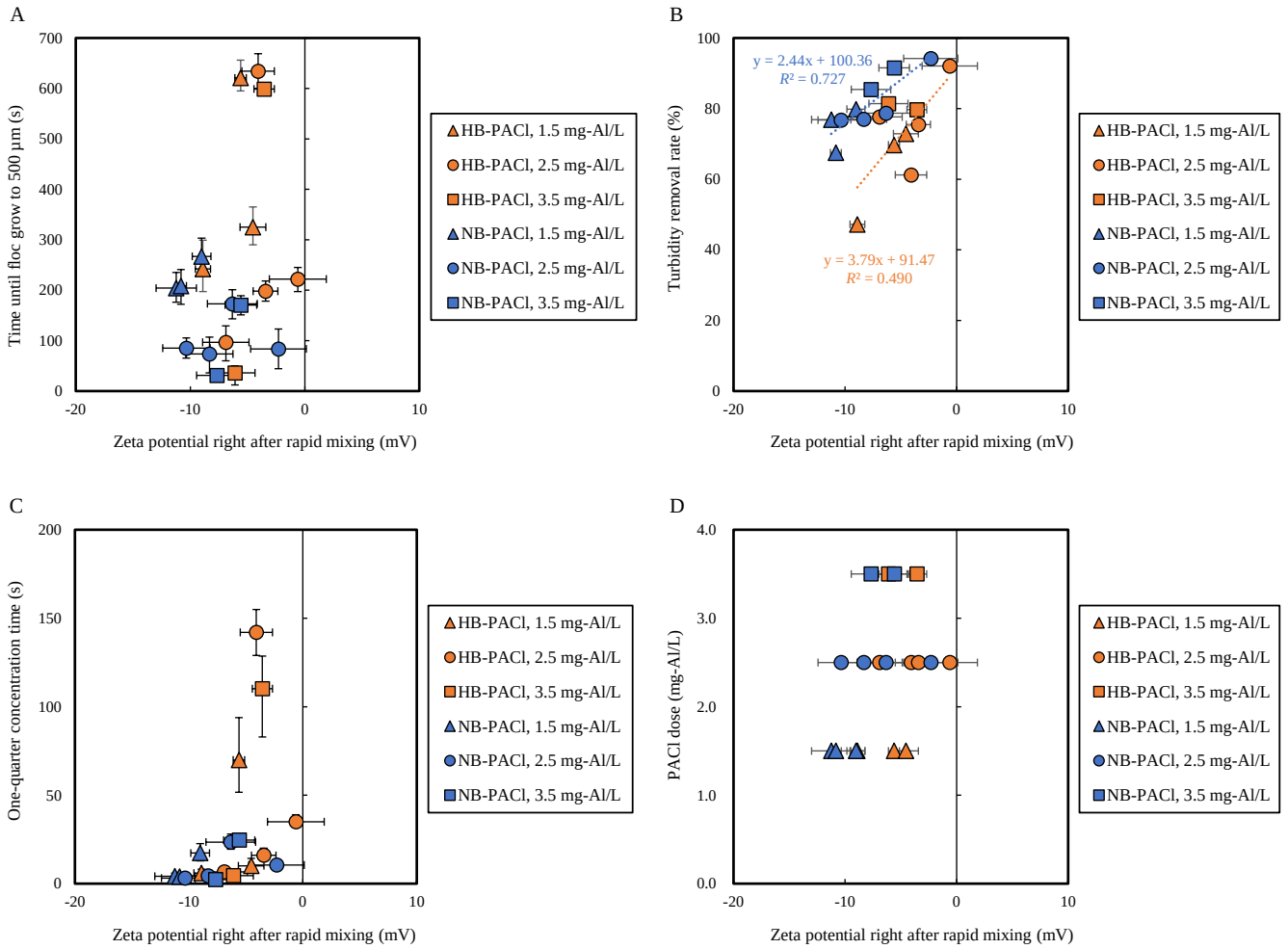


Fig. 3-10. Plots of the time until floc grow to 500 µm (Panel A), turbidity removal rate (Panel B), one-quarter concentration time in hydrolysis-precipitation rate test (Panel C), and PACl dose (Panel D) against zeta potential right after rapid mixing. HB-PACl and NB-PACl were used. The PACl doses were 1.5, 2.5, and 3.5 mg-Al/L. Coagulation experiments were conducted in M and T series waters. The coagulation pH was 7.0. Error bars in *x*-axis indicate standard deviations. Error bars in *y*-axis in Panel A and C indicate 95% confidence intervals.

### 3.3.4 Correlation between PACl hydrolysis-precipitation and coagulation performance

A previous study dealing with coagulation of superfine powdered activated carbon particles (Chen et al., 2020) mentions an Al hydrolysis–precipitation reaction and proposes that the change of dissolved Al concentration, which is related to the polymerization of aluminum species, is a key property, besides charge-neutralization capacity, for proper coagulation, including formation of large floc particles. Chu et al (2008) indicate that zeta potential is not the only indicator for the coagulant efficiency when aluminum precipitation significantly improves coagulation. An et al. (2021) also mention the importance of hydrolysis and have reported that $Al_{13}$ polycation hydrolyzes while retaining its structure.

In this study, we used one-quarter concentration time (the time required to reduce the soluble Al concentration fourfold from the initial concentration, as described in Section 3.2.5) as the index of the rate of PACl hydrolysis-precipitation. As shown in Fig. 3-11, when the rate of floc formation was slow (a long time was required for the floc to grow to a size of 500 μm), the one-quarter concentration time was long (the rate of PACl hydrolysis-precipitation was slow). The rates of floc formation, which depended on the type of coagulant (HB-PACl or NB-PACl) and dose, water quality (sulfate and bicarbonate ion concentrations), and pH, were correlated to the rates of PACl hydrolysis-precipitation ($R^2$ = 0.614). The correlation became somewhat stronger ($R^2$ = 0.672) when we omitted the datum associated with the lowest dose (1.5 mg/L), which resulted in low particle charge neutralization (Fig. 3-12). Hydrolysis of aluminum was therefore found to be an important factor for floc formation. The rate of turbidity removal was also measured, and the results are shown in Fig. 3-13. Low turbidity removal (< 70%) was observed when the rates of PACl hydrolysis-precipitation were slow (the one-quarter concentration time exceeded 30 s) or the zeta potential was lower than −5 mV (Fig. 3-10 panel B). In summary, the dependence of coagulation performance on PACl type and water quality (sulfate ion

concentration) was related to the hydrolysis-precipitation of aluminum species in the PACl. The rate of hydrolysis-precipitation was identified as an indicator that could be used to evaluate the compatibility of the raw water with HB-PACl.

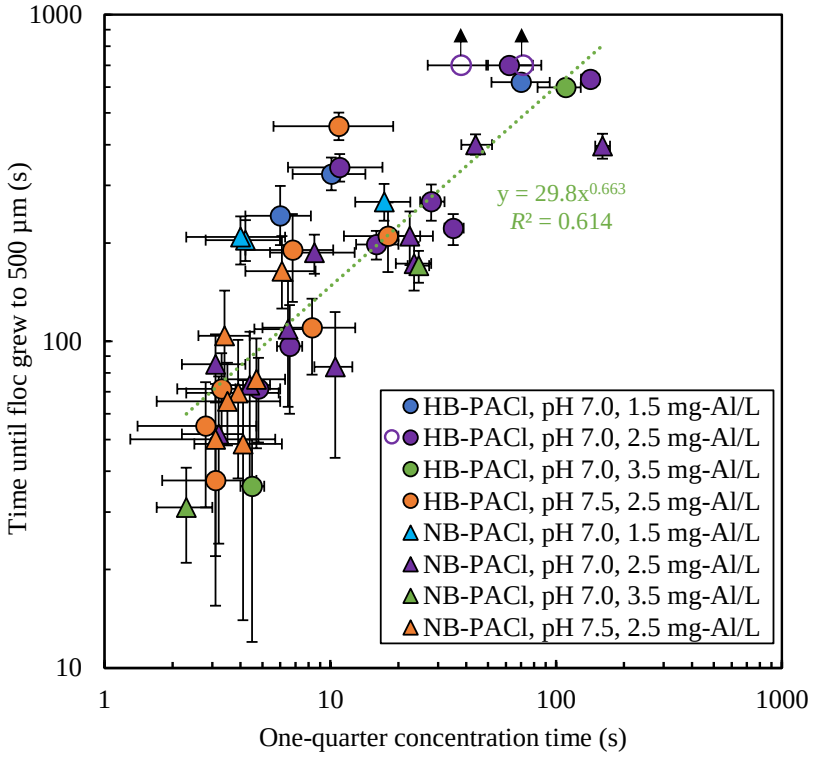


Fig. 3-11. Relationship between the time until floc grew to 500 µm and one-quarter concentration times in coagulation experiments. The results for HB-PACl and NB-PACl at pHs of both 7.0 and 7.5 are shown. Y-1–6, M-1,2, and T-1,2 waters were used in these experiments. Results for PACl doses of 1.5, 2.5, and 3.5 mg-Al/L are shown. Open circles indicate that floc size did not grow to 500 µm during flocculation. Error bars indicate 95% confidence intervals.

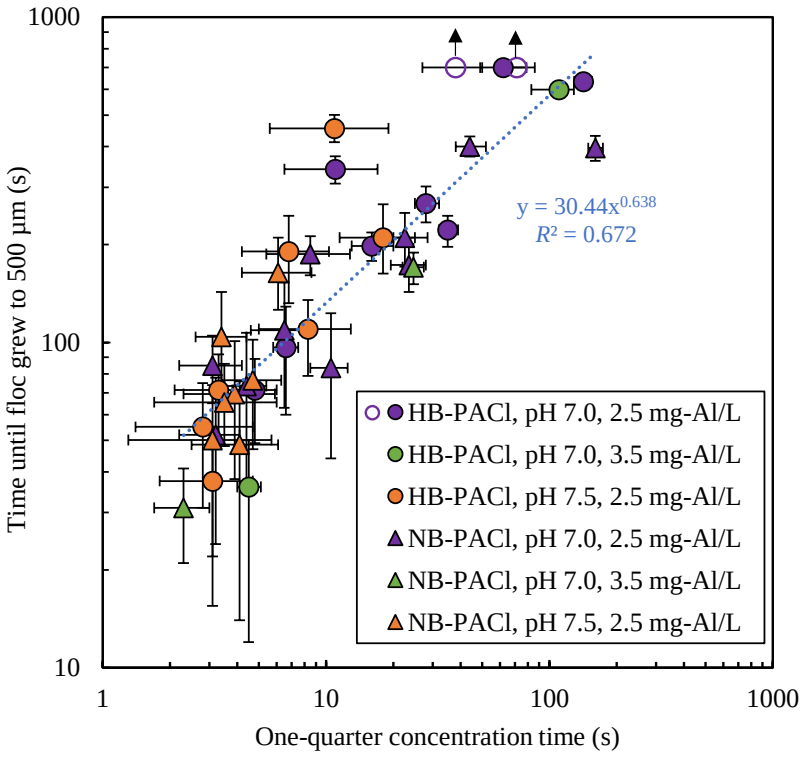


Fig. 3-12. Relationship between the time until floc grew to 500 µm and one-quarter concentration times in coagulation experiments. The results for HB-PACl and NB-PACl at pHs of both 7.0 and 7.5 are shown. Y-1–6, M-1,2, and T-1,2 waters were used in these experiments. Results for PACl doses of 2.5 and 3.5 mg-Al/L are shown. Open circles indicate that floc size did not grow to 500 µm during flocculation. Error bars indicate 95% confidence intervals.

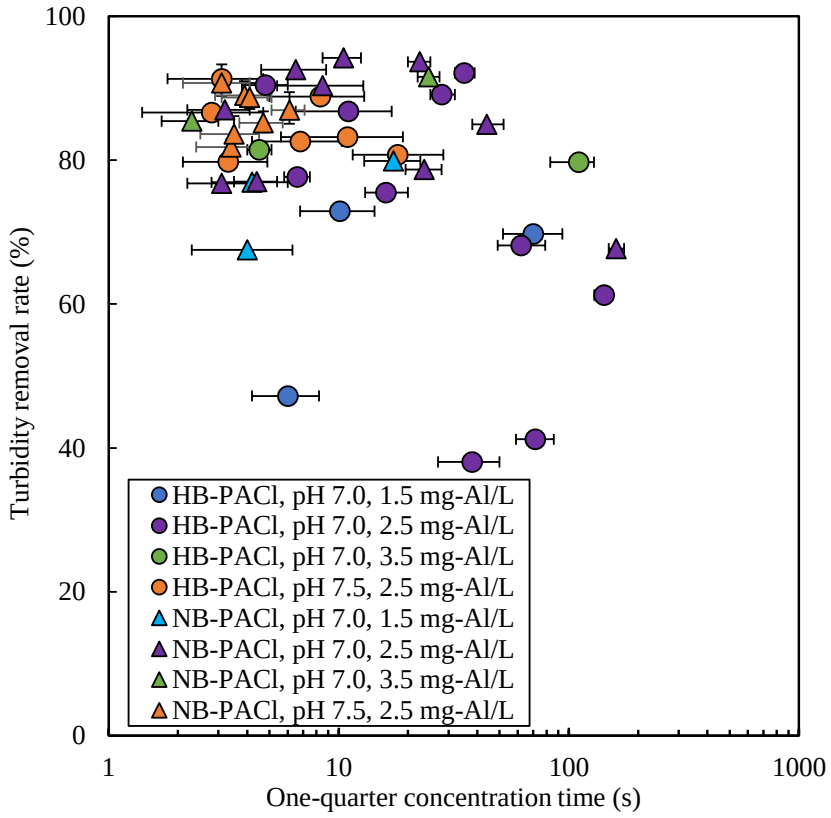


Fig. 3-13. Relationship between the rate of turbidity removal and the one-quarter concentration time. HB-PACl and NB-PACl were used. Y-1–6, M-1,2, and T-1,2 waters were used. The PACl doses were 1.5, 2.5, and 3.5 mg-Al/L. Coagulation pHs were 7.0 and 7.5. Error bars indicate 95% confidence intervals.

## 3.4 Chapter summary

In this chapter, the coagulation performance and hydrolysis-precipitation of HB-PACl and NB-PACl were tested using various natural raw waters under different condition.

1) Under different conditions of pH and PACl dose, the rate of floc formation by PACls with different basicities and polymerization degrees (HB-PACl and NB-PACl) varied as a function of the characteristics of the raw water. Those variations were related to the hydrolyze ability of the PACls.

2) Zeta potential is an important and necessary factor when evaluating the coagulation process. However, zeta potential was not able to explain why the coagulation performance of HB-PACl and NB-PACl was correlated with raw water. It still cannot explain the fail of coagulation when using HB-PACl in a low sulfate ion concentration water.

3) Rates of floc formation were strongly correlated with the rate of aluminum hydrolysis-precipitation rate irrespective of raw waters and coagulation conditions. The hydrolysis-precipitation rate of PACl is a key property besides charge neutralization capacity for proper coagulation and can be used to evaluate the compatibility of the raw water with HB-PACl.

## 3.5 Reference

An, G., Yue, Y., Wang, P., Liu, L., Demissie, H., Jiao, R., & Wang, D. (2021). Deprotonation and aggregation of Al13 under alkaline titration: A simulating study related to coagulation process. Water Research, 203(June), 117562. https://doi.org/10.1016/j.watres.2021.117562

Chassagne, C. (2021). A simple model to study the flocculation of suspensions over time. Chemical Engineering Research and Design, 172, 302–311. https://doi.org/10.1016/j.cherd.2021.06.006

Chen, Y., Nakazawa, Y., Matsui, Y., Shirasaki, N., & Matsushita, T. (2020). Sulfate ion in raw water affects performance of high-basicity PACl coagulants produced by Al(OH)3 dissolution and base-titration: Removal of SPAC particles by coagulation-flocculation, sedimentation, and sand filtration. Water Research, 183, 116093. https://doi.org/10.1016/j.watres.2020.116093

Chen, Z., Luan, Z., Fan, J., Zhang, Z., Peng, X., & Fan, B. (2007). Effect of thermal treatment on the formation and transformation of Keggin Al13 and Al30 species in hydrolytic polymeric aluminum solutions. Colloids and Surfaces A: Physicochemical and Engineering Aspects, 292(2–3), 110–118. https://doi.org/10.1016/j.colsurfa.2006.06.005

Chu, Y., Gao, B., Yue, Q., & Wang, Y. (2008). Investigation of dynamic processing on aluminum floc aggregation: Cyclic shearing recovery and effect of sulfate ion. Science in China, Series B: Chemistry, 51(4), 386–392. https://doi.org/10.1007/s11426-007-0129-2

Kimura, M., Matsui, Y., Kondo, K., Ishikawa, T. B., Matsushita, T., & Shirasaki, N. (2013). Minimizing residual aluminum concentration in treated water by tailoring properties of polyaluminum coagulants. Water Research, 47(6), 2075–2084. https://doi.org/10.1016/j.watres.2013.01.037

Parker, D. R., & Bertsch, P. M. (1992). Identification and Quantification of the “Al13” Tridecameric Aluminum Polycation Using Ferron. Environmental Science and Technology, 26(5), 908–914. https://doi.org/10.1021/es00029a006

Sato, F., & Matsuda, S. (2009). Novel Basic Aluminum Chloride, Its Manufacturing Method and Its Application. Japanese Patent, Application, 2008–047932.

Sposito, G. (1995). The Environmental Chemistry of Aluminum, Second Edition. Taylor & Francis. https://books.google.co.jp/books?id=lNxltQeVP9UC

Yan, M., Wang, D., Ni, J., Qu, J., Chow, C. W. K., & Liu, H. (2008). Mechanism of natural organic matter removal by polyaluminum chloride: Effect of coagulant particle size and hydrolysis kinetics. Water Research, 42(13), 3361–3370. https://doi.org/10.1016/j.watres.2008.04.017

Ye, C., Wang, D., Shi, B., Yu, J., Qu, J., Edwards, M., & Tang, H. (2007). Alkalinity effect of coagulation with polyaluminum chlorides: Role of electrostatic patch. Colloids and Surfaces A: Physicochemical and Engineering Aspects, 294(1–3), 163–173. https://doi.org/10.1016/j.colsurfa.2006.08.005

# Chapter 4. Quantifying the effects of inorganic ions on PACl hydrolysis

## 4.1 Introduction

The PACl hydrolysis-precipitation has been proved to have a strong correlation with floc formation in coagulation-flocculation process (Chapter 3). The hydrolysis-precipitation can reflect the PACl coagulation performance at different pH, PACl dosage, and alkalinity, therefore it is supposed to be an important factor besides conventional index. Sulfate ions are able to strongly facilitate PACl hydrolysis-precipitation (Chapter 2). However, it is necessary to consider the effects of multi-ions because various types of inorganic ions exist in different concentration in natural water (Nikanorov & Brazhnikova, 2009). To use hydrolysis-precipitation rate in a multi-ions condition, it is necessary to figure out the effect of each common ion on PACl hydrolysis-precipitation respectively. One of the objectives of this chapter is to comprehensively investigate the correlation between raw water characteristics and PACl hydrolysis-precipitation. To achieve this objective, we investigated and compared the effect of common ions (sulfate ion, bicarbonate ion, chloride ion, nitrate ion, and cations) and natural organic matter (NOM) on PACl hydrolysis by hydrolysis-precipitation rate test. Another objective is to quantify the effects of inorganic ions and NOM on PACl hydrolysis-precipitation, thus the hydrolysis can be estimated and calculated when applying PACl on new water condition. Additionally, by comparing with other divalent ions, we considered the mechanism related to why sulfate ion can strongly facilitate PACl hydrolysis-precipitation.

The contents of Chapter 3 and Chapter 4 have been summarized as a journal article. The journal article has been submitted to Water Research and is now under peer review. The information is described as follows:

Title: Overlooked effect of ordinary inorganic ions on polyaluminum-chloride coagulation treatment

Author: Yize Chen, Yoshihiko Matsui, Tsutomu Sato, Nobutaka Shirasaki, Taku Matsushita

Journal: Water Research

Condition: Under peer review

## 4.2 Materials and methods

### 4.2.1 PACl coagulants

The PACl coagulants used in this chapter were HB-PACl and NB-PACl, which were the same as that mentioned in Section 3.2.1.

### 4.2.2 Water

Waters tested in this study were given 16 designations. Table 4-1, Table 4-2, and Table 4-3 show the water characteristics. Waters designated Y-1, J-1, M-1, T-1, and S-1 (Table 4-1) were natural waters sampled from the Kuromorigawa Reservoir (Akita, Japan), Jyoganji River (Toyama, Japan), Toyohira River (Hokkaido, Japan), Jyoganji River, and Shiraikawa water treatment plant (Hokkaido, Japan), respectively. Waters J-1 and T-1 were sampled from the same river on different dates. Waters designated Y-2–6, J-2, M-2, and T-2 were prepared by adding $Na_2SO_4$ and $NaHCO_3$ to the respective natural water.

Series of $Na_2SO_4$, $NaHCO_3$, NaCl, $NaNO_3$, $K_2SO_4$, $MgSO_4$, $CaSO_4$, $Na_2SeO_4$, $Na_2S_2O_3$, and $Na_2CrO_4$ were prepared by dissolving $Na_2SO_4$, $NaHCO_3$, NaCl, $NaNO_3$, $K_2SO_4$, $MgSO_4$, $Ca(OH)_2$ (99.9%), $Na_2SeO_4$, $Na_2S_2O_3 \cdot 5H_2O$, and $Na_2CrO_4 \cdot 4H_2O$ (FUJIFILM Wako Pure Chemical Corporation., Osaka, Japan), respectively, into pure water (Elix water, Elix Advantage; Merck KGaA, Darmstadt, Germany) slightly buffered with bicarbonate (0.24 mmol/L, 12 mg/L as $CaCO_3$). SRNOM series water was prepared by dissolving Suwannee River Natural Organic Matter (International Humic Substances Society, FUJIFILM Wako Pure Chemical Corporation) into pure water slightly buffered with bicarbonate. The water was then filtered through a polytetrafluoroethylene (PTFE) membrane filter (Φ90 mm, 0.45-μm pore size; Toyo Roshi Kaisha, Ltd., Tokyo, Japan).

These waters were stored at 4 °C prior to experiments, which were begun after the temperature of the waters had returned to room temperature (~20 °C). Concentrations of ions in the water were measured by ion chromatography (Integrion and ICS-1100; Thermo Scientific, Bremen, Germany). At the experimental pH of 7.0, almost all the alkalinity is associated with bicarbonate ions. The alkalinity was measured by titration with sulfuric acid (0.01 M $H_2SO_4$, FUJIFILM Wako Pure Chemical Corporation), and then the concentration of bicarbonate ions was determined from the alkalinity. For measurements of dissolved organic carbon (DOC) and ultraviolet (UV) light absorbance, a water sample was filtered through a membrane filter (0.45-μm pore size; Toyo Roshi Kaisha, Ltd., Tokyo, Japan). The DOC was measured with a TOC analyzer (TOC900; GE Analytical Instruments, Inc., Boulder, CO, USA). The UV absorbance was measured at 260 nm (UV260 value) with a spectrophotometer (UV-1800; Shimadzu, Kyoto, Japan). Turbidity was measured with a turbidity meter (WA7700; Nippon Denshoku Industries Co., Ltd; Tokyo, Japan).

Table 4-1.

Ion components, alkalinity, DOC, UV260, and turbidity of the Y, J, M, T, and S water series used in this study

| Series | Water | $Na^+$ | $K^+$ | $Mg^{2+}$ | $Ca^{2+}$ | $Cl^-$ | $NO_3^-$ | $SO_4^{2-}$ | Alkalinity meq/L | DOC | UV260 | Turbidity | Source |
|---|---|---|---|---|---|---|---|---|---|---|---|---|---|
| | | mmol/L | mmol/L | mmol/L | mmol/L | mmol/L | mmol/L | mmol/L | $\approx HCO_3^-$ mmol/L | mg-C/L | $cm^{-1}$ | NTU | |
| Y | Y-1 | 0.34 | 0.02 | 0.05 | 0.04 | 0.37 | 0.00 | 0.04 | 0.08 | 1.9 | 0.04 | 5.2 | Kuromorigawa Reservoir |
| | Y-2 | 0.40 | 0.02 | 0.05 | 0.03 | 0.34 | 0.01 | 0.07 | 0.08 | 1.8 | 0.04 | 5.6 | |
| | Y-3 | 0.51 | 0.02 | 0.05 | 0.04 | 0.33 | 0.01 | 0.12 | 0.08 | 1.8 | 0.04 | 5.4 | |
| | Y-4 | 0.62 | 0.02 | 0.05 | 0.04 | 0.34 | 0.01 | 0.04 | 0.34 | 1.9 | 0.04 | 4.9 | |
| | Y-5 | 0.68 | 0.02 | 0.05 | 0.04 | 0.34 | 0.00 | 0.07 | 0.34 | 1.8 | 0.04 | 5.1 | |
| | Y-6 | 1.10 | 0.02 | 0.05 | 0.04 | 0.34 | 0.02 | 0.12 | 0.66 | 1.9 | 0.04 | 5.9 | |
| J | J-1 | 0.08 | 0.01 | 0.04 | 0.16 | 0.05 | 0.01 | 0.04 | 0.32 | 0.5 | NM | NM | Joganji River |
| | J-2 | 0.35 | 0.01 | 0.04 | 0.16 | 0.05 | 0.01 | 0.16 | 0.32 | 0.5 | NM | NM | |
| M | M-1 | 0.24 | 0.02 | 0.05 | 0.14 | 0.19 | 0.01 | 0.09 | 0.20 | 0.4 | 0.03 | 3.2 | Toyohira River |
| | M-2 | 0.45 | 0.04 | 0.09 | 0.23 | 0.37 | 0.02 | 0.15 | 0.34 | 0.4 | 0.03 | 1.1 | |
| T | T-1 | 0.08 | 0.01 | 0.04 | 0.18 | 0.04 | 0.01 | 0.06 | 0.32 | 0.4 | 0.02 | 1.4 | Jyoganji River |
| | T-2 | 0.55 | 0.01 | 0.04 | 0.18 | 0.04 | 0.01 | 0.12 | 0.66 | 0.4 | 0.02 | 1.6 | |
| S | S-1 | 0.31 | 0.04 | 0.06 | 0.18 | 0.29 | 0.02 | 0.13 | 0.23 | 2.9 | 0.10 | 67.7 | Shiraikawa Treatment Plant |

Table 4-2.

Ion components, alkalinity, DOC, and UV260 values of waters used in this study

| Series | Water | $Na^+$ | $K^+$ | $Mg^{2+}$ | $Ca^{2+}$ | $Cl^-$ | $NO_3^-$ | $SO_4^{2-}$ | Alkalinity meq/L | DOC | UV260 | Source |
|---|---|---|---|---|---|---|---|---|---|---|---|---|
| | | mmol/L | mmol/L | mmol/L | mmol/L | mmol/L | mmol/L | mmol/L | $\approx HCO_3^-$ mmol/L | mg-C/L | $cm^{-1}$ | |
| $Na_2SO_4$ | $Na_2SO_4$-1 | 1.21 | 0.00 | 0.00 | 0.00 | 0.00 | 0.00 | 0.47 | 0.24 | 0.0 | 0.00 | Elix water |
| | $Na_2SO_4$-2 | 0.60 | 0.00 | 0.00 | 0.00 | 0.00 | 0.00 | 0.18 | 0.24 | 0.0 | 0.00 | |
| | $Na_2SO_4$-3 | 0.43 | 0.00 | 0.00 | 0.00 | 0.00 | 0.00 | 0.09 | 0.24 | 0.0 | 0.00 | |
| | $Na_2SO_4$-4 | 0.52 | 0.00 | 0.00 | 0.00 | 0.00 | 0.00 | 0.13 | 0.24 | 0.0 | 0.00 | |
| | $Na_2SO_4$-5 | 0.33 | 0.00 | 0.00 | 0.00 | 0.00 | 0.00 | 0.04 | 0.24 | 0.0 | 0.00 | |
| | $Na_2SO_4$-6 | 0.88 | 0.00 | 0.00 | 0.00 | 0.00 | 0.00 | 0.32 | 0.24 | 0.0 | 0.00 | |
| | $Na_2SO_4$-7 | 0.38 | 0.00 | 0.00 | 0.00 | 0.00 | 0.00 | 0.06 | 0.24 | 0.0 | 0.00 | |
| | $Na_2SO_4$-8 | 1.37 | 0.00 | 0.00 | 0.00 | 0.00 | 0.00 | 0.17 | 1.00 | 0.0 | 0.00 | |
| | $Na_2SO_4$-9 | 0.45 | 0.00 | 0.00 | 0.00 | 0.00 | 0.00 | 0.16 | 0.10 | 0.0 | 0.00 | |
| | $Na_2SO_4$-10 | 0.95 | 0.00 | 0.00 | 0.00 | 0.00 | 0.00 | 0.16 | 0.61 | 0.0 | 0.00 | |
| | $Na_2SO_4$-11 | 0.35 | 0.00 | 0.00 | 0.00 | 0.00 | 0.00 | 0.13 | 0.10 | 0.0 | 0.00 | |
| | $Na_2SO_4$-12 | 0.87 | 0.00 | 0.00 | 0.00 | 0.00 | 0.00 | 0.13 | 0.61 | 0.0 | 0.00 | |
| | $Na_2SO_4$-13 | 1.27 | 0.00 | 0.00 | 0.00 | 0.00 | 0.00 | 0.13 | 1.00 | 0.0 | 0.00 | |
| | $Na_2SO_4$-14 | 2.04 | 0.00 | 0.00 | 0.00 | 0.62 | 0.00 | 0.17 | 1.00 | 0.0 | 0.00 | |
| $NaHCO_3$ | $NaHCO_3$-0 | 0.25 | 0.00 | 0.00 | 0.00 | 0.00 | 0.00 | 0.00 | 0.24 | 0.0 | 0.00 | |
| | $NaHCO_3$-1 | 1.04 | 0.00 | 0.00 | 0.00 | 0.00 | 0.00 | 0.00 | 1.00 | 0.0 | 0.00 | |
| | $NaHCO_3$-2 | 0.62 | 0.00 | 0.00 | 0.00 | 0.00 | 0.00 | 0.00 | 0.60 | 0.0 | 0.00 | |

| | | | | | | | | | | | |
|---|---|---|---|---|---|---|---|---|---|---|---|
| | $NaHCO_3$-3 | 4.09 | 0.00 | 0.00 | 0.00 | 0.00 | 0.00 | 0.00 | 4.09 | 0.0 | 0.00 |
| | $NaHCO_3$-4 | 8.20 | 0.00 | 0.00 | 0.00 | 0.00 | 0.00 | 0.00 | 8.20 | 0.0 | 0.00 |
| | $NaHCO_3$-5 | 2.00 | 0.00 | 0.00 | 0.00 | 0.00 | 0.00 | 0.00 | 2.00 | 0.0 | 0.00 |
| | $NaHCO_3$-6 | 3.00 | 0.00 | 0.00 | 0.00 | 0.00 | 0.00 | 0.00 | 3.00 | 0.0 | 0.00 |
| | $NaHCO_3$-7 | 0.80 | 0.00 | 0.00 | 0.00 | 0.00 | 0.00 | 0.00 | 0.80 | 0.0 | 0.00 |
| NaCl | NaCl-1 | 0.86 | 0.00 | 0.00 | 0.00 | 0.60 | 0.00 | 0.00 | 0.24 | 0.0 | 0.00 |
| | NaCl-2 | 1.41 | 0.00 | 0.00 | 0.00 | 1.15 | 0.00 | 0.00 | 0.25 | 0.0 | 0.00 |
| | NaCl-3 | 5.15 | 0.00 | 0.00 | 0.00 | 4.63 | 0.00 | 0.00 | 0.24 | 0.0 | 0.00 |
| | NaCl-4 | 7.24 | 0.00 | 0.00 | 0.00 | 6.61 | 0.00 | 0.00 | 0.24 | 0.0 | 0.00 |
| | NaCl-5 | 10.58 | 0.00 | 0.00 | 0.00 | 9.90 | 0.00 | 0.00 | 0.24 | 0.0 | 0.00 |
| | NaCl-6 | 29.60 | 0.00 | 0.00 | 0.00 | 29.35 | 0.00 | 0.00 | 0.24 | 0.0 | 0.00 |
| | NaCl-7 | 20.05 | 0.00 | 0.00 | 0.00 | 19.75 | 0.00 | 0.00 | 0.24 | 0.0 | 0.00 |
| | NaCl-8 | 15.48 | 0.00 | 0.00 | 0.00 | 15.23 | 0.00 | 0.00 | 0.24 | 0.0 | 0.00 |
| $NaNO_3$ | $NaNO_3$-1 | 16.37 | 0.00 | 0.00 | 0.00 | 0.00 | 16.13 | 0.00 | 0.24 | 0.0 | 0.00 |
| | $NaNO_3$-2 | 12.25 | 0.00 | 0.00 | 0.00 | 0.00 | 12.00 | 0.00 | 0.24 | 0.0 | 0.00 |
| | $NaNO_3$-3 | 20.25 | 0.00 | 0.00 | 0.00 | 0.00 | 20.00 | 0.00 | 0.24 | 0.0 | 0.00 |
| | $NaNO_3$-4 | 29.31 | 0.00 | 0.00 | 0.00 | 0.00 | 29.06 | 0.00 | 0.24 | 0.0 | 0.00 |
| | $NaNO_3$-5 | 8.32 | 0.00 | 0.00 | 0.00 | 0.00 | 8.07 | 0.00 | 0.24 | 0.0 | 0.00 |
| | $NaNO_3$-6 | 4.85 | 0.00 | 0.00 | 0.00 | 0.00 | 4.60 | 0.00 | 0.24 | 0.0 | 0.00 |
| | $NaNO_3$-7 | 1.45 | 0.00 | 0.00 | 0.00 | 0.00 | 1.20 | 0.00 | 0.24 | 0.0 | 0.00 |
| $K_2SO_4$ | $K_2SO_4$-1 | 0.25 | 0.25 | 0.00 | 0.00 | 0.00 | 0.00 | 0.12 | 0.24 | 0.0 | 0.00 |
| $MgSO_4$ | $MgSO_4$-1 | 0.25 | 0.00 | 0.12 | 0.00 | 0.00 | 0.00 | 0.11 | 0.24 | 0.0 | 0.00 |
| $CaSO_4$ | $CaSO_4$-1 | 0.25 | 0.00 | 0.00 | 0.19 | 0.00 | 0.00 | 0.18 | 0.24 | 0.0 | 0.00 |

| | | | | | | | | | | | |
|---|---|---|---|---|---|---|---|---|---|---|---|
| | $CaSO_4$-2 | 0.25 | 0.00 | 0.00 | 0.04 | 0.00 | 0.00 | 0.04 | 0.24 | 0.0 | 0.00 |
| | $CaSO_4$-3 | 0.26 | 0.00 | 0.00 | 0.08 | 0.00 | 0.00 | 0.09 | 0.24 | 0.0 | 0.00 |
| | $CaSO_4$-4 | 0.26 | 0.00 | 0.00 | 0.13 | 0.00 | 0.00 | 0.12 | 0.24 | 0.0 | 0.00 |
| SRNOM | SRNOM-1 | 0.25 | 0.00 | 0.00 | 0.00 | 0.00 | 0.00 | 0.00 | 0.24 | 0.1 | 0.16 |
| | SRNOM-2 | 0.26 | 0.00 | 0.00 | 0.00 | 0.00 | 0.00 | 0.00 | 0.24 | 0.5 | 0.04 |
| | SRNOM-3 | 0.26 | 0.00 | 0.00 | 0.00 | 0.00 | 0.00 | 0.00 | 0.24 | 1.3 | 0.08 |
| | SRNOM-4 | 0.40 | 0.00 | 0.00 | 0.00 | 0.00 | 0.00 | 0.07 | 0.24 | 1.3 | 0.08 |
| | SRNOM-5 | 1.16 | 0.00 | 0.00 | 0.00 | 0.00 | 0.00 | 0.07 | 1.00 | 1.4 | 0.08 |
| | SRNOM-6 | 0.59 | 0.00 | 0.00 | 0.00 | 0.00 | 0.00 | 0.16 | 0.24 | 1.4 | 0.09 |
| | SRNOM-7 | 1.34 | 0.00 | 0.00 | 0.00 | 0.00 | 0.00 | 0.16 | 1.00 | 1.5 | 0.09 |
| | SRNOM-8 | 1.38 | 0.00 | 0.00 | 0.00 | 0.00 | 0.00 | 0.14 | 1.00 | 0.5 | 0.04 |
| | SRNOM-9 | 0.26 | 0.00 | 0.00 | 0.00 | 0.00 | 0.00 | 0.00 | 0.24 | 1.0 | 0.06 |
| | SRNOM-10 | 0.26 | 0.00 | 0.00 | 0.00 | 0.00 | 0.00 | 0.00 | 0.24 | 2.0 | 0.12 |

Table 4-3.

Ion components and alkalinity of the $Na_2SeO4$, $Na_2S_2O_3$, and $Na_2CrO_4$ water series used in this study

| Series | Water | $Na^+$ | $SeO_4^{2-}$ | $S_2O_3^{2-}$ | $CrO_4^{2-}$ | Alkalinity | Source |
|---|---|---|---|---|---|---|---|
| | | | | | | meq/L | |
| | | mmol/L | mmol/L | mmol/L | mmol/L | ≈ $HCO_3^-$ mmol/L | |
| $Na_2SeO_4$ | $Na_2SeO_4$-1 | 0.89 | 0.31 | 0.00 | 0.00 | 0.24 | Elix water |
| | $Na_2SeO_4$-2 | 0.50 | 0.13 | 0.00 | 0.00 | 0.24 | |
| | $Na_2SeO_4$-3 | 0.42 | 0.08 | 0.00 | 0.00 | 0.24 | |
| $Na_2S_2O_3$ | $Na_2S_2O_3$-1 | 0.89 | 0.00 | 0.32 | 0.00 | 0.24 | |
| | $Na_2S_2O_3$-2 | 0.50 | 0.00 | 0.13 | 0.00 | 0.24 | |
| | $Na_2S_2O_3$-3 | 0.42 | 0.00 | 0.09 | 0.00 | 0.24 | |
| $Na_2CrO_4$ | $Na_2CrO_4$-1 | 0.89 | 0.00 | 0.00 | 0.32 | 0.24 | |
| | $Na_2CrO_4$-2 | 0.51 | 0.00 | 0.00 | 0.13 | 0.24 | |
| | $Na_2CrO_4$-3 | 0.42 | 0.00 | 0.00 | 0.09 | 0.24 | |

### 4.2.3 Coagulation experiment, hydrolysis-precipitation rate test, and floc particle size measurement

The process for coagulation experiment, hydrolysis-precipitation rate test, and floc size measurement were the same as that described in Section 3.2.3 and 3.2.4 (Chapter 3).

## 4.3 Results and discussion

### 4.3.1 Effects of anions

We investigated the effect on PACl hydrolysis-precipitation of inorganic ions commonly found in natural water, including sulfate and bicarbonate ions, by using artificial waters containing one major anion and one major cation each. The time for the Al concentration in the filtrate to decrease to one-fourth of the original concentration (one-quarter concentration time) was calculated from the experimental data and used as an index of the rate of hydrolysis-precipitation, as in Section 3.2.5, Chapter 3. If the rates of hydrolysis-precipitation were very slow in the waters with monovalent ions and the one-quarter concentration time was not obtainable, the one-quarter concentration time was calculated from the one-half concentration time by using the linear relationship between the one-half concentration time and one-quarter concentration time (Section 3.2.5 in Chapter 3 and Fig. 4-1). Fig. 4-2 shows the one-quarter concentration times of PACl hydrolysis-precipitation plotted against anion concentrations. Bicarbonate ions hydrolyzed both HB-PACl and NB-PACl at higher concentrations than sulfate ions. Much higher concentrations of chloride and nitrate ions were required to hydrolyze HB-PACl and NB-PACl. The concentrations of sulfate, bicarbonate, chloride, and nitrate ions required for a one-quarter concentration time of 60 s for hydrolysis-precipitation of HB-PACl were approximately 0.174, 2.20, 34, and 42 mmol/L. Those of NB-PACl were 0.168, 1.00, 14, and 12 mmol/L, respectively (Table 4-4). Because such high chloride and nitrate ion

concentrations are not normally found in natural river waters, nitrate and chloride ions do not have a substantial effect on the hydrolysis-precipitation of PACl in river water. The bicarbonate ion concentration of 1.0 mmol/L (corresponding to alkalinity of 1 meq/L) required for hydrolysis-precipitation of NB-PACl was similar to the concentrations sometimes observed in natural surface waters. The bicarbonate concentration required for hydrolysis-precipitation of HB-PACl (2.20 mmol/L) was relatively high. Therefore, the bicarbonate ion concentration of ~0.1–0.8 mmol/L (corresponding to alkalinity of 0.1–0.8 meq/L) observed in the natural surface waters we used would contribute to the hydrolysis-precipitation of NB-PACl but contribute to a much lesser extent to the hydrolysis-precipitation of HB-PACl. This conclusion explains why the effect of bicarbonate was more clearly apparent in the formation of floc particles by NB-PACl than HB-PACl (Fig. 3-9 in Section 3.3.2, Chapter 3).

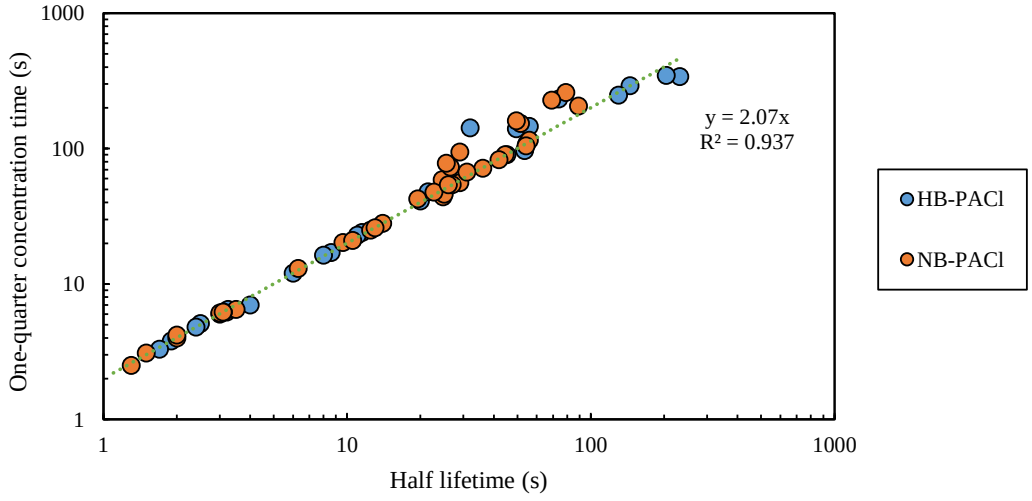


Fig. 4-1. The relationship between one-quarter concentration times and half lifetime. NOM-free waters ($Na_2SO_4$, $NaHCO_3$, NaCl, $NaNO_3$, $K_2SO_4$, $MgSO_4$, $CaSO_4$, $Na_2SeO_4$, $Na_2S_2O_3$, and $Na_2CrO_4$ series) were used. The PACl dose was 2.5 mg-Al/L. The coagulation pH was 7.0. Error bars indicate 95% confidence intervals.

The concentrations of sulfate ions required for hydrolysis-precipitation of NB-PACl and HB-PACl also differed, but the difference (0.174 vs. 0.168 mmol/L) was not large compared with the difference of bicarbonate ion concentrations (2.20 vs. 1.00 mmol/L). Therefore, the reason

for the poor performance of HB-PACl in water with low sulfate ion concentrations was partly the high concentration of sulfate ions required for the hydrolysis-precipitation of HB-PACl but mainly the small contribution of bicarbonate ions to the hydrolysis-precipitation of HB-PACl. Conversely, because bicarbonate ions contribute to the hydrolysis-precipitation of NB-PACl, hydrolysis-precipitation proceeds satisfactorily, even in water with a low concentration of sulfate ions, and NB-PACl is a better coagulant than HB-PACl in water with a low concentration of sulfate ions (Section 3.3.1 in Chapter 3). Furthermore, a review of previous data in Chapter 2 (Chen et al., 2020) revealed that PACl produced by high-temperature heating and base-titration requires 3 times the concentration of sulfate ions for hydrolysis-precipitation and floc formation than HB-PACl produced by the widely and commercially applied dissolution method even at the same basicity. This difference suggests that the effect of anions on the hydrolysis-precipitation of PACl (i.e., which ion hydrolyzes each component in the PACl) influences the suitability of PACl for raw water. This study revealed that HB-PACl, which contains a larger amount of $Al_b$+$Al_c$ and thus has a high charge-neutralization capacity than NB-PACl, is not easily hydrolyzed by bicarbonate ions and requires a higher concentration of sulfate ions than NB-PACl. If various types of PACl are manufactured, sold, and used around the world (Jiang, 2001; Wang et al., 2017; Zouboulis & Tzoupanos, 2010), and if each of them is suitable for a region, the diversity of PACls may be related to the anion concentrations in the raw water.

Bicarbonate ions were about 11 times more effective than nitrate and chloride ions in promoting hydrolysis-precipitation. Because the concentration of carbonate ions is 1% of the concentration of bicarbonate ions at the experimental pH of 7.0, its effect would be small compared to that of bicarbonate. Because the hydrolysis-precipitation of PACl consumes alkalinity, bicarbonate ions play a role as a source of alkalinity (Bratby, 2016; Dousma & de Bruyn, 1978), and their influence is thus likely to be greater than that of monovalent ions such as chloride ions. The sulfate ion was ~200 times more effective than chloride and nitrate ions

in hydrolyzing PACl. It was also >6 times more effective than the bicarbonate ion. This difference was not eliminated by basing the calculations on ionic strengths rather than molar concentrations. The effect of the sulfate ion on aluminum coagulant (including PACl) performance is explained by its capacity to neutralize the positive charge of hydrolyzing colloids of aluminum (Edzwald, 2011). However, there is roughly a 60-fold difference in the relative effectiveness of charge neutralization by divalent ions compared with monovalent ions according to the Schulze–Hardy rule (Bratby, 2016) but less than a 60-fold difference according to the modified Schulze–Hardy rules by the DLVO theory of the electric double layer (Rakshit et al., 2021). The relative effectiveness on the critical coagulation concentration has been reported to be around 60 or less (Nowicki & Nowicka, 1994). These values are still smaller than the observed relative effectiveness of PACl hydrolysis-precipitation (~200). The charge neutralization mechanism on the basis of these rules is therefore insufficient to explain the effect of sulfate, chloride, and nitrate ions on PACl hydrolysis-precipitation.

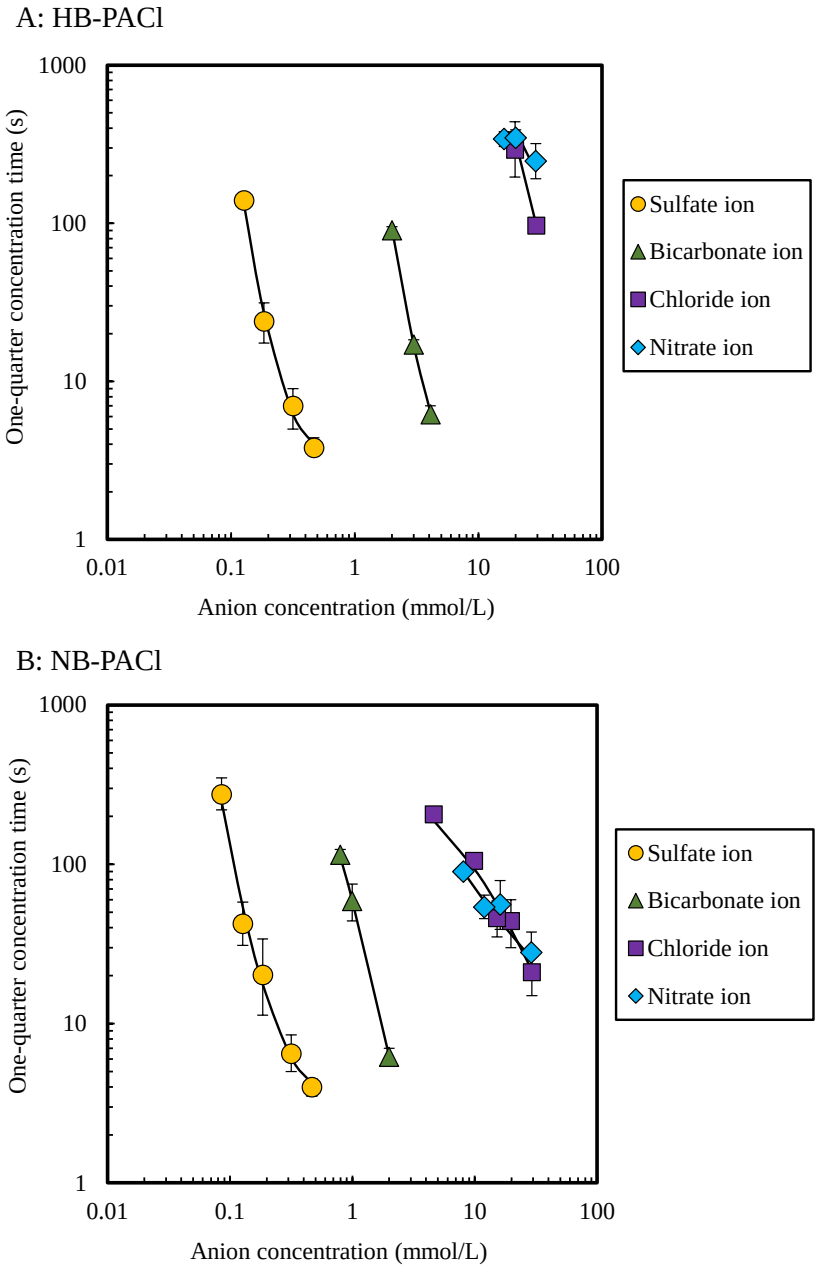


Fig. 4-2. Relationship between one-quarter concentration times and anion concentrations in tests of hydrolysis-precipitation rates. Panel A shows the data for HB-PACl in $Na_2SO_4$-1–6, $NaHCO_3$-3,5,6, NaCl-8,9, and $NaNO_3$-1,3,4 waters. Panel B shows the data for NB-PACl in $Na_2SO_4$-2–4, $NaHCO_3$-1,5,7, NaCl-5,7–10, and $NaNO_3$-1,2,4,5 waters. The PACl dose was 2.5 mg-Al/L. The coagulation pH was 7.0. Error bars indicate 95% confidence intervals.

Table 4-4

Concentrations required for one-quarter concentration times of 60 s and relative intensities for PACl hydrolysis.

| | | Sulfate ion | Bicarbonate ion | Chloride ion | Nitrate ion | DOC | UV260 |
|---|---|---|---|---|---|---|---|
| Concentrations required for a one-quarter concentration time of 60 s | HB-PACl | 0.174 mmol/L | 2.20 mmol/L | 34.3 mmol/L | 41.8 mmol/L | N/A | N/A |
| | | 16.7 mg-$SO_4^{2-}$/L | 134 mg-$HCO_3^-$/L | 1220 mg-$Cl^-$/L | 2590 mg-$NO_3^-$/L | 1.46 mg-C/L | 0.088 $cm^{-1}$ |
| | NB-PACl | 0.168 mmol/L | 1.00 mmol/L | 14.5 mmol/L | 11.5 mmol/L | N/A | N/A |
| | | 16.1 mg-$SO_4^{2-}$/L | 61 mg-$HCO_3^-$/L | 514 mg-$Cl^-$/L | 714 mg-$NO_3^-$/L | 0.99 mg-C/L | 0.066 $cm^{-1}$ |
| Intensity for PACl hydrolysis relative to the intensity of sulfate ions | HB-PACl | 1 mol/mol | 0.079 [ah)] mol/mol | 0.0051 mol/mol | 0.0042 mol/mol | 0.12 mol/(g-C) | 1.97 [bh)] (mmol/L)/$cm^{-1}$ |
| | | 1 g/g | 0.12 (g-$SO_4^{2-}$)/(g-$HCO_3^-$) | 0.014 (g-$SO_4^{2-}$)/(g-$Cl^-$) | 0.0064 (g-$SO_4^{2-}$)/(g-$NO_3^-$) | 11.4 (g-$SO_4^2$)/(g-C) | 190 (mg-$SO_4^{2-}$/L)/ $cm^{-1}$ |
| | NB-PACl | 1 mol/mol | 0.17 [an)] mol/mol | 0.012 mol/mol | 0.015 mol/mol | 0.17 mol/(g-C) | 2.54 [bn)] (mmol/L)/$cm^{-1}$ |
| | | 1 g/g | 0.26 (g-$SO_4^{2-}$)/(g-$HCO_3^-$) | 0.031 (g-$SO_4^{2-}$)/(g-$Cl^-$) | 0.022 (g-$SO_4^{2-}$)/(g-$NO_3^-$) | 16.3 (g-$SO_4^{2-}$)/(g-C) | 244 (mg-$SO_4^{2-}$/L)/ $cm^{-1}$ |

Note: Because the waters used in the experiments for sulfate, chloride, and nitrate ions contained a slight bicarbonate, the effect of bicarbonate ions was subtracted from the apparent effective concentration for the one-quarter concentration time of 60 s.
The numbers with superscripts ah) and an) are the values of "a" in equation (1) for HB-PACl and NB-PACl, respectively.
The numbers with superscripts bh) and bn) are the values of "b" in equation (1) for HB-PACl and NB-PACl, respectively.

### 4.3.2 Effect of cations

The effects of cations were also investigated by using waters containing sulfate ion as the major counter anion. As shown in Fig. 4-3, the rate of hydrolysis-precipitation was not influenced by whether the counter cation was $Na^+$ or $Ca^{2+}$. $K^+$ and $Mg^{2+}$ slightly retarded the rate of hydrolysis-precipitation of HB-PACl compared with $Na^+$ or $Ca^{2+}$, whereas $K^+$, $Mg^{2+}$, $Na^+$, and $Ca^{2+}$ did not have any effect on the rate of hydrolysis-precipitation of NB-PACl. Because $K^+$ and $Mg^{2+}$ are not as abundant as $Na^+$ or $Ca^{2+}$ in normal natural river water and the effects of cation type are much smaller than those of anion type, the types of cations would not be expected to substantially affect PACl hydrolysis-precipitation.

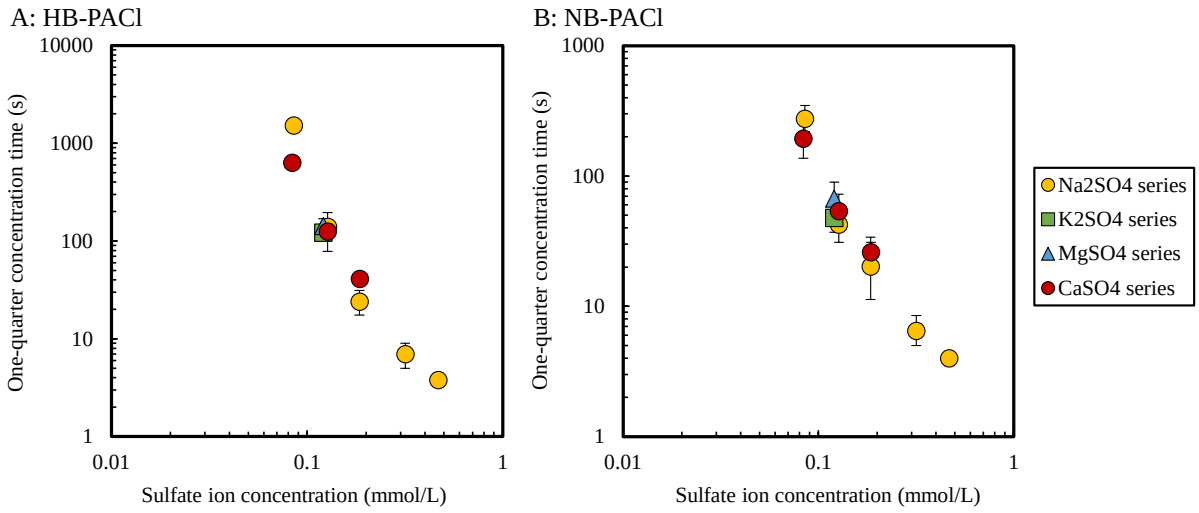


Fig. 4-3. Plots of one-quarter concentration times against sulfate ion concentrations with different counter cations. Panel A shows the data for HB-PACl in $Na_2SO_4$-1–4,6 and $CaSO_4$-1,3,4 waters. Panel B shows the data for NB-PACl in $Na_2SO_4$-2–4 and $CaSO_4$-1,3,4 waters. The PACl dose was 2.5 mg-Al/L. The coagulation pH was 7.0. Error bars indicate 95% confidence intervals.

### 4.3.3 Effect of NOM

Because it is commonly known that NOM affects coagulation performance, we investigated its role in PACl hydrolysis-precipitation. We conducted a test of hydrolysis-precipitation rates

by using artificial waters with the same NOM (SRNOM series) and different DOC concentrations. The results for HB-PACl and NB-PACl are shown in Fig. 4-4. Rates of hydrolysis-precipitation were slower in waters with lower NOM concentration, and the presence of NOM accelerated the hydrolysis-precipitation of PACl. These results may be related to the fact that NOM is a target compound for coagulation treatment and reacts with PACl coagulants to form precipitates. At the same DOC concentration, HB-PACl was hydrolyzed at a slower rate (longer one-quarter concentration time) than NB-PACl, a trend consistent with the results for anions, including sulfate ions (Section 3.3.1). Although the DOC concentrations required for hydrolysis-precipitation were not very high (~1.5 mg/L and ~1.0 mg/L for HB-PACl and NB-PACl, respectively, for a one-quarter concentration time of 60 s), surface waters with DOC concentrations lower than 1.0 mg/L are not uncommon in Japan. For such water, the ionic composition required for PACl hydrolysis-precipitation is key for floc formation when HB-PACl is applied. In contrast, the influence of the nature of the NOM must not be forgotten. Chromophoric NOM with high specific ultraviolet absorbance values is removed by aluminum coagulation, but non-chromophoric NOM is less amenable to removal (Archer and Singer, 2006; Edwards, 1997; Edzwald, 2011; Ou et al., 2014). Therefore, UV absorbance is considered more suitable than the concentration of DOC as a metric of the concentration of NOM that affects the rate of PACl hydrolysis-precipitation: this is discussed further in Section 4.3.5.

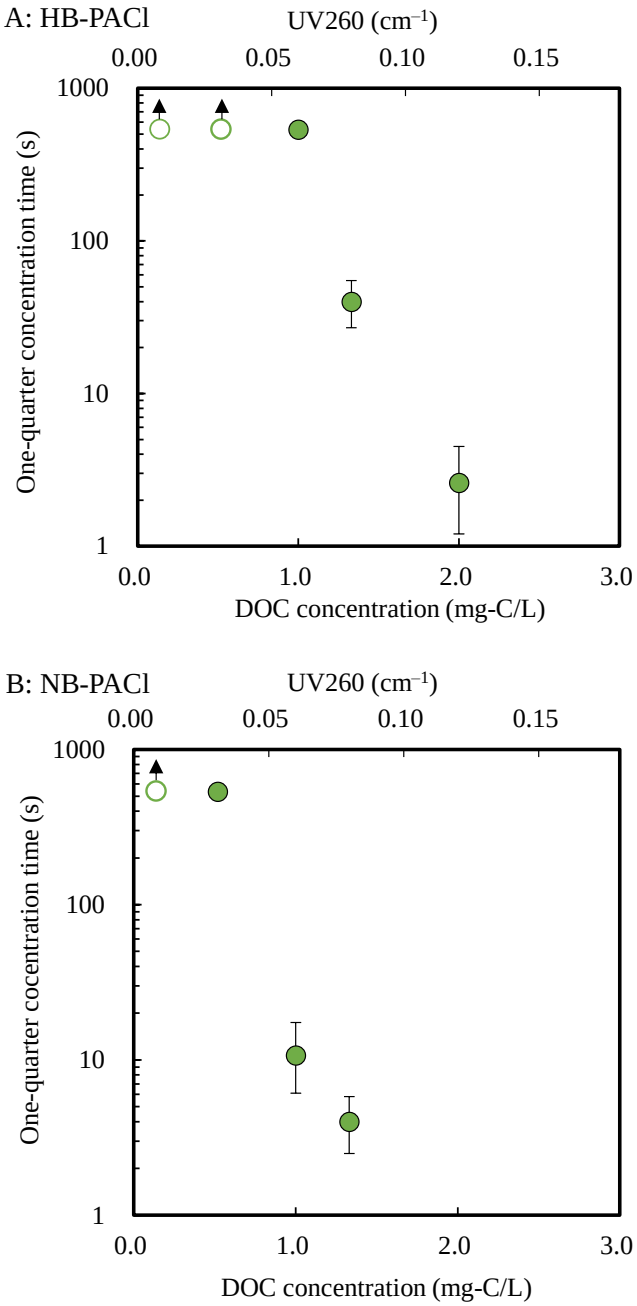


Fig. 4-4. Plots of one-quarter concentration times against DOC concentrations. Panel A shows the data for HB-PACl in SRNOM-1–3,9,10 waters. Panel B shows the data for NB-PACl in SRNOM-1–3,9 waters. The PACl dose was 2.5 mg-Al/L. The coagulation pH was 7.0. Open circles indicate that one-quarter concentration times exceeded 540 s. Error bars indicate 95% confidence intervals.

The mechanisms responsible for the effects of NOM and anions on the hydrolysis-precipitation of PACl would be expected to differ. The correlation between the one-half and the one-quarter concentration times regardless of anion species suggests that anions accelerate the

rate of hydrolysis-precipitation of PACl by the same mechanism (Al concentration vs. time, Fig. 4-1). In contrast, the hydrolysis-precipitation of PACl by NOM followed a different trend from hydrolysis-precipitation by anions because the relationship between the half-lives and one-quarter concentration times in the case of hydrolysis-precipitation by NOM differed significantly from the relationship for hydrolysis-precipitation by anions (Fig. 4-5). The fact that the initial rate of the hydrolysis-precipitation reaction was very rapid in the presence of NOM compared with the rate in the absence of NOM (calculated by the method in Section 3.2.5, Chapter 3) was probably due to the direct reaction of NOM with PACl (Barrett et al., 2000; Bratby, 2016; J. K. Edzwald, 1993; Yue et al., 2021). This study did not examine in depth the detailed properties of NOM and its stoichiometric relationship to hydrolysis-precipitation because such an examination would have been beyond the scope of this study (Hussain et al., 2013; Li et al., 2021; Su et al., 2017), but it should definitely be a subject of future research.

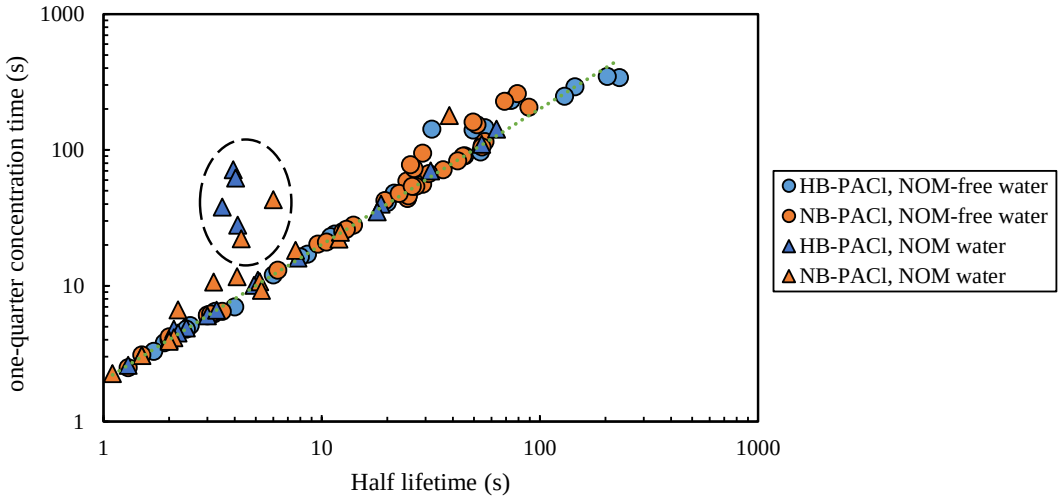


Fig. 4-5. Relationship between one-quarter concentration times and half lifetimes. NOM-free water ($Na_2SO_4$, $NaHCO_3$, NaCl, $NaNO_3$, $K_2SO_4$, $MgSO_4$, $CaSO_4$, $Na_2SeO_4$, $Na_2S_2O_3$, and $Na_2CrO_4$ series) and NOM water (SRNOM, Y, M, T series) were used. The PACl doses were 1.5, 2.5, and 3.5 mg-Al/L. The coagulation pH was 7.0. Error bars indicate 95% confidence intervals.

### 4.3.4 Effect of sulfate ions and its mechanism

To further clarify the mechanism by which sulfate ions accelerate PACl hydrolysis-precipitation and improve coagulation performance, we selected three other oxo anions (the selenate ion [$SeO_4^{2-}$], thiosulfate ion [$S_2O_3^{2-}$], and chromate ion [$CrO_4^{2-}$]) that have the same valency and/or similar structure to sulfate ion, and we investigated their abilities to accelerate PACl hydrolysis-precipitation. Figure 4-6 shows the relationship between the one-quarter concentration times and the concentrations of anions in raw water. For the rates of hydrolysis-precipitation of both HB-PACl and NB-PACl, water containing chromate ions or selenate ions was as effective as water containing sulfate ions (Panel B in Fig. 4-6). The effect of thiosulfate ions was somewhat smaller than that of sulfate ions, but the difference was much smaller than the difference between sulfate ions and monovalent ions (chloride, nitrate, and bicarbonate ions). The main reason for the effect of sulfate ions on the hydrolysis-precipitation of PACl therefore seemed to be its divalency, but the effect was not explained solely by the electric double layer theory that divalent ions are more effective, as mentioned in Section 4.3.1.

The difference between the effects of sulfate ions and thiosulfate ions on the rate of hydrolysis-precipitation indicates that the effect of sulfate ions is not due only to their divalency. There is another property of sulfate ions that affects PACl hydrolysis-precipitation. A possible explanation is related to their pKa2, which reflects the tendency of the ion to keep a proton, $H^+$. A lower pKa2 value means that the ion tends to donate a proton. Among the four anions, the thiosulfate ion, which had the least effect on PACl hydrolysis-precipitation, has the lowest pKa2. However, the chromate ion has the largest pKa2 but had an effect on PACl hydrolysis-precipitation similar to that of the sulfate and selenate ions (Fig. 4-7). Sulfate, selenate, and chromate ions have a similar structure consisting of a central atom surrounded by four equivalent oxygen atoms in a tetrahedral arrangement, whereas the thiosulfate ion is a sulfate ion with one oxygen replaced by sulfur. The effect on hydrolysis-precipitation may therefore be related not only to the valence but also to the structure of the anion. Duan et al. (2014) have

mentioned that sulfate ions chemically bound to an Al precipitate increase its negative surface charge and thereby prompt the aggregation of precipitates. Because of their structure, sulfate ions would chemisorb onto colloidal aluminum species and thereby effectively neutralize their charge and promote further hydrolysis-precipitation and the formation of coarse aluminum colloidal aggregates. This supports the possibility that sulfate ions form complexes with aluminum (Hanna et al., 1970; Matijević and Stryker, 1966). This process could result in sulfate ions' promoting hydrolysis-precipitation of PACl more efficiently than the Schulze–Hardy rule predicted by DLVO theory.

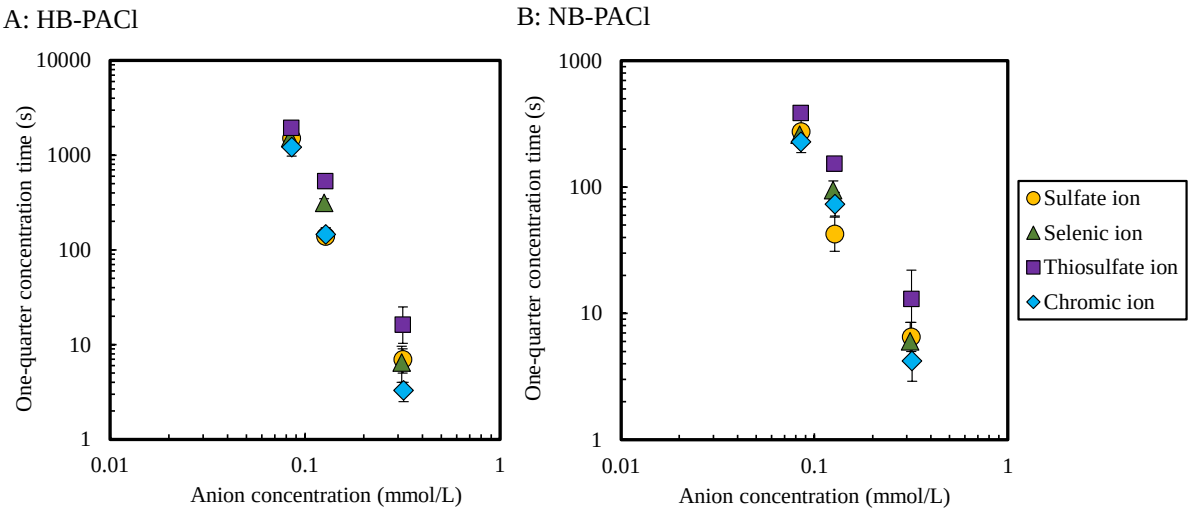


Fig. 4-6. Relationship between one-quarter concentration time and oxyanion concentration in tests of hydrolysis-precipitation rates. Panel A shows the data for HB-PACl. Panel B shows the data for NB-PACl. $Na_2SO_4$-3,4,6, $Na_2SeO_4$-1–3, $Na_2S_2O_3$-1–3, and $Na_2CrO_4$-1–3 waters were used in these experiments. The PACl dose was 2.5 mg-Al/L. The coagulation pH was 7.0. Error bars indicate 95% confidence intervals.

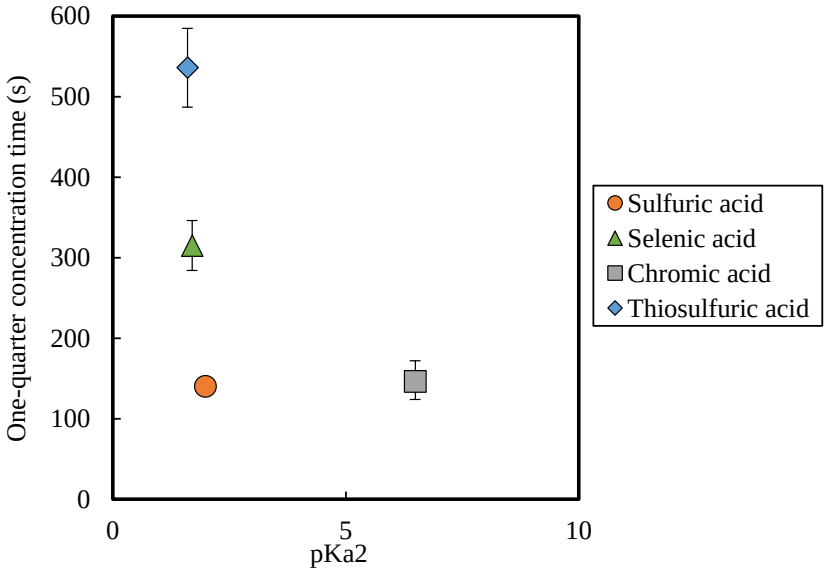


Fig. 4-7. Plots of one-quarter concentration times in waters that contained sulfate ions, selenate ions, chromate ions, or thiosulfate ions against the pKa2 value of these ions. $Na_2SO_4$-4, $Na_2SeO_4$-2, $Na_2CrO_4$-1, and $Na_2S_2O_3$-2 waters were used. The PACl dose was 2.5 mg-Al/L, and the coagulation pH was 7.0. The pKa2 data for sulfuric acid, selenic acid, and chromic acid are from Lide (2004). The pKa2 data for thiosulfuric acid is from Macintyre et al. (1992). Error bars indicate 95% confidence intervals.

### 4.3.5 Effect of sulfate and bicarbonate ions and NOM mixture

The simultaneous effects of anions and NOM in water need to be considered because natural waters contain a variety of ions, not just cation–anion pairs as described in Section 4.3.2. Because sulfate ions, bicarbonate ions, and NOM had the largest effects on PACl hydrolysis-precipitation, we investigated their synergistic/additive effects. Chloride and nitrate ions were omitted from this study because they affected PACl hydrolysis-precipitation only at concentrations much higher than those found in surface waters. The fact that increasing the concentration of either sulfate ions, bicarbonate ions, or NOM shortened the one-quarter concentration time of hydrolysis-precipitation (Figs. 4-8 and 4-9) indicated that the rate of hydrolysis-precipitation had increased. Increasing the concentrations of both sulfate and bicarbonate ions led to a much shorter one-quarter concentration time than increasing the concentration of sulfate or bicarbonate ions separately. We therefore analyzed the experimental

data on the assumption that the effects of sulfate and bicarbonate ions and NOM were additive. Table 4-4 summarizes the concentrations required for a one-quarter concentration time of 60 s (see Section 4.3.1). If the effects of sulfate ion, bicarbonate ion, and NOM are additive, the total concentration of the components affecting the hydrolysis-precipitation rate can be expressed in terms of the sulfate ion concentration by the following equation.

$$C_{SE} = C_S + aC_{BC} + bC_{NOM} \quad (1)$$

Here, $C_{SE}$ is the sulfate-ion-equivalent concentration for the overall effect of sulfate ions, bicarbonate ions, and NOM (mmol/L). $C_S$, $C_{BC}$, and $C_{NOM}$ are the concentrations of sulfate ions (mmol/L), bicarbonate ions (mmol/L), and NOM ($cm^{-1}$). UV absorbance at 260 nm was used as a measure of the NOM that reacts with PACl. The parameter *a* is the ratio of the effects of bicarbonate ions to sulfate ions, and *b* is the corresponding ratio of the effects of NOM to sulfate ions. Table 4-4 shows the values of *a* and *b*.

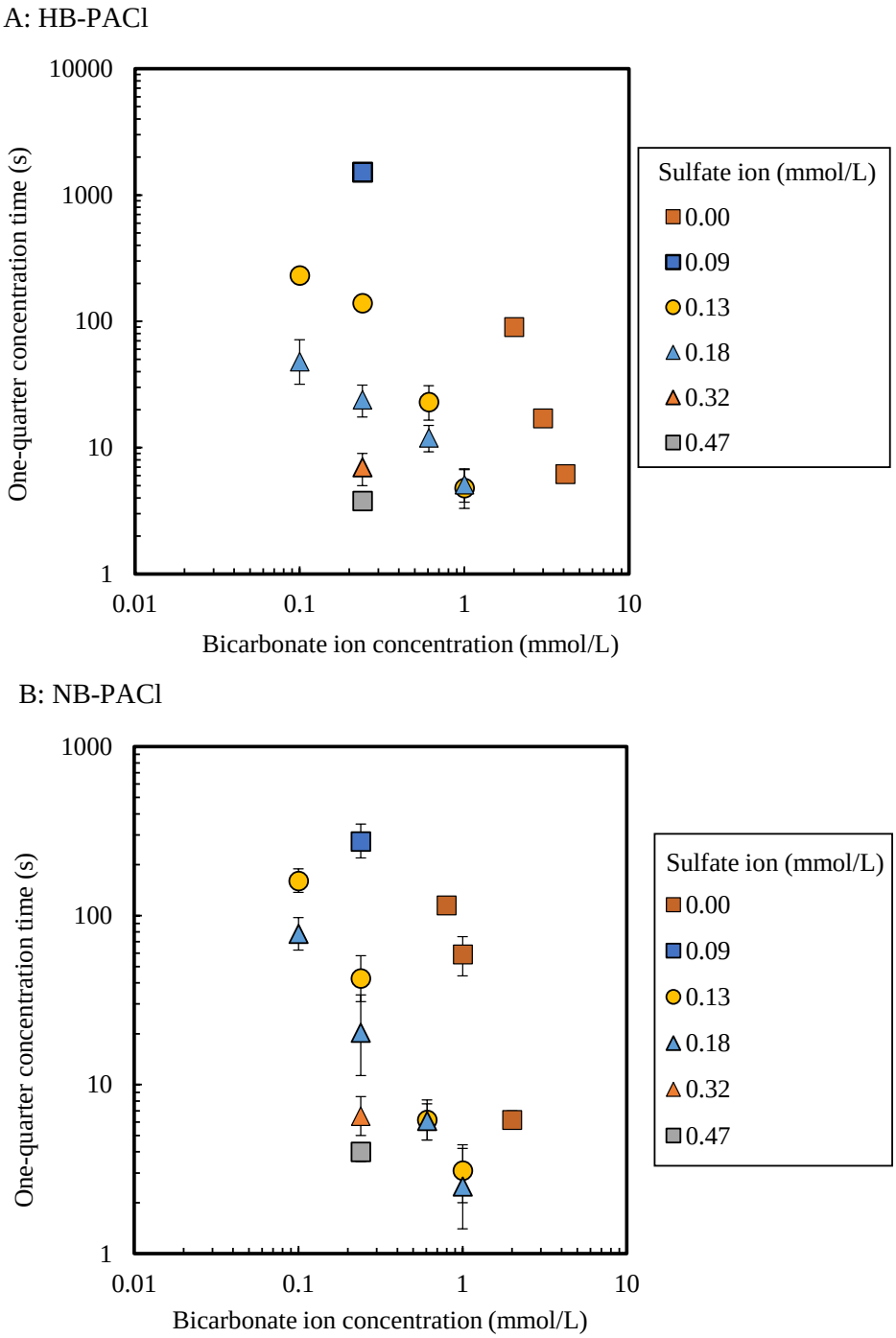


Fig. 4-8. One-quarter concentration times for various bicarbonate and sulfate ion concentrations. Panel A: HB-PACl was used in waters $Na_2SO_4$-1–3,6,8–13, and $NaHCO_3$-3,5,6 waters. Panel B: NB-PACl was used in $Na_2SO_4$-1–4,6,8–13, and $NaHCO_3$-1,5,7 waters. The PACl dose was 2.5 mg-Al/L. The coagulation pH was 7.0. Error bars indicate 95% confidence intervals.

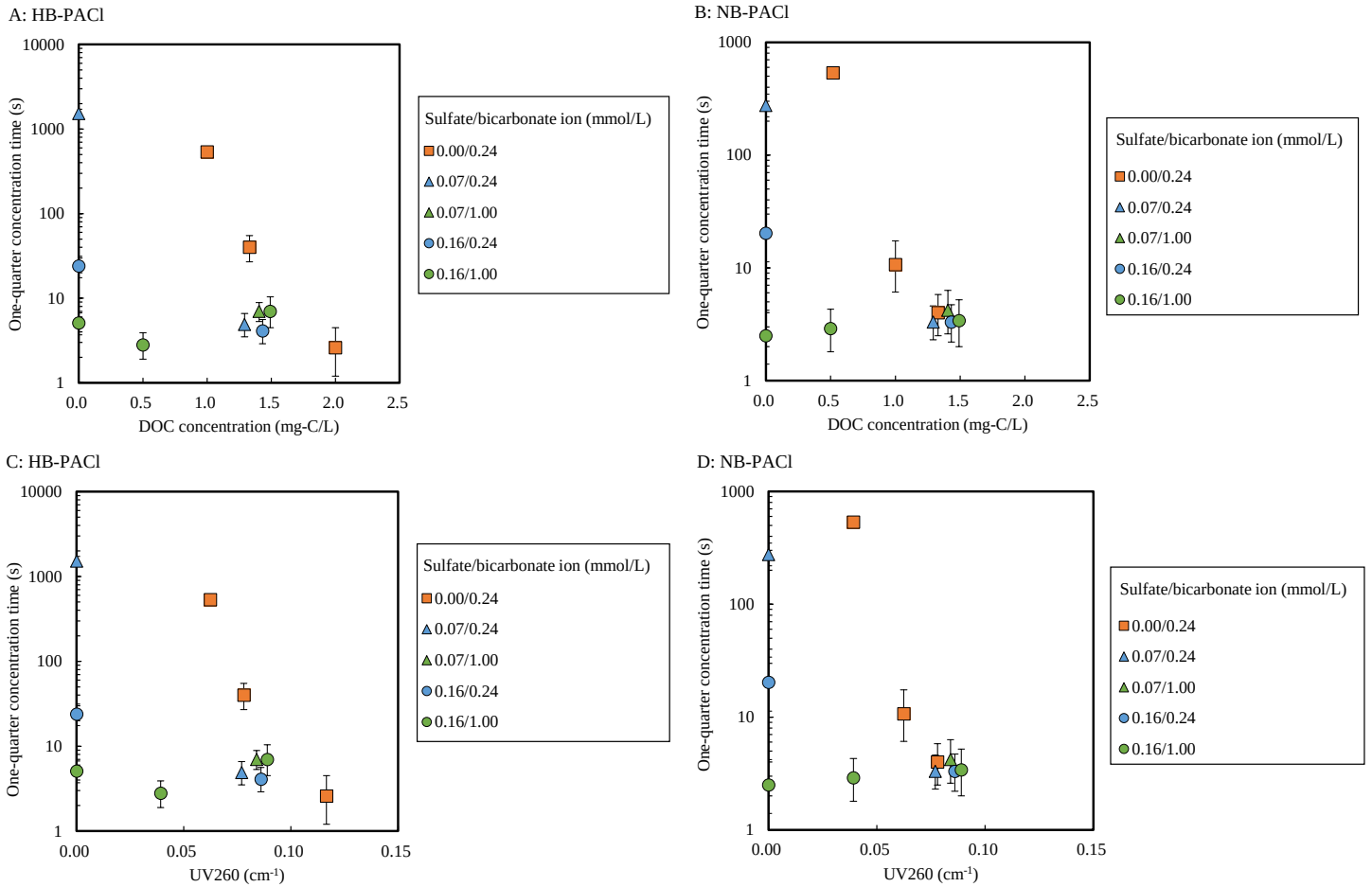


Fig. 4-9. One-quarter concentration times for various concentrations of NOM (DOC in Panels A and B, UV260 in Panels C and D), sulfate ions, and bicarbonate ions. Panels A and C; HB-PACl was used in SRNOM-3–5,7–10 and $Na_2SO_4$-2,3,6,8 waters. Panel B and D: NB-PACl was used in SRNOM-2–5,7–9, and $Na_2SO_4$-2,3,6,8 waters. The coagulation pH was 7.0. The PACl dose was 2.5 mg-Al/L. Numerical values in the legends indicate the concentrations of sulfate ion and bicarbonate ion. Error bars indicate 95% confidence intervals.

We then obtained Fig. 4-10 by plotting the one-quarter concentration times for PACl hydrolysis-precipitation versus the $C_{SE}$ values of the water. Despite the various concentrations of sulfate ions, bicarbonate ions, and NOM, the data appear to reflect a single relationship (the values for one-quarter concentration times of less than 5 s were scattered and imprecise because the aluminum concentrations decreased rapidly). The results shown in Fig. 4-10 indicate that the effects of sulfate ion, bicarbonate ion, and NOM on the hydrolysis-precipitation of PACl vary greatly, but the interactions between the effects are additive. The graph shows that the rate of hydrolysis-precipitation begins to decrease when the $C_{SE}$ falls below 0.2 mmol/L. Incidentally, when the DOC concentration was used instead of UV260 as the metric of the NOM concentration, the functional relationship shown in Fig. 4-10 was not obtained (Fig. 4-11 and Fig. 4-12). This confirms that UV260 is more appropriate as the concentration of NOM that reacts with PACl and promotes hydrolysis-precipitation.

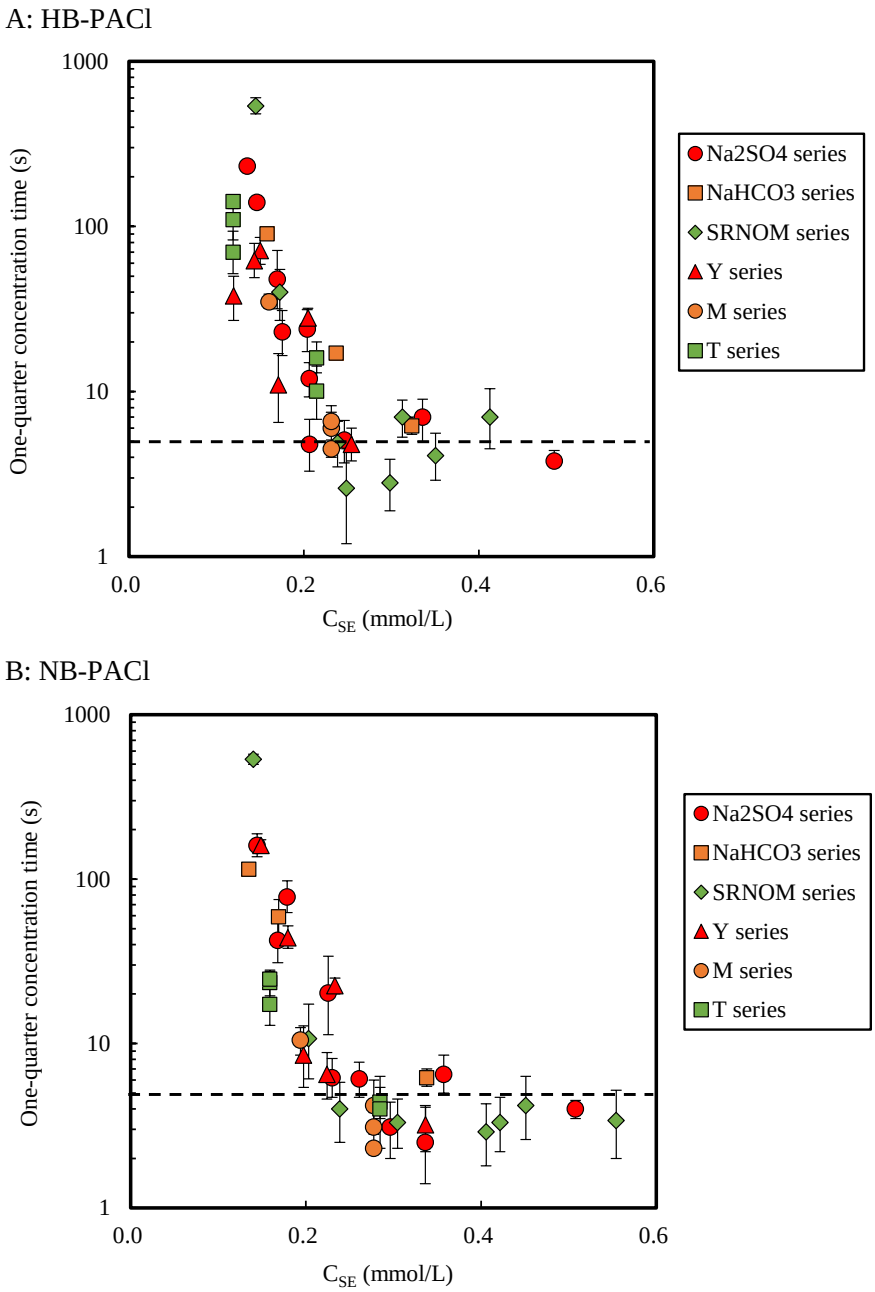


Fig. 4-10. One-quarter concentration times versus $C_{SE}$ values. Panel A shows the data for HB-PACl in $Na_2SO_4$-1,2,4,6,8–13, $NaHCO_3$-3,5,6, SRNOM-3–10, Y-1–6, M-1,2, and T-1,2 waters, and Panel B shows the data for NB-PACl in $Na_2SO_4$-1,2,4,6,8–13, $NaHCO_3$-1,5,7, SRNOM-2–9, Y-1–6, M-1,2, and T-1,2 waters. The PACl dose was 2.5 mg-Al/L, but doses of 1.5 and 3.5 mg-Al/L were also used in the experiments with M-1,2 and T-1,2 waters. The coagulation pH was 7.0. Error bars indicate 95% confidence intervals.

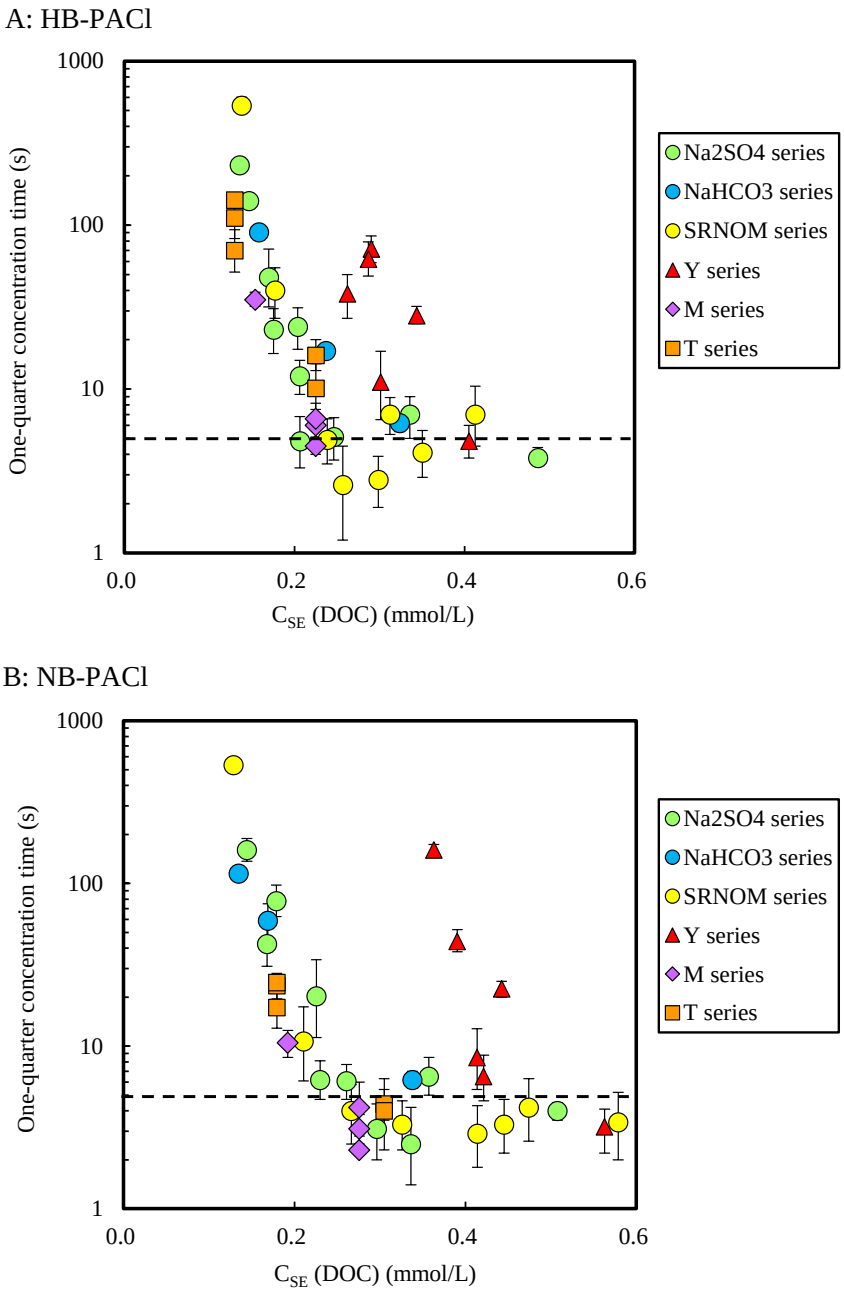


Fig. 4-11. One-quarter concentration times versus $C_{SE}$ values, where DOC was used instead of UV260 for the NOM concentration. Panel A shows the data for HB-PACl in $Na_2SO_4$-1,2,4,6,8–13, $NaHCO_3$-3,5,6, SRNOM-3–10, Y-1–6, M-1,2, and T-1,2 waters, and Panel B shows the data for NB-PACl in $Na_2SO_4$-1,2,4,6,8–13, $NaHCO_3$-1,5,7, SRNOM-2–9, Y-1–6, M-1,2, and T-1,2 waters. The PACl dose was 2.5 mg-Al/L, but doses of 1.5 and 3.5 mg-Al/L were also used in the experiments with M-1,2 and T-1,2 waters. The coagulation pH was 7.0. Error bars indicate 95% confidence intervals.

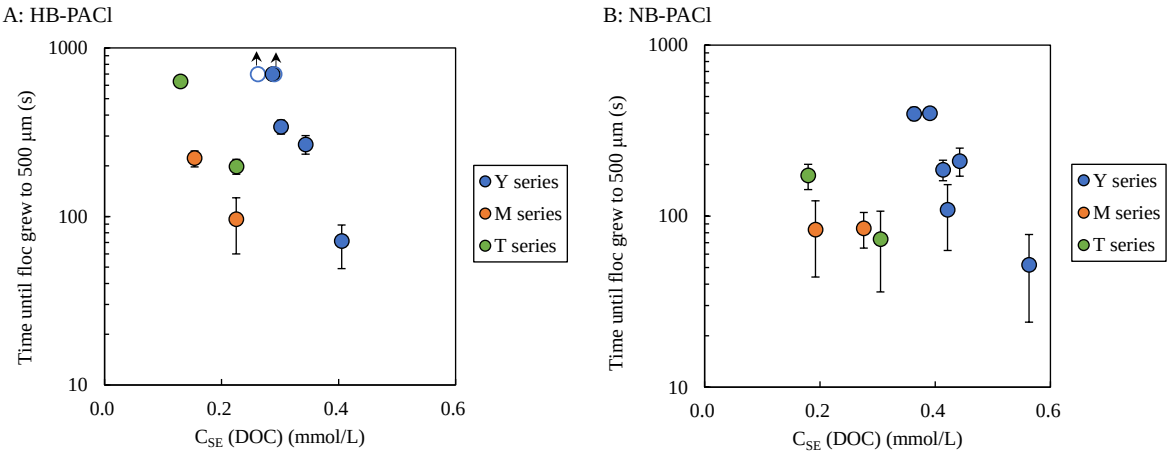


Fig. 4-12. Plots of the time until floc grew to 500 μm for HB-PACl (Panel A) and NB-PACl (Panel B) against $C_{SE}$, where DOC was used instead of UV260 for the NOM concentration. Y, M, and T series waters were used. The coagulation pH was 7.0. The PACl dose was 2.5 mg-Al/L. The open circle in Panel A indicates that the floc size did not increase to 500 μm during the experiment. Error bars indicate 95% confidence intervals.

Using the *a* and *b* values, we analyzed the contributions of sulfate and bicarbonate ions and NOM to $C_{SE}$ and the hydrolysis-precipitation of HB-PACl and NB-PACl in T-1 and T-2 waters (Fig. 4-13). The reciprocal of the one-quarter concentration times for hydrolysis-precipitation when HB-PACl was added to the T-1 water was 0.007 $s^{-1}$. Sulfate ions, bicarbonate ions, and NOM were estimated to contribute 47%, 21%, and 32%, respectively, to the hydrolysis-precipitation. In T-2 water, in which the concentrations of sulfate and bicarbonate ions were higher, the reciprocal one-quarter concentration time was 0.063 $s^{-1}$ for HB-PACl, and the contributions of sulfate ions, bicarbonate ions, and NOM to hydrolysis-precipitation were 58%, 24%, and 18%, respectively. In contrast, when NB-PACl was added to the T-1 water, the reciprocal one-quarter concentration was 0.043 $s^{-1}$, and the contributions of sulfate ions, bicarbonate ions, and NOM to the hydrolysis-precipitation were estimated to be 35%, 34%, and 31%, respectively. In T-2 water, the reciprocal one-quarter concentration time for NB-PACl was 0.22 $s^{-1}$, and the corresponding contributions to hydrolysis-precipitation were 44%, 39%, and 17%, respectively. The much larger reciprocal one-quarter concentration times for NB-PACl versus HB-PACl indicated that the former was much more effective than the latter. Use of Eq.

(1) enabled us to determine the contribution of each component to the hydrolysis-precipitation and thus to coagulation as well as how the contributions varied with the components in the raw water.

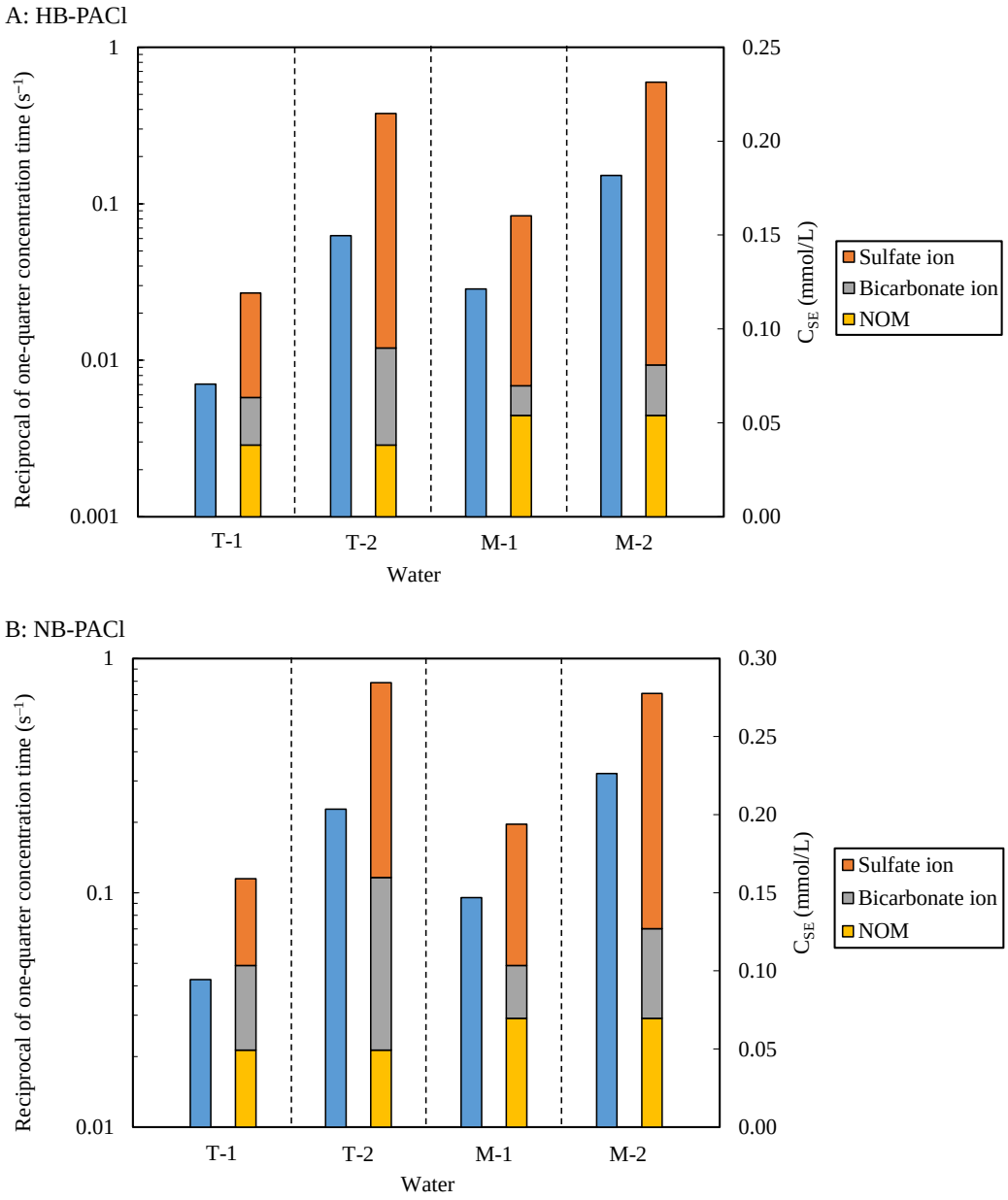


Fig. 4-13. The reciprocal of one-quarter concentration time and the contribution from sulfate ions, bicarbonate ions, and NOM in $C_{SE}$ units. Blue bars show the reciprocal of one-quarter concentration time indicated by the left axis scale. Contributions of sulfate ion (orange bars), bicarbonate ion (grey bars), and NOM (yellow bars) to $C_{SE}$ value are indicated by the right axis scale. Results of HB-PACl are shown in Panel A, and the results of NB-PACl are shown in Panel B. T-1,2 and M-1,2 waters were used.

The main substances in the water that affected PACl hydrolysis-precipitation were sulfate ions, bicarbonate ions, and NOM. These substances interacted additively to enhance the hydrolysis-precipitation of PACl. This additive interaction may have led to better PACl coagulation performance. But the enhancement depended on whether the PACl was a HB-PACl or NB-PACl. We then used natural waters (Y and S series) containing different concentrations of sulfate ions, bicarbonate ions, and NOM to verify that the effects on coagulation, flocculation, and sedimentation were in all cases additive. The flocculation time (the time for the D50 of floc particles to reach 500 μm) was strongly correlated with the sulfate-ion-equivalent concentration for the overall effect of sulfate ions, bicarbonate ions, and NOM (by UV260) as shown in Fig. 4-14 (note: as shown in Fig. 4-12, no correlations were obtained for $C_{\mathrm{SE}}(\mathrm{DOC})$, which supports that some NOM sensitive to UV is more effective for hydrolysis-precipitation of PACl than the entire NOM measured by DOC). The $C_{SE}$ was therefore a useful metric of the effectiveness of a PACl coagulant.

In this study, it was shown that high-basicity PACl, in which the polymerization of aluminum is more advanced than that of normal-basicity PACl, is difficult to hydrolyze, and therefore, PACl hydrolysis is important for the coagulation-flocculation by the PACl, in addition to neutralizing the charge on the particles to be removed. Anions such as sulfate ion are important for the hydrolysis of PACl. On the other hand, it has been reported that mixing intensity during rapid mixing for coagulation process is important for high-basicity PACl (Nakazawa et al., 2018), so it is also important to study how physical condition, such as mixing intensity and water temperature, affect PACl hydrolysis-precipitation. We feel the high-intensity mixing promotes the hydrolysis-precipitation of PACl.

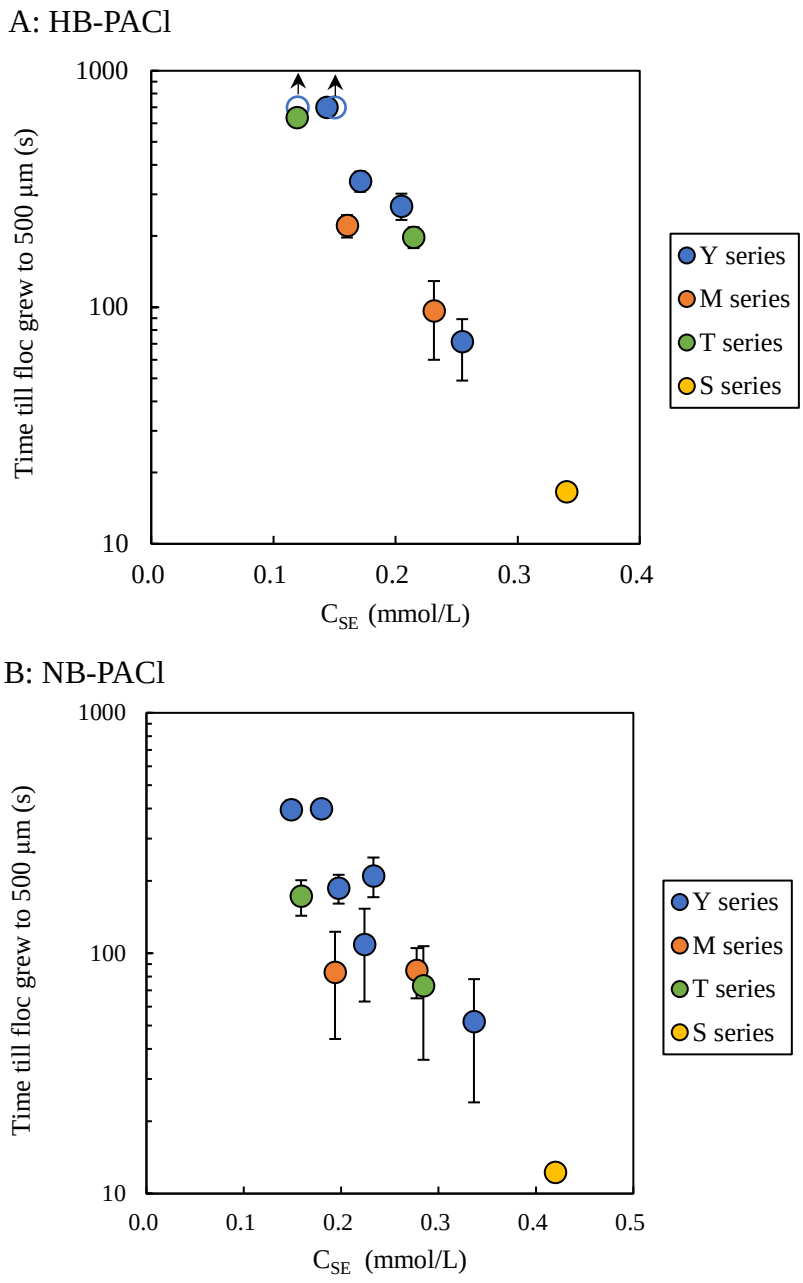


Fig. 4-14. Time until floc grew to 500 µm against $C_{SE}$ values in coagulation experiments. Panels A and B show the data for HB-PACl and NB-PACl, respectively, in Y, M, T, and S series waters. The coagulation pH was 7.0. The PACl dose was 2.5 mg-Al/L for Y, M, T series, and 5.6 mg-Al/L for S series water. Open circles in Panel A indicate that floc size did not increase to 500 µm during the experiment. Error bars indicate 95% confidence intervals.

## 4.4 Chapter summary

In this chapter, the effects of common inorganic ions and NOM on PACl hydrolysis-precipitation are comprehensively investigated.

Among the common ions in natural water, the sulfate ions had the greatest ability to hydrolyze PACl because of its divalency and tetrahedral structure. This conclusion followed from experimental results using selenate, chromate, and thiosulfate ions.

Bicarbonate ions and natural organic matter affected PACl hydrolysis-precipitation, but chloride ions, nitrate ions, and cations had little effect on PACl hydrolysis-precipitation.

The abilities of sulfate ions to hydrolyze HB-PACl and NB-PACl were very similar. Bicarbonate ions were less effective in hydrolyzing HB-PACl than NB-PACl, and bicarbonate ions contributed little to the hydrolysis-precipitation of HB-PACl in raw water with normal alkalinity. Sufficient coagulation with HB-PACl therefore usually requires a certain concentration of sulfate ions.

Sulfate ions, bicarbonate ions, and NOM affected the rate of hydrolysis-precipitation of PACl in an additive manner. The overall effect can be expressed by sulfate-ion-equivalent concentrations.

The rate of floc formation was low when the sulfate-ion-equivalent concentration in the raw water was low. Sulfate-ion-equivalent concentration could be applied as an index to estimate the coagulation performance when applying PACl.

## 4.5 Reference

Archer, A. D., & Singer, P. C. (2006). Effect of SUVA and enhanced coagulation on removal of TOX precursors. *Journal-American Water Works Association*, *98*(8), 97–107.

Barrett, S. E., Krasner, S. W., & Amy, G. L. (2000). *Natural organic matter and disinfection by-products: Characterization and control in drinking water—an overview*.

Bratby, J. (2016). *Coagulation and flocculation in water and wastewater treatment*. IWA publishing.

Chen, Y., Nakazawa, Y., Matsui, Y., Shirasaki, N., & Matsushita, T. (2020). Sulfate ion in raw water affects performance of high-basicity PACl coagulants produced by Al(OH)3 dissolution and base-titration: Removal of SPAC particles by coagulation-flocculation, sedimentation, and sand filtration. *Water Research*, *183*, 116093. https://doi.org/10.1016/j.watres.2020.116093

David R. Lide. (2004). CRC Handbook of Chemistry and Physics, 84th Edition Edited by David R. Lide (National Institute of Standards and Technology). CRC Press LLC: Boca Raton. 2003. 2616 pp. $139.95. ISBN 0-8493-0484-9. In *Journal of the American Chemical Society* (Vol. 126, Issue 5). American Chemical Society. https://doi.org/10.1021/ja0336372

Dousma, J., & de Bruyn, P. L. (1978). Hydrolysis-precipitation studies of iron solutions. II. Aging studies and the model for precipitation from Fe(III) nitrate solutions. *Journal of Colloid And Interface Science*, *64*(1), 154–170. https://doi.org/10.1016/0021-9797(78)90345-4

Duan, J., Wang, J., Guo, T., & Gregory, J. (2014). Zeta potentials and sizes of aluminum salt precipitates - Effect of anions and organics and implications for coagulation mechanisms. *Journal of Water Process Engineering*, *4*(C), 224–232. https://doi.org/10.1016/j.jwpe.2014.10.008

Edwards, M. (1997). Predicting DOC removal during enhanced coagulation. *Journal-American Water Works Association*, *89*(5), 78–89.

Edzwald, J., & Association, A. W. W. (2011). *Water quality & treatment: a handbook on drinking water*. McGraw-Hill Education.

Edzwald, J. K. (1993). Coagulation in drinking water treatment: Particles, organics and coagulants. *Water Science and Technology*, *27*(11), 21–35. https://doi.org/10.2166/wst.1993.0261

Hanna, & Rubin, A. J. (1970). Effect of Sulfate and Other Ions in Coagulation With Aluminum(Iii. *Journal / American Water Works Association*, *62*(5), 315–321. https://doi.org/10.1002/j.1551-8833.1970.tb03912.x

Hussain, S., van Leeuwen, J., Chow, C., Beecham, S., Kamruzzaman, M., Wang, D., Drikas, M., & Aryal, R. (2013). Removal of organic contaminants from river and reservoir waters by three different aluminum-based metal salts: Coagulation adsorption and kinetics studies. *Chemical Engineering Journal*, *225*, 394–405. https://doi.org/10.1016/j.cej.2013.03.119

Jiang, J. Q. (2001). Development of coagulation theory and pre-polymerized coagulants for water treatment. *Separation and Purification Methods*, *30*(1), 127–141. https://doi.org/10.1081/SPM-100102986

Li, M., Cheng, J., Zou, F., Zhang, C., Wang, M., Li, Y., Gu, J., & Yan, M. (2021). Effects of pre-oxidation on residual dissolved aluminum in coagulated water: A pilot-scale study. *Water Research*, *190*, 116682. https://doi.org/10.1016/j.watres.2020.116682

Macintyre, J. E., Daniel, F. M., & Stirling, V. M. (1992). *Dictionary of Inorganic Compounds*. Chapman & Hall. https://books.google.co.jp/books?id=macRAQAAMAAJ

Matijević, E., & Stryker, L. J. (1966). Coagulation and reversal of charge of lyophobic colloids by hydrolyzed metal ions. III. Aluminum Sulfate. *Journal of Colloid And Interface Science*, *22*(1), 68–77. https://doi.org/10.1016/0021-9797(66)90068-3

Nakazawa, Y., Matsui, Y., Hanamura, Y., Shinno, K., Shirasaki, N., & Matsushita, T. (2018). Minimizing residual black particles in sand filtrate when applying super-fine powdered activated carbon: Coagulants and coagulation conditions. *Water Research*, *147*, 311–320. https://doi.org/10.1016/j.watres.2018.10.008

Nikanorov, A. M., & Brazhnikova, L. V. (2009). Water Chemical Composition of Rivers, Lakes and Wetlands. In *Encyclopedia of Life Support Systems (EOLSS)* (Vol. 2). https://www.eolss.net/Sample-Chapters/C07/E2-03-04-02.pdf

Nowicki, W., & Nowicka, G. (1994). Verification of the Schulze-Hardy rule - A colloid chemistry experiment. *Journal of Chemical Education*, *71*(7), 624–626. https://doi.org/10.1021/ed071p624

Ou, H.-S., Wei, C.-H., Deng, Y., & Gao, N.-Y. (2014). Principal component analysis to assess the efficiency and mechanism for ultraviolet-C/polyaluminum chloride enhanced coagulation of algae-laden water. *Water Science and Technology: Water Supply*, *14*(3), 493–503.

Rakshit, A. K., Naskar, B., & Moulik, S. P. (2021). Performance of modified Schulze-Hardy rule on the stability of nano, micro, and macro colloidal dispersions: A comprehensive account. *Colloids and Surfaces A: Physicochemical and Engineering Aspects*, *626*(May), 127084. https://doi.org/10.1016/j.colsurfa.2021.127084

Su, Z., Liu, T., Yu, W., Li, X., & Graham, N. J. D. (2017). Coagulation of surface water: Observations on the significance of biopolymers. *Water Research*, *126*, 144–152. https://doi.org/10.1016/j.watres.2017.09.022

Wang, X., Tang, X., Feng, P., Li, X., Zhao, C., Chen, W., & Zheng, H. (2017). A novel preparation method of polyaluminum chloride/polyacrylamide composite coagulant: Composition and characteristic. *Journal of Applied Polymer Science*, *134*(11), 1–6. https://doi.org/10.1002/app.44500

Yue, Y., An, G., Liu, L., Lin, L., Jiao, R., & Wang, D. (2021). Pre-aggregation of Al13 in optimizing coagulation for removal of humic acid. *Chemosphere*, *277*, 130268. https://doi.org/10.1016/j.chemosphere.2021.130268

Zouboulis, A. I., & Tzoupanos, N. (2010). Alternative cost-effective preparation method of polyaluminium chloride (PAC) coagulant agent: Characterization and comparative application for water/wastewater treatment. *Desalination*, *250*(1), 339–344. https://doi.org/10.1016/j.desal.2009.09.053

# Chapter 5. Summary and conclusions

In this study, the important role of PACl hydrolysis-precipitation in coagulation process was comprehensively investigated. From the different performance of high-basicity $AlCl_3$-titration PACl and $Al(OH)_3$-dissolution PACl in removing SPAC particles in coagulation-flocculation, sedimentation, and sand-filtration (CSF) process, the important role of hydrolysis-precipitation was revealed. The effects of water characteristics on PACl hydrolysis-precipitation and performance were investigated. The total study has been described in Chapter 1 ~ Chapter 4 and the contents can be summarized as follows.

Chapter 1 introduced the background and objectives of this study. As a popular method in coagulation-flocculation water treatment process, the application of PACl is widely used around the world. In the experiment conducted in my laboratory, the high-basicity PACl prepared by $AlCl_3$-titration method and $Al(OH)_3$-dissolution method showed totally different performance in removing particles. However, this difference cannot be explained by conventional indices such as ferron assay and zeta potential. On the other hand, high-basicity $Al(OH)_3$-dissolution PACl is sometimes inferior to normal-basicity PACl. PACls with a variety of characteristics are used in different regions with different water quality around the world, however, the effects of water characteristics are not fully investigated yet. Therefore, this study sets the objectives to find the factor or method that can explain the different PACl performance, and to figure out the effects of water characteristics on PACl coagulation.

Chapter 2 introduced the finding of hydrolysis-precipitation rate as a factor of PACl coagulation performance, and the effect of sulfate ion on PACl hydrolysis-precipitation. I comprehensively investigated the difference between HB-PACl ($Al(OH)_3$-dissolution PACl) and HB-PACl-t ($AlCl_3$-titration PACl) as well as the difference between HB-PACl and NB-

PACl (normal-basicity PACl) in terms of their coagulation ability to form floc particles and to reduce the concentration of SPAC particles in CSF-treated water. The ferron distribution, colloid charge, zeta potential cannot explain their different performance, however, the hydrolysis-precipitation rate, measured by the membrane filtration, showed correlation between PACl performance. On the other hand, sulfate ion in raw water was found to facilitate the hydrolysis-precipitation, therefore affected PACl performance.

Chapter 3 confirmed the universality of PACl hydrolysis-precipitation as a factor related to PACl coagulation performance. The coagulation experiment and hydrolysis-precipitation rate test were conducted in natural raw water at various of pH, PACl dose, and alkalinity condition. The floc formation rates during coagulation experiments were strongly correlated with PACl hydrolysis-precipitation, irrespectively the pH, PACl dose, and alkalinity. Therefore, the correlation between PACl hydrolysis-precipitation and PACl coagulation performance was established.

Chapter 4 introduced the effects of inorganic ions and NOM in raw water on PACl hydrolysis. Because natural water contains various types of ions besides sulfate ion in different concentrations, it is necessary to figure out the respective effect of other ions in water. The effects of sulfate ion, bicarbonate ion, chloride ion, nitrate ion, and NOM on PACl hydrolysis were investigated in different concentrations by hydrolysis-precipitation rate test. The respective effect can be additively calculated as the overall effect. Then, I built the connection between the overall effects caused by water characteristics and the PACl performance. Thus, the overall effect can be applied as an index to estimate the coagulation performance when applying PACl.

I would like to summarize the findings of this study.

1) The coagulation performance of HB-PACl was superior to that of HB-PACl-t, although the ferron distribution, colloid charge, and sulfate ion content were the same. Charge neutralization capacities were likewise sufficient for HB-PACl-t and HB-PACl, but the very low hydrolysis-precipitation of aluminum species in HB-PACl-t versus HB-PACl resulted in poor floc formation by the former. HB-PACl was superior to NB-PACl in reducing residual carbon particles after CSF, although the rate of floc particle formation was somewhat slower for HB-PACl than for NB-PACl.

2) Sulfate ion was required in raw water for HB-PACl to be effective. When the raw water contained very low concentrations of sulfate ions, the aluminum species in HB-PACl hydrolyzed very slowly and did not form floc particles. In contrast, NB-PACl did not need sulfate ions. HB-PACl was inferior to NB-PACl when sulfate ion concentrations in raw water were very low. Hydrolysis, therefore, is a key determinant of coagulation performance.

3) The rates of floc formation by PACls with different basicities and polymerization (HB-PACl and NB-PACl) varied as a function of the characteristics of the raw water. Floc formation rates were strongly correlated with the rates of PACl hydrolysis-precipitation.

4) Hydrolysis-precipitation of PACls was enhanced by sulfate, selenate, chromate, thiosulfate, and bicarbonate ions, and NOM. Sulfate, selenate, and chromate ions had >200 times greater ability to hydrolyze and precipitate PACl than chloride ions and nitrate ions. This greater ability was attributable to both the divalency and tetrahedral structure of the sulfate ion, which supports the possible mechanism of the complexing of sulfate with aluminum. Cations in the water had little effect on the rate of PACl hydrolysis-precipitation. The ability of bicarbonate ions to hydrolyze PACls was more than tenfold that of chloride and nitrate ions but much less than that of sulfate ions.

5) HB-PACl was hydrolyzed more slowly than NB-PACl. In particular, HB-PACl was very slowly hydrolyzed by bicarbonate ions. The hydrolysis-precipitation of HB-PACl is needed for sufficient flocculation performance, therefore, required a certain concentration of sulfate ions in natural surface water. In contrast, because NB-PACl was hydrolyzed to some extent by bicarbonate ions, the concentration of sulfate ions required for hydrolysis-precipitation was low and in practice was rarely insufficient.

6) Sulfate ions, bicarbonate ions, and NOM affected the rate of hydrolysis-precipitation of PACl in an additive manner. The rates of PACl hydrolysis-precipitation were therefore described rather well by sulfate-ion-equivalent concentrations, which represent the additive effects of sulfate ions, bicarbonate ions and NOM. The rate of floc formation was low when the sulfate-ion-equivalent concentration in the raw water was low.

7) In this study, it was found that hydrolysis-precipitation of PACl, besides charge neutralization, is necessary for coagulation-flocculation. Sulfate ion, bicarbonate ion, and NOM accelerate the hydrolysis-precipitation, but their effects are different depending on the type of PACl. The effectiveness of PACl, which has a high charge-neutralization capacity due to its high content of Alb and AlC, has been demonstrated in a number of papers. However, such PACl is difficult to hydrolyze in raw water with low sulfate ion concentrations, resulting in poor coagulation-flocculation. Since PACl is composed of a variety of aluminum polymeric species, clarifying which aluminum species is hydrolyzed by which anion or NOM and at what rate will undoubtedly be an important research theme in the future.